LOMONOSOV MOSCOW STATE UNIVERSITY

FACULTY OF CHEMISTRY

POLYMER DEPARTMENT

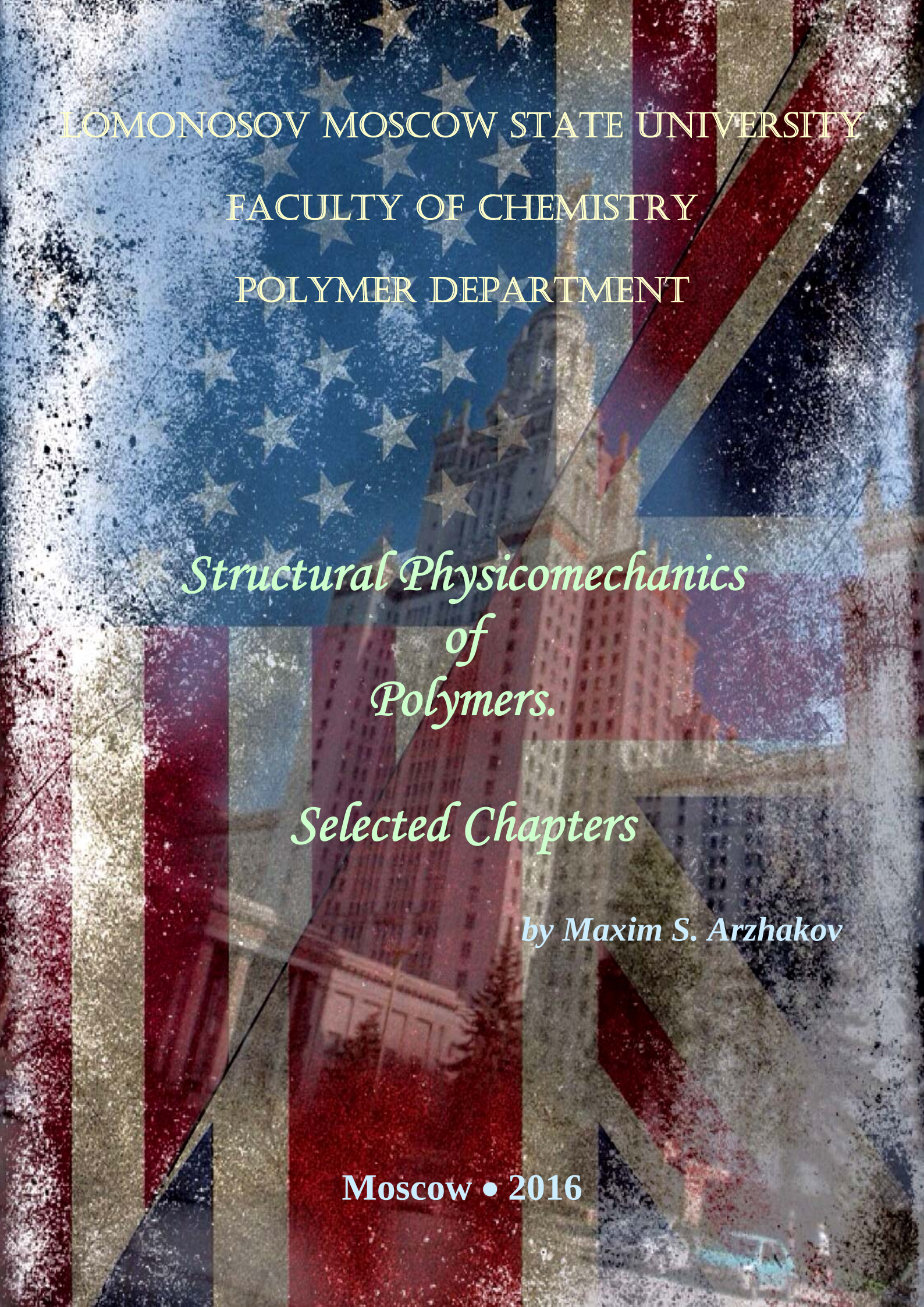

Structural Physicomechanics of Polymers.

Selected Chapters

by Maxim S. Arzhakov

Moscow • 2016

This textbook contributes to the Educational Course

"SELECTED CHAPTERS OF CHEMISTRY"

Selected Chapters of Polymer Science

lectured for students of Faculty of Chemistry
Lomonosov Moscow State University

The fundamentals of physics of polymers
as well as
the basic principles of production of modern construction polymeric materials
are outlined

For students and post-graduated students who are specialized and/or interested in
Polymer Science

CONTENT

Chapter 1. WHAT IS "STRUCTURAL PHYSICOMECHANICS"?
Basic Principles and Definitions

The basic principle of the "Structural Physicomechanics" is the fundamental and intrinsic interrelation between microscopic structure and macroscopic physicomechanical property.

> Macroscopic property of any material is controlled by microscopic structure or, in other words, physicomechanical behavior is the macroscopic manifestation of microscopic structural organization of the material.

By physicomechanical behavior we mean the set of

- combination of physical parameters of material (temperatures of phase and physical transitions, thermal properties, sorption properties, *etc*.) and mechanical properties (strength, elasticity, ductility, *etc*);
- the changes of the mechanical parameters of material with the change of physical operating parameters such as temperature, humidity, pressure, *etc*.

From this standpoint, for any material, development of the desired operating properties is possible only via controlled design or synthesis of the appropriate structure.

This statement is of the utmost importance for polymers because, for them, the term "structure" is a more comprehensive as compared with that for the low-molar-mass bodies. Unique chain molecular structure of macromolecules is responsible for the wide possibilities to form complicated supramolecular structure, and this sophisticated structural organization controls specific mechanical properties of polymers.

> "The properties of polymers are designed at the level of their molecular structure but come into a play at the level of their supramolecular structure".
>
> V.A. Kargin[1]

For example, for *rubbers* (or *elastomers*), structural design of the macromolecular three-dimensional *networks* via chemical cross-linking of the linear macrochains manifests itself in the appearance of the well-pronounced *high elasticity*, that is, the unique ability to high (till several hundreds percents) reversible deformations. Appropriate chemical structure of macromolecules provides a possibilities for polymer crystallization with the appearance of crystalline supramolecular structure which results in noticeable changes in physicomechanical properties. Chain chemical structure of polymer allow formation of anisotropic *oriented* supramolecular structure which controls the enormous growth of the strength mechanical characteristics of the material.

To demonstrate the validity of the "Structural Physicomechanics" approach, let us overview the general concepts concerning the physicomechanical behavior of physical bodies.

[1] V.A. Kargin (1907 - 1969), Russian chemist, one of the founder of Russian Polymer Science

Typically, real bodies exist in solid, liquid, and gaseous *physical states*. Solid and liquid states are identified as the *condensed state* of a physical body. To simplify the problem, let us take into consideration only molecular organic substances composed of molecules with no invoking the atomic and ionic bodies such as metals and inorganic crystals. This point of view is quite appropriate due to the fact that polymers are organic molecular substances, and their behavior is more close to that of molecular bodies. Note that the following analysis concerning the behavior of molecular substances is also applied to atomic and ionic substances except the nature of physical interactions within body and some quantitative differences.

The majority of the organic molecular substances exhibit the ability to be transformed from solid to liquid at *melting point*, and from liquid to gas (or vapor) at *boiling point*, and can be obtained in all above states. Obviously, physical bodies in solid, liquid, and gaseous states are characterized by the quite different physical and mechanical behavior.

Solid bodies show the high resistance to applied loading and high stability of shape and volume. Liquids demonstrate well-pronounced fluidity, that is, the ability to flow with the change of the shape by gravity or under rather small loading, and, as a result, they do not possess shape stability. However, for liquids, volume stability is rather high because of low compressibility which is comparable with that for solids. Gases do not exhibit stability of both shape and volume.

In the framework of "Structural Physicomechanics", to understand the origin of the dramatic differences between the behavior of the same physical body in solid, liquid, and gaseous states as well as the nature of the transitions from one state to another, let us consider the problem from the standpoint of the intrinsic correlation between the following factors:

- structural organization of the physical body;
- the interplay of (i) intermolecular interactions (van der Waals interactions (dipole - dipole, induction, and dispersion interactions), hydrogen bonding, *etc*.) and (ii) thermal motion of molecules.

In the framework of *Systems Approach*, structure may be identified as a mutual arrangement, interrelation, and interconnection of the *structural units* or subsystems (in our case, molecules) of a given system (in our case, molecular physical body). **Quantitatively, structure is characterized by degree of ordering and packing density of the above structural units.**

Packing density (or ***density***) controls the degree of aggregation of molecules.

Note that the transition from liquid to gas is accompanied by the dramatic (for several orders of magnitude) decrease in density while density does not noticeably change when transition from solid to liquid takes place.

Hence, ***the density term describes the difference between liquids and gases but is not sufficient to explain the difference between solids and liquids.***

From the standpoint of the ***ordering*** of the structural units, *long-range order* and *short-range order* are recognized in condensed bodies. This speculation allows us to introduce the term **"*phase state*"** which involves crystalline and amorphous states.

Crystalline phase state is characterized by the three-dimensional long-range order, and amorphous phase state is characterized by the short-range order.

For crystalline bodies, well-pronounced long-range order is observed when structural units are strictly embedded at the nodes of *crystalline lattice*. For a given crystalline body, crystalline lattice is a typical arrangement of structural units which is characterized by the sharp and specified regularity in all three dimensions. As a result, for crystalline substances, anisotropy, that is, the difference of the physicomechanical properties (thermal conductance and expansion, strength, refractive index, *etc*.) is observed.

In the framework of the ***Molecular Kinetics Approach***, a physical body exists in the crystalline state at temperatures when the energy of interatomic and intermolecular interactions of *kinetic units*, U, is much higher than their thermal energy, that is, $U >> kT$.

Kinetic unit – structural unit which possesses translational and/or vibrational degrees of freedom.

For low-molar-mass crystalline bodies, translational degree of freedom is lost, and the sample shows the specific physical and mechanical behavior of the solid body, primarily, shape and volume stability. Hence, solid physical state is always crystalline phase state.

When temperature increases the noticeable thermal motion of kinetic units appears and start to compete with their interatomic and intermolecular interactions. At the critical temperature which is called melting point, the appeared thermal motion destroys the crystalline lattice, and melting, that is, "solid - liquid" transition is observed.

Liquids are characterized by the short-range order in the arrangement of the molecules. Short-range order implies the fact that the number of adjacent molecules around each molecule and their mutual arrangement are the same for all molecules. Liquids are isotropic bodies, and their physicomechanical properties are identical in all three directions.

In this case, $U \sim kT$, and intermolecular interactions are still sufficient to hold liquids in the condensed state but low enough to allow *self-diffusion*, that is, continuous migration of the molecules relative to each other because of well-pronounced thermal mobility. This intrinsic interconnection between structural features of liquids, intermolecular interactions and thermal motion of molecules control the liquid fluidity, that is, shape instability and stability of volume.

With increasing temperature till the boiling point, liquids easily vaporize, and "liquid - gas (vapor)" transition takes place. This transition is realized when thermal energy becomes much higher than the energy of intermolecular interaction ($U << kT$), and molecules are not hold together. As a result, gases are not considered as condensed bodies, and, for them, no order is observed.

Hence, the above discussion demonstrates that the features of structural organization of physical bodies and balance between energy of intermolecular interaction and thermal energy are in intrinsic interconnection and should be considered together to understand the origin of the physical and mechanical behavior of the real bodies in all possible physical states. The above reasoning suggests that, at the first approximation, physicomechanical behavior of the real physical bodies is controlled by their phase and physical states. However, in some cases, this

relationship is ambiguous. Actually, the boundaries between the above physical and phase states are not distinct. To clarify this problem, let us assess the following examples.

When temperature decreases, a lot of liquids tend to solidify with no crystallization and formation of three-dimensional crystalline lattice. This super-cooled solidified liquid is called *glass*.

From the phase and structural standpoints,
glass is amorphous liquid with well-pronounced isotropy of the properties and without long-range order.

From the physical standpoint,
glass is solid body, and its both shape and volume are stable for a long period of time.

The origin of these structural and physical features is associated with the fact that, at the critical temperature which is called *glass transition temperature*, the thermal energy becomes too low to provide molecular translational mobility. As a result, liquid fluidity disappears.

Glassy state may be identified as solid physical state which is characterized by the absence of crystalline structure.

Note that the physicomechanical behavior of physical body becomes more complicated under dynamic conditions. To get a deeper insight into the problem, let us analyze the following examples.

Hurricane-force wind breaks trees and destroys buildings because, at the speed more than 73 miles per hour, air becomes more hard than typical solid bodies such as wood and stone. Under instantaneous compression, the resistance of the gas is comparable to that for liquid. Under impact loading, for example, bullet blow, the stream of water is broken down as a brittle solid body. On keeping for a long period of time, solid bitumen tends to flow by gravity with the distortion of the shape as viscous liquid. In all these examples, real bodies in a certain physical state show the mechanical behavior and response which are characteristic for another physical state in dependence on the rate or duration of loading. Hence, actually, physical and mechanical behavior depends on both physical and phase state of a body and kinetic factors.

Note that, in general, the above speculations concerning the physical, structural, and kinetic aspects of the physical and mechanical behavior of low-molar-mass bodies may be applied to high-molar-mass polymer substances. However, in many cases, ***polymers demonstrate the unique features of physical and mechanical behavior because of their macromolecular nature.***

The prime example is the fact that polymers do not exist in gaseous state and may be obtained only in solid or liquid condensed states. The reason of it is associated with the extremely high energy of intermolecular interaction based on the cooperative system of intermolecular physical bonds, well-pronounced entanglements of macromolecules, formation of the physical network, *etc*. As a result, the temperature required to evaporate polymer via separation of individual macromolecules in polymeric liquids is much higher as compared with the temperature of the chemical decomposition. In other words, polymer macromolecules "prefer" to be burned but not to be separated.

As compared with low-molar-mass bodies, for polymers, the nature of kinetic and structural units responsible for the structural organization and physicomechanial behavior may change from atomic groups to segments to macromolecules in dependence on various factors. However, for polymers as for any physical body, "Structural Physicomechanics" allows one to understand the structural and physical origin of their behavior.

The objective of the following chapters is

to provide scientific fundamentals and define the problems related to following structural design of polymeric materials via

- structural analysis of the physical and mechanical behavior of polymeric substances within different physical and phase states to understand the origin of their specific and, in many cases, unique properties;
- examination of the temperature-induced transitions from one state to another state to predict and control operating temperature intervals of polymers.

Chapter 2. VISCOELASTICITY AND RELAXATION

In the previous section, we touched on the problem concerning the influence of the kinetic factors on the physical and mechanical behavior of physical bodies. In dependence on the duration of loading, physical bodies in a given physical and phase state show the response to applied loading which is characteristic for another state. Liquids behave themselves as solid body. Gases respond to loading as liquids or solids. Solids demonstrate typical liquid-like behavior. The objective of this section is to understand the origin of the kinetic nature of the mechanical behavior of physical bodies and to introduce quantitative kinetic parameters which control the response of the body to applied loading.

Under loading with the applied external force, the response of the body is associated with deformation of the material, that is, changes in its shape and geometrical dimensions. Deformation is estimated as a *strain* which is the relative (fractional) change in the dimension of a given sample. There are two general laws describing the relationship between applied stress σ (force per unit of area) and strain ε or *vice versa*.

For the ***ideal elastic bodies,*** mechanical response to applied loading is described by Hooke's law

$$\sigma = E\varepsilon = E\frac{\Delta l}{l}, \qquad (1)$$

where σ is applied stress, that is, the applied force normalized to cross-section area; ε is the strain equal to the ratio between the increment of the dimension after deformation Δl and the initial linear dimension of the sample l; E is the elastic modulus or Young's modulus, that is, the stress realized at the strain equal to unity.

Hooke's law predicts the linear dependence of applied stress and resulting strain with the slope equal to elastic modulus. For a variety of solids, mechanical behavior obeys Hooke's law at rather low strains not more than a percent.

Hookean elastic deformation is associated with the disturbance of intermolecular and interatomic physical interactions and short-range displacement of molecules or atoms from their equilibrium positions without leaving surrounding. Under unloading, molecules or atoms return in their initial equilibrium states providing reversible character of Hookean deformation.

For ***ideal viscous liquids,*** their response to applied loading is associated with slippage of molecules relative to each other. As a result, well-pronounced *flow* is observed. On contrary to Hookean elastic deformation, flow deformations are irreversible. In ideal case, the viscous flow obeys Newton's law

$$\sigma = \eta\frac{d\varepsilon}{dt} \qquad (2)$$

where $d\varepsilon/dt$ is the rate of deformation; η is the coefficient of viscous resistance, or viscosity.

Actually, a variety of real bodies (polymers are the prime example of them), exhibit more complicated response to applied loading. This mechanical behavior is intermediate between ideal elastic and ideal viscous response and is called *viscoelasticity*.

In 19th century, to explain time-dependent mechanical behavior of natural materials such as tar and pitch Maxwell proposed a mechanical model which combines in series two basic components – elastic spring of modulus E and viscous dashpot of viscosity η (Fig. 1A). Deformation of elastic spring obeys Hooke's law, and deformation controlled by the movement of piston in viscous dashpot is described by Newton's law.

Under applied loading, the total strain of the model is a sum of elastic strain of the spring, ε_{el}, and strain associated with the viscous movement of piston in dashpot, ε_v

$$\varepsilon = \varepsilon_{el} + \varepsilon_v .$$

Differentiation of this equation with respect to Hooke's law and Newton's law gives

$$\frac{d\varepsilon}{dt} = \frac{1}{E}\frac{d\sigma}{dt} + \frac{\sigma}{\eta} \tag{3}$$

or

$$\frac{d\sigma}{dt} = E\frac{d\varepsilon}{dt} - \frac{\sigma}{\eta / E} \tag{4}$$

Let us consider the behavior of Maxwell model under the following regimes of loading.

When Maxwell model is instantaneously subjected to deformation of strain ε, and this strain is kept constant during test, that is, ε = const and $d\varepsilon / dt = 0$, Eq. (4) is written as

$$\frac{d\sigma}{dt} = -\frac{\sigma}{\eta / E}.$$

Integration of the above equation gives

$$\ln\frac{\sigma_t}{\sigma_0} = -\frac{t}{\eta / E}$$

or

$$\sigma_t = \sigma_0 e^{-\frac{t}{\eta / E}} \tag{5}$$

where σ_0 and σ_t are the initial and current stresses, respectively.

The above mathematical expression predicts an exponential decay of stress in Maxwell model deformed with a constant strain (Fig. 1B). Obviously, this process is controlled by elastic contraction of drawn spring retarded by the movement of piston in viscous dashpot.

In general, the behavior observed reflects the tendency of instantaneously deformed, that is, excited Maxwell model to release excitation and approach equilibrium state.

Transition from excited non-equilibrium state to equilibrium state is called *relaxation*.

In this case, the relaxation of the model manifests itself as *stress relaxation*.

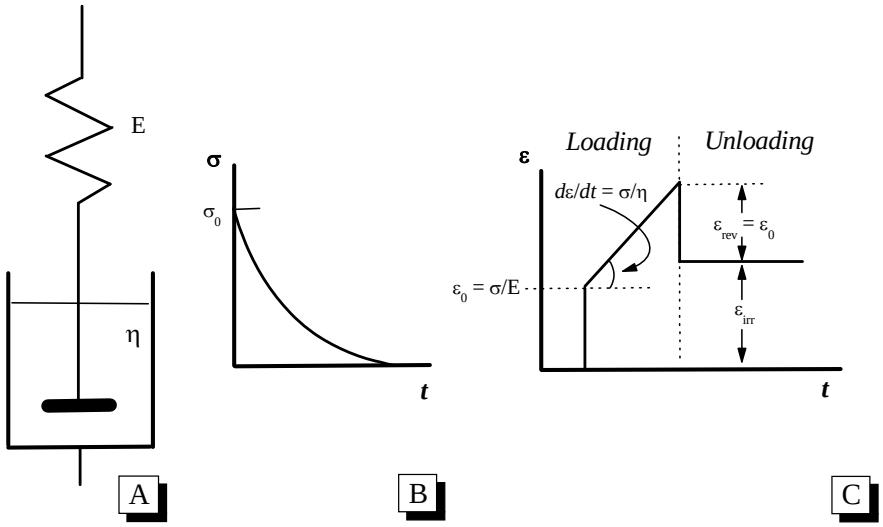

Figure 1. Maxwell model of viscoelastic body (A), time dependence of stress in deformed model (B), and mechanical response of the model under creep conditions (C).

For a given Maxwell model, the term η / E (Eq. 5) is the constant and controls the rate of relaxation. This term has a dimension of time and is called *relaxation time*, τ.

The higher relaxation time, the longer a period of time required to approach equilibrium.

Equation (5) allows the following formal definition of relaxation time. When $t = \tau$, $\sigma_t = \sigma_t / e$, and, from this standpoint,

relaxation time of a system is a time during which a given relaxing macroscopic parameter (stress, in this case) decreases for *e* times.

From the physical viewpoint, $\tau = \eta / E$ reflects the ratio between the elastic response and viscous resistance of a system. The higher viscosity and the lower elastic modulus, the higher relaxation time and *vice versa*.

Under *creep* testing, when Maxwell model is instantaneously subjected to stress σ at the time $t = 0$, and the stress is kept constant during testing, that is, σ = const and $d\sigma / dt = 0$, Eq. (3) is written as

$$\frac{d\varepsilon}{dt} = \frac{\sigma}{\eta} \quad \text{or} \quad \frac{d\varepsilon}{dt} = \frac{\sigma}{E\tau}.$$

Integration gives the following time dependence of resulting strain

$$\varepsilon_t = \varepsilon_0 + \frac{\sigma}{\eta} t \tag{6}$$

or

$$\varepsilon_t = \varepsilon_0 + \frac{\sigma}{E\tau} t \tag{7}$$

The above equations suggest that, under constant stress, strain of Maxwell model grows with time in linear fashion with the rate which is proportional to applied stress and reciprocal to viscosity, elastic modulus, and relaxation time according to Newton's law. The corresponding mechanical response of the model is shown in Fig. 1C.

Under instantaneous loading at t = 0, model responds to applied stress immediately because of instantaneous extension of a spring for strain $\varepsilon_0 = \sigma / E$ (Eq. (6)). With increasing loading time, deformation proceeds due to movement of piston in viscous dashpot. Unloading of the model is accompanied by the instantaneous contraction of a spring, and strain ε_0 recovers immediately. The strain associated with the movement of piston in dashpot is stored in unloaded model.

Hence, for viscoelastic bodies, Maxwell model predicts the co-existence of reversible elastic component of strain ε_{rev} and irreversible viscous component ε_{irr}. Obviously, the total strain is the sum of the above components $\varepsilon = \varepsilon_{rev} + \varepsilon_{irr}$.

`

Note that, at a given stress, the ratio ε_{rev} / ε_{irr} is time-dependent and decreases with increasing loading time. In other words, the nature of the response of Maxwell model to loading is controlled by the loading duration. When $t \to 0$, only elastic response is recognized, and, under loading for a long period of time, viscous response prevails.

To be more correct, the ratio between elastic and viscous response of Maxwell model is associated mainly with the ratio between loading time t and relaxation time τ which may be varied by the ratio η / E. When $\tau << t$ (stiff spring and liquid with low viscosity), viscous response prevails, and, when $\tau >> t$ (weak spring and liquid with high viscosity), elastic component mainly contributes to strain.

Another mechanical model proposed by Voigt and Kelvin consists of the same elastic and viscous units combined in parallel (Fig. 2A). In this case, the strain is uniform

$$\varepsilon = \varepsilon_{el} = \varepsilon_{v},$$

and the total stress is a sum of the corresponding components

$$\sigma = \sigma_{el} + \sigma_{v}.$$

With respect to Hooke's law and Newton's law the total stress is written as

$$\sigma = E\varepsilon + \eta\frac{d\varepsilon}{dt} \tag{8}$$

Integration gives the following time dependence of strain under loading with constant stress

$$\varepsilon = \frac{\sigma}{\varepsilon}\left[1 - e^{-\frac{E}{\eta}t}\right] \tag{9}$$

Under creep testing, mechanical response of Voigt-Kelvin is shown in Fig. 2B. Note that this model predicts retarded development of deformation when strain rate decreases with time. Under unloading, when $\sigma \to 0$, Eq. (6) is written as

$$\frac{d\varepsilon}{dt} = -\frac{E}{\eta}\varepsilon = -\frac{\varepsilon}{\tau}.$$

Integration gives the following time dependence of strain

$$\varepsilon_t = \varepsilon_0 e^{-\frac{E}{\eta}t} = \varepsilon_0 e^{-\frac{t}{\tau}} . \qquad (10)$$

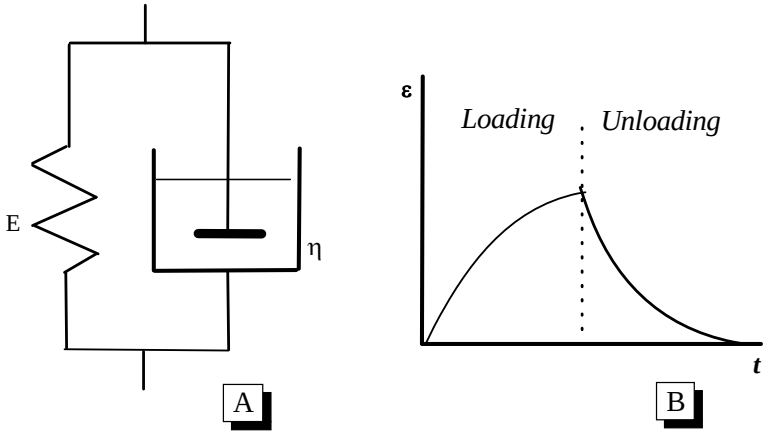

Figure 2. Voigt-Kelvin model of viscoelastic body (A) and mechanical response of the model under creep conditions (B).

Deformed and unloaded Voigt-Kelvin model tends to initial equilibrium state, exponential decay of strain is observed, that is, strain relaxation takes place.

The Voigt-Kelvin model predicts the retarded origin of elastic reversible deformation and relaxation in contrary Maxwell model when Hookean elastic reversible strain proceeds and relaxes instantaneously. This phenomenon is called *delayed elasticity*.

For delayed elasticity, time dependences of strain development (Eq. (9)) and strain relaxation (Eq. (10)) are controlled by the parameter η / E which, in this model, is identified as *retardation time*.

Voigt-Kelvin model does not predict the stress relaxation because, when the applied strain is kept constant, that is, $d\varepsilon / dt = 0$, Eq. (II.8) transforms into Hooke's law, and linear elastic response is observed.

To summarize, each of the above models describes some of the following aspects of general viscoelastic behavior:

1. Co-existence of reversible and irreversible components of total viscoelastic strain;
2. The influence of loading time on the ratio between elastic and viscous components of strain, that is, time-dependent nature of the viscoelastic behavior;
3. Relaxation nature of viscoelasticity which manifests itself as stress and strain relaxation;
4. Retarded character of elastic deformation and elastic strain recovery, that is, delyed elasticity.

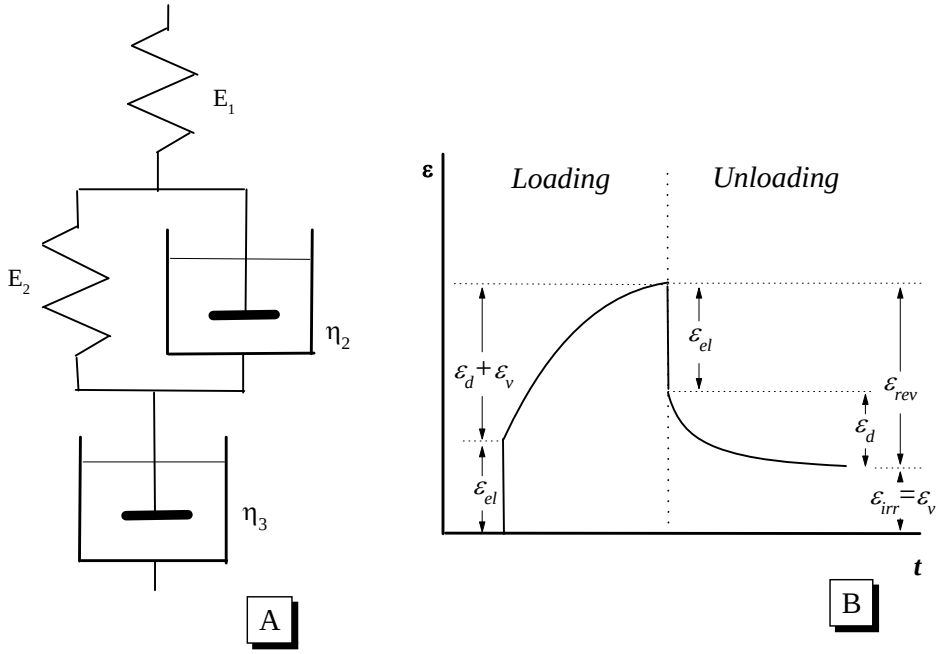

Figure 3. Combined mechanical model of viscoelastic body (A) and mechanical response of the model under creep conditions (B).

Figure 3A shows the mechanical model which allows one to visualize all above features of viscoelastic behavior. In this case, total strain is a sum of instantaneous Hookean elastic strain ε_{el} provided by a spring of modulus E_1, delayed elastic strain ε_d provided by Voigt-Kelvin unit (spring of modulus E_2 and dashpot of viscosity η_2), and viscous flow strain ε_v provided by dashpot of viscosity η_3

$$\varepsilon = \varepsilon_{el} + \varepsilon_d + \varepsilon_v .$$

After appropriate substitutions, for combined model, the general time dependence of strain is written as

$$\varepsilon = \frac{\sigma}{E_1} + \frac{\sigma}{E_2}\left[1 - e^{-\frac{t}{\tau}}\right] + \sigma\frac{t}{\eta_3}. \qquad (11)$$

Under creep testing (Fig. 3B), the loading of the model at time t_1 is accompanied by the instantaneous deformation of spring of modulus E_1 for strain $\varepsilon_{el} = \sigma / E_1$. With increasing loading time till t_2 model is deformed for the strain which is a combination of delayed elastic strain of Voigt-Kelvin unit and viscous flow strain of dashpot of viscosity η_3

$$\varepsilon_d + \varepsilon_v = \frac{\sigma}{E_2}\left[1 - e^{-\frac{(t_2 - t_1)}{\tau}}\right] + \sigma\frac{t_2 - t_1}{\eta_3}.$$

Under unloading at time t_2, the Hookean elastic portion ε_{el} of the total strain recovers immediately. Within period of time $t_3 - t_2$ relaxation of Voigt-Kelvin unit provides recovery of delayed elastic component ε_d of strain. Hence, combined model describes reversible portion of strain as a sum of Hookean elastic component and delayed elastic component

$$\varepsilon_{rev} = \varepsilon_{el} + \varepsilon_d .$$

Irreversible portion ε_{irr} of strain is associated with the movement of piston in dashpot of viscosity η_3 which controls viscous component of strain ε_v, and $\varepsilon_{irr} = \varepsilon_v$.

The above mechanical simulation provides phenomenological description of the of viscoelastic behavior when the following assumptions are taken into account.

1. Viscoelastic deformation is divided into elastic component and viscous irreversible component;
2. These deformation components obey Hooke's law and Newton's law, and viscoelastic behavior is controlled by the combination of these two laws;
3. Activation parameters and relaxation times of the kinetic units which are responsible for the viscoelastic deformation do not depend on loading parameters (primarily, stress and strain) and do not change during deformation.

When the above assumptions are fulfilled, we deal with the *linear viscoelasticity* of linear viscoelastic response of a body to mechanical loading.

In connection with this,

the above mechanical models are called *linear viscoelastic mechanical models*.

Actually, the real viscoelastic bodies obey linear viscoelasticity only at rather low stress and strain. Increasing stress and strain as well as changing the loading time and testing temperature are responsible for the inclination of viscoelastic behavior of polymers from linear viscoelasticity. For real polymeric materials, the reasoning of it will be discussed below.

However, the relaxation origin of viscoelasticity predicted by the above considerations is of prime importance. Deformation of physical body is associated with the permanent disturbance of its equilibrium state. In its turn, under these conditions, the body tends to relax permanently to recover the equilibrium state. In other words, deformation may be considered as a continuous set of "excitation – relaxation" cycles. To clarify the situation, let us consider the simplified scheme of flow of viscous liquids or plastic deformation of solids (Fig. 4).

Under applied external stress σ or by gravity, deformation is associated with the translations and mutual displacements of the molecules (or, in general, kinetic units) along the direction of applied loading. These microscopic events proceed via transition of a molecule to adjacent “hole” (Fig. 4A) with overcoming of potential barrier (Fig. 4B) because of the presence adjacent molecules. The overcoming of potential barrier involves “excitation” of the initial state “1” with minimum of energy and relaxation via transition to another potential dwell “2”.

Obviously, these microscopic transitions do not proceed just immediately and require a finite period of time which is considered as relaxation time τ. Relaxation time is reciprocal to the frequency ν at which kinetic units jump through the barrier and move to the new position. The temperature dependence of these two parameters is represented by an Arrhenius type equation

$$\tau = \frac{1}{\upsilon} = Ae^{\frac{U}{kT}} \qquad (12)$$

where A is temperature-dependent constant, and k is Boltzmann’s constant.

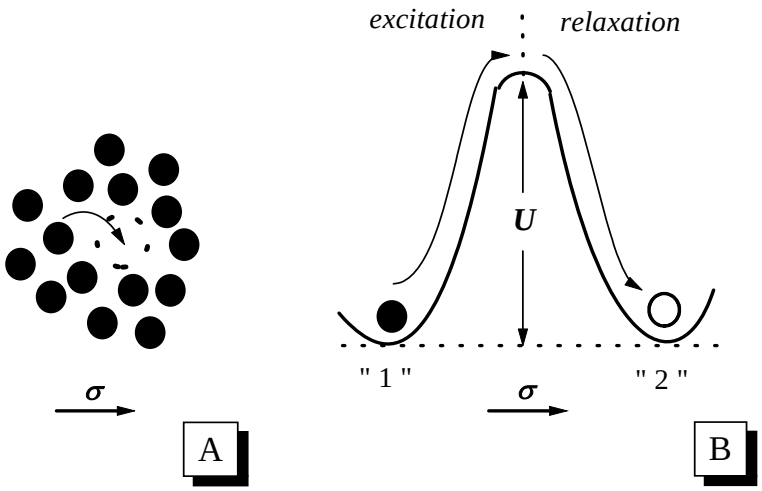

Figure 4. Schematic representation of flow or plastic deformation as a transition of a molecule to adjacent "hole" (A) with overcoming of potential barrier U (B).

Under the given loading conditions, mechanical response of physical body is expected to be dependent on the ratio between loading time t and relaxation time τ. If relaxation time is much less than loading time physical body behaves itself as purely viscous material. The reason is that the body has enough time for the inner rearrangements and well-pronounced fluidity and plasticity is observed. In contrary, when relaxation time is much higher than loading time, inner rearrangements do not occur, and purely elastic Hookean response is observed.

The relation between these two time scales (loading time t and relaxation time τ) was formalized by Reiner[1] [*M. Reiner, Physics Today, January, 1964, p. 62*] in terms of *Deborah number De*

$$De = \tau / t$$

after a phrase in the song by prophetess Deborah (Judges V, 5): "...the mountains flow before the Lord". It reflects the role of observation time scale: the objects which seem to be unchangeable within finite observation time scale of the human beings, deform or flow within infinite time scale accessible for the Lord.

From the physical viewpoint,

material may be considered as purely elastic when $De \to \infty$, and purely viscous when $De \to 0$. For typically viscoelastic bodies De is in the vicinity of unity.

Consideration of viscoelastic behavior of materials provides the fundamentals for the studying molecular or structural mechanism of deformation. As for the applied aspects, one should take into account the fact that, under operating conditions, construction materials are often subjected to loading for a long period of time. Obviously, prediction of material behavior requires detailed knowledge of its viscoelastic properties.

[1] Marcus Reiner (1886-1976), austrian civil engineer.

Chapter 3. AMORPHOUS POLYMERS

To study physicomechanical behavior of amorphous polymers let us invoke the *thermomechanical analysis*.

Thermomechanical analysis is based on the studying temperature dependence of deformation ε of a material under applying to the sample a specified stress for a specified period of time at each temperature.

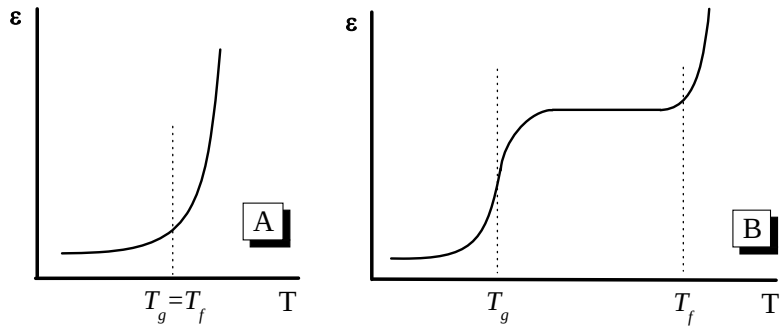

Figure 5. Typical thermomechanical curves for low-molar-mass amorphous body (A) and amorphous polymer (B).

For low-molar-mass amorphous substance, typical *thermomechanical curve* is shown in Fig. 5A. Transition which corresponds to the inflection point on this curve may be discussed from the two standpoints (see Ch.1). At first, it is a typical transition from solid physical state to liquid physical state which takes place at, T_f. On the other hand, it is glass transition, that is, transition from glassy to viscous flow state within amorphous phase state at glass transition temperature, T_g.

For low-molar-mass amorphous bodies, flow temperature and glass transition temperature coincide, that is T_f is equal to T_g.

For amorphous linear polymer, thermomechanical behavior is quite different (Fig. 5B). In this case, T_f and T_g are separated, and appearance of new state is observed between these temperatures. The polymer in this state is characterized by reversible high elastic deformations, and this state is called *rubbery* or *high-elastic* state.

The above experimental evidence allows one to suggest that the appearance of rubbery state is controlled by the transition from low-molar-mass substances to polymers. To verify this idea let us consider thermomechanical curves of polymer homologous series consisted substances with the same chain chemical structure and with different molar masses (Fig. 6A). For polymer homologues, with rather low molar masses (M_1 ..... M_3), only glassy and viscous flow states are observed. Increasing molar mass from M_1 to M_3 results in the shift of both T_g and T_f towards higher temperatures. Further increasing molar mass of polymer homologues to M_4, M_5, *etc* does not lead to growth in T_g, and is accompanied by increasing T_f.

With increasing molar mass, the separation of T_f and T_g is observed, and temperature range of rubbery physical state increases.

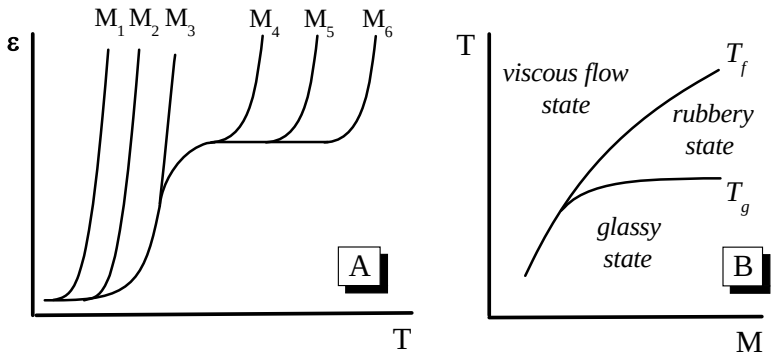

Figure 6. Thermomechanical curves for polymer homologues with molar masses $M_1 < M_2 < ... < M_6$ (A) and typical dependence of flow temperature T_f and glass transition temperature T_g on molar mass M (B).

Hence, the appearance of rubbery state and the property of high elasticity take place when the critical molar mass (or length of the chain) is attained. To explain this phenomenon, let us invoke the molecular mechanism of high elasticity. Elastic entropic response of the polymer chain to applied deformation is controlled by its flexibility. Flexibility of macrochain is associated with the quasi-independent mobility of specific fragments of a given macrochain which are called segments. Hence, rubbery state and high elasticity are expected to be observed for polymer chains with the length much higher as compared with the length of segment.

From this standpoint, the lengths of the chains with molar masses M_1, M_2, and M_3 (Fig. 6A) seem to be shorter than segment length. For these short chains, flexibility is poor, and, as a result, rubbery state is not observed. When the length of polymer chain exceeds the segment length (macromolecules with molar masses M_4, M_5, and M_6), segmental mobility comes to a play, and resulting well-pronounced flexibility is responsible for the appearance of rubbery state and high elasticity.

With increasing temperature, transition from one state to another state is controlled by the thermal activation of mobility of the specified kinetic units which compose this physical body. For low-molar-mass substances (Fig. 5A) and polymer homologues with low molar masses (Fig. 6A, curves $M_1 – M_3$), at $T_g = T_f$, the samples exhibit transition from solid (glassy) state to liquid (viscous flow) state because of the thermal activation of translation mobility of their basic kinetic unit – molecule as a whole. The resulting mutual displacements and slippage of the above kinetic units control the appearance of well-pronounced fluidity under applied loading or by gravity. For polymer chains with sufficiently high molar mass and length (Fig. 6A, curves $M_4 – M_5$), a new kinetic unit, that is, segment appears.

Macromolecular substances are characterized by two basic kinetic units – segment and macromolecule as a whole.

Thermal activation of segmental mobility takes place at T_g, and transition from glassy state to rubbery state is observed at this temperature. For amorphous polymers in the rubbery state, well-pronounced segmental mobility controls their specific physicomechanical properties, primarily, high elastic deformation. Hence, for a given polymer, the value of T_g is controlled by the segment characteristics such as the length, activation parameters, *etc*. which are associated, primarily, with the molecular chemical structure. The influence of the chemical structure on T_g will be discussed below. Here, let us note that, at the first approximation, the segment length and activation parameters of segmental mobility do not depend on the polymer molar mass. This is a reason that, for polymers with sufficient chain length, T_g approaches the constant value and do not change with increasing molar mass (Fig. 6B).

At $T = T_f$, mobility of the macromolecules is thermally activated. The slippage of these kinetic units becomes allowed, and transition from rubbery state to viscous flow state is observed. With increasing molar mass of polymer homologues, flow temperature grows (Fig. 6B). Increasing molar masses of macromolecules restricts their mobility. As a result, for polymers with higher molar masses, to activate their mobility the higher thermal energy is required, and transition to viscous flow state is observed at higher temperatures.

Hence, with increasing molar mass, the separation of T_g and T_f and appearance of rubbery state is associated with the appearance of the new kinetic unit – segment. When molar mass increases, permanent growth of T_f at the constant T_g is responsible for the widening of the temperature interval of rubbery high elastic state. The relationship between these two temperatures and molar mass was given by Kargin and Sogolova with the following empirical expression:

$$\lg n = \lg n_s + \frac{B(T_f - T_g)}{C + (T_f - T_g)},$$

where n and n_s are degrees of polymerization of macromolecule and segment, respectively, and B and C are constants for a given polymer.

Note that all above three states (glassy, rubbery, and viscous flow) are observed only for linear flexible amorphous polymers. Increase in stiffness of polymer chain and resulting growth of segment length are responsible for the degeneration of rubbery state when the length of segment becomes comparable to the length of macromolecule. As a result, these polymers tend to go from glassy state to viscous flow state. The following increase in stiffness controls the fact that these polymers exist only in glassy state because, for them, the flow temperature becomes higher that the temperature of thermal decomposition.

Rare cross-linking of polymer chains results in the restriction of molecular mobility and degeneration of viscous flow state. With increasing density of cross-links restriction of segmental mobility controls degeneration of rubbery state, and these polymers exist only in glassy state.

Note that amorphous polymer in glassy and rubbery states are characterized by quite different mechanical properties and used for the production of different polymeric materials. Amorphous polymers with low T_g (generally, below 0^oC) serve for production of rubbers or elastomers. Amorphous polymers with T_g more than 60 - 80^oC are used for production of plastics.

Glass transition temperature is the upper operating temperature for plastics and lower operating temperature for rubbers.

Hence, for solid amorphous polymers,

T_g is a most important physicomechanical parameter, and control for T_g is of prime importance.

In this section, to provide scientific background for the following structural design of elastomers and plastics, we will discuss

- the structural origin of physicomechanical behavior of amorphous polymers in rubbery and glassy states;
- the nature of glass transition to understand the effect of different factors on T_g, for the following physicochemical control for this physicomechanical operating parameter.

3.1. Structure of Amorphous Polymers

As discussed in Ch.1, with decreasing temperature, a variety of low-molar-mass liquids solidify at T_g with formation of amorphous glasses. For polymers, this behavior is much more complicated because, under cooling, polymer melt transforms in rubber at T_f and in glass at T_g (Fig. 5B). For both low-molar-mass substances and polymers, the above transitions are not accompanied by the structural transformation associated with the crystallization and appearance of three-dimensional long-range order. These transitions are only controlled by the freezing of the mobility of the specified kinetic units (for polymers, macromolecular coils at T_f and segments at T_g) with no changes of structure and phase state.

Rubbers and both low-molar-mass and polymer glasses may be considered as super-cooled (or frozen) liquids.

From the standpoint of the ordering of the structural units, liquids are characterized by the short-range order when, in the vicinity of any molecule, a certain ordering of the neighboring molecules is observed because of their intermolecular interaction. These local micro-regions of ordering are characterized by the increased density as compared with that for non-ordered regions, and, as a result, in liquids, distribution of density is not homogeneous. In low-molar-mass liquids, these ordered micro-regions are characterized by the extremely short lifetime ($10^{-8} \div 10^{-10}$ s) and well-pronounced dynamics: they are dissolved because of molecular thermal mobility and re-appear continuously. From these standpoint, they are usually identified as *density fluctuations*. However, despite of the fluctuation nature, these molecular aggregates may be considered as supramolecular structural units of liquids.

In contrary to thermodynamically stable crystals with long-range order, these density fluctuations are stable kinetically. The kinetic stability is characterized by the lifetime τ which depends on the ambient conditions, primarily, temperature and external excitation by, for example, mechanical loading. With increasing temperature and mechanical stress τ decreases and *vice versa*. Decreasing temperature below T_g is responsible for increasing stability of density fluctuations, and, as a result, glass is expected to be characterized by the high stability of fluctuation supramolecular structural units. In general, the kinetic stability of fluctuation structural units is controlled by the ratio between loading or observation time t and τ. These fluctuations are considered as stable units when $t < \tau$.

Another approach to describe dynamic fluctuation structure is associated with the nature of the thermal mobility of molecules. Note that, in thermodynamically stable crystalline structure, the particles vibrates near equilibrium positions. In liquids, both vibration of the molecules near equilibrium positions and translation of the molecules from one position to another position are allowed. Kinetics of the above thermal motion is characterized by the *"settled" life time* which may be identified as a time when the molecule vibrates near equilibrium position with no translational transition to the other position.

Let us try to apply the above general speculations concerning the dynamic nature of the fluctuation structural units of low-molar-mass amorphous bodies to amorphous polymers composed of macrochains.

According to Flory[1], in amorphous polymers, macromolecules exist in the conformation of *macromolecular coil* with unperturbed dimension.

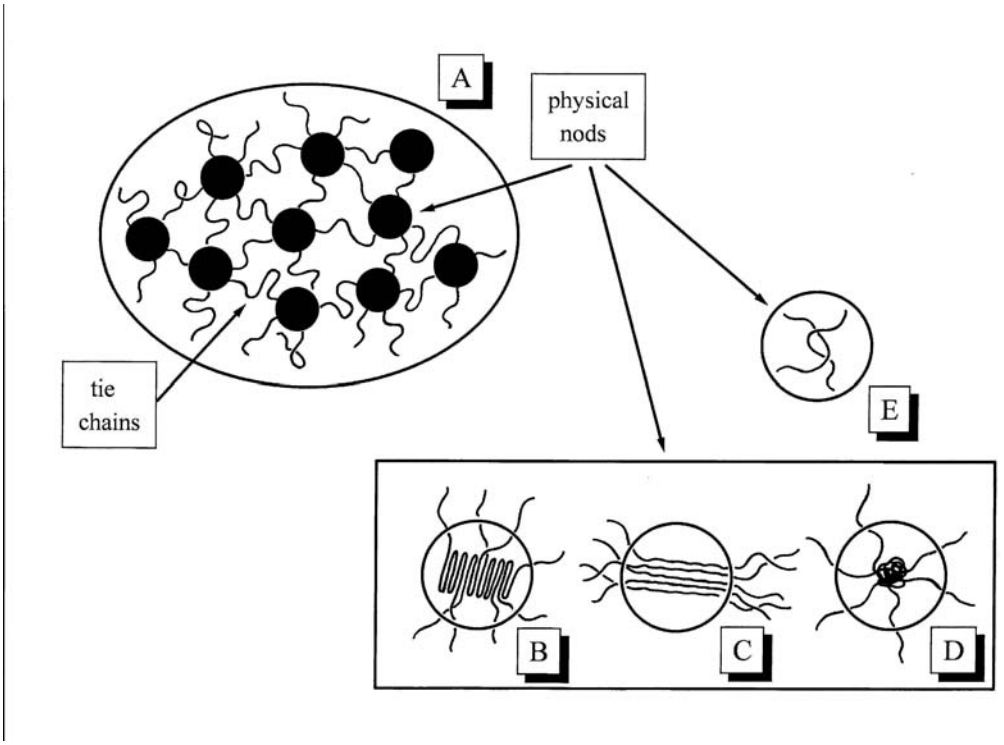

Figure 7. Schematic representation of the structure of linear amorphous polymer (A) and fine structure of physical nods as fluctuation nods with folded chains (B), extended chains (C), chains with globular conformation (D), and physical entanglement (E).

In macromolecular coil, the volume of polymer chain is not more that 1 – 3 % of the effective volume of the coil. In condensed state, the empty space inside macromolecular coils is occupied by the fragments of the neighboring macromolecular coils, and, from this standpoint, the structure of amorphous polymer may be considered as interpenetrating macromolecular coils. However, as in the low-molar-mass liquids, intermolecular interaction is responsible for the aggregation of the segments of the macromolecules with the formation of domains of order. In other words, amorphous polymers (melts, rubbers, and glasses) are characterized by the existence of the micro-regions with a certain amount of molecular order. Hence, supramolecular (or, to be more correct, suprasegmental) structure of amorphous polymer is characterized by the existence of physical nods, that is, aggregation of segments via intermolecular interaction. This nodular structure is shown in Fig. 7A. As compared with the supramolecular structure of low-molar-mass liquids, in polymers, all these nods which can be also considered as density fluctuations are interconnected with each others by *tie-chains* because a certain macromolecule takes part in the formation of several nods. This particular type of supermolecular structural organization is called *physical fluctuation network*. According to the semi-quantitative estimation concerning the characteristics of the fluctuation network for non-polar elastomer at ambient temperature, the time of "settled life" of segment within tie-chain is approximately $10^{-6} \div 10^{-4}$ s. For segment within physical nod, this time is $10 \div 10^{4}$ s.

[1] Paul J. Flory (1910-1985) – American chemist. A pioneer in the field of Polymer Science. Nobel Prize in Chemistry (1974).

As for the fine structure of physical nods, the following types may be considered: physical nod with folded chains (Fig. 7.B), extended chains (Fig. 7C), and chains in globular conformation (Fig. 7D).

Together with the above fluctuation nods, another type of the nods of physical network is associated with entanglement of the neighboring macromolecules (Fig. 7E).

Note that the above speculations concerning the structure of amorphous polymers are mainly hypothetical but sufficient to understand and explain the general features of their physicomechanical behavior.

3.2. Rubbers

Rubbers (alternative name, *elastomers*) are referred to as amorphous polymers for which glass transition temperature is lower and flow temperature is higher than operating temperature.

In rubbery state, amorphous polymers exhibit the ability to be deformed at very low stress up to enormous (hundreds percents) strain. In general, these large deformations are reversible (elastic) and, under unloading, the polymer sample regains its initial shape and size.

These large reversible deformations are called *high-elastic* deformations, and the phenomenon is called *high-elasticity*.

High-elasticity is a unique property of polymers and is not observed for low-molar-mass substances.

Elasticity of individual macromolecule is associated with the thermally activated segmental mobility.

The origin of high-elasticity is attributed to the chain chemical structure of polymers.

Actually, rubbers under operating conditions exhibit more complicated viscoelastic mechanical response to applied loading. To gain a deeper insight into physicomechanical behavior of rubbers, let us discuss the problem as follows.

3.2.1. High-Elasticity

At the first approximation, elasticity may be defined as an ability of deformed physical body to recover the original shape and size under unloading, that is, removal of external forces.

Two typical types of low-molar-mass elastic bodies: crystalline solids and gases.

In crystalline lattice, the distances between atoms, ions, or molecules are controlled by the compensation of attractive and repulsive forces. Under applied external force, deformation of crystal is accompanied by the disturbance of equilibrium distances between the above structural units and energy of their interactions. Under unloading, atoms, ions, or molecules tend to return to their initial equilibrium position providing the macroscopic recovery of deformed crystalline body.

For crystalline body, both deformation and elastic recovery are controlled by the energy of interaction between structural units, and, as a result, crystal elasticity demonstrates well-pronounced energetic nature.

Note that the high energy of interaction between atoms, ions, or molecules is responsible for the high resistance of crystalline body to applied loading and high elastic modulus. This behavior is formalized by the Hooke's law (see Eq. (1)), and the elasticity of crystalline bodies is identify as Hookean elasticity.

For gases, under compression in closed volume, deformation, that is, decrease in volume is accompanied by the increasing gas pressure. Under unloading, both volume and pressure tend to their initial equilibrium value, and macroscopic recovery of deformed gas is observed. From this standpoint, gas behaves itself as typical elastic body.

The origin of gas elasticity is associated with the temperature activated mobility of molecules. Hence, gas elasticity is of molecular kinetic nature.

The difference between the nature of Hookean elasticity and gas elasticity may be clearly demonstrated by the effect of temperature on the elastic response. For crystalline solids, increasing temperature results in the increasing intensity of vibration of atoms, ions, or molecules near equilibrium positions. As a result, the energy of interaction between these structural units decreases, and elastic response to the applied loading decreases. Hence, for crystals, increasing temperature leads to decreasing elastic modulus. For gases, increasing temperature is accompanied by the increasing intensity of thermal mobility of molecules. As a result, both pressure and elastic response to applied loading increase.

The above differences control the different thermal effects which accompany elastic deformation and elastic recovery of crystalline solids and gases. For crystals, elastic deformation is characterized by the endo-thermal effect, and, during deformation, cooling of the sample is observed. Elastic recovery proceeds with the heating of the sample because of the exo-thermal effect. For gases, the situation is opposite. Elastic deformation is accompanied by the exo-effect while, during elastic recovery, gas is cooled because of endo-effect.

To gain a deeper insight in the origin of elasticity, let us consider the phenomenon from the thermodynamic viewpoint.

For the case when the work is done over the system, the first law of thermodynamics predicts that the changes in inner energy of a system dU is a sum of the heat delivered to a system dQ and the work done over the system dA

$$dU = dQ + dA. \qquad (13)$$

The heat and work terms of this expression are represented as follows

$$dQ = TdS, \qquad (14)$$

$$dA = fdl - pdV, \qquad (15)$$

where dS is the change of entropy; and f is external force, dl is the change of linear dimension, p is pressure, and dV is the change of volume.

For isothermal elastic deformation of solid body, the term pdV in Eq. (15) is negligible as compared with the term fdl. For example, for elastomers, the term pdV is lower than the term fdl for $10^3 \div 10^4$ times. When the term pdV is ignored the Eq. (13) may be re-written as follows

$$fdl = dU - TdS. \qquad (16)$$

Differentiation of the above expression gives

$$f = \left(\frac{\partial U}{\partial l}\right)_{T,V} - T\left(\frac{\partial S}{\partial l}\right)_{T,V} \qquad (17)$$

or

$$f = f_U + f_S, \qquad (18)$$

where $f_u = \left(\frac{\partial U}{\partial l}\right)_{T,V}$ and $f_S = -T\left(\frac{\partial S}{\partial l}\right)_{T,V}$.

For isothermal compression of the gas, the work which is done over the system (Eq. (15)) is written as $dA = - pdV$, and applied pressure

$$p = \left(\frac{\partial U}{\partial V}\right)_T - T\left(\frac{\partial S}{\partial V}\right)_T \qquad (19)$$

may be also divided into two components as follows

$$p = p_U + p_S, \qquad (20)$$

where $p_u = \left(\frac{\partial U}{\partial V}\right)_T$ and $p_S = \left(\frac{\partial S}{\partial V}\right)_T$.

For elastic loading, the above thermodynamic analysis predicts the existence of two types of parameters: elastic force or pressure which are associated with the change of inner energy (f_U or p_U) and elastic force or pressure which are associated with the change of entropy (f_S or p_S).

Note that, for elastic deformation of ideal crystal, elastic response is controlled by the energy of interaction between atoms, ions, or molecules without noticeable changes of their mutual rearrangements. In connection with this, $f_S \to 0$ (Eq. (18)), and ideal Hookean elasticity is only associated with the changes of inner energy of a system. In contrary, for compression of ideal gas, disturbance of intermolecular interaction is negligible ($p_U \to 0$, Eq. (20)), and elastic response is associated with the kinetics of thermal motion of molecules, their mutual rearrangements, and, from this standpoint, elasticity of a gas is controlled by the changes of entropy. On the basis of this thermodynamic analysis, let us discuss the nature of high-elasticity.

For isolated ideal macrochain with no physical interactions between its fragments, elastic response is controlled by the thermal motion of segments or, in other words, their mutual rearrangements. For this system, similar to ideal gas and contrary to ideal crystal, elastic deformation and recovery are not accompanied by the changes of inner energy, and $f_U \to 0$.

The elasticity of isolated ideal polymer chain is associated with the changes of entropy as for elastic behavior of gases.

To clarify the molecular mechanism of the elastic behavior of macrochain, let us apply to this system the Boltzmann relation

$$S = k \ln \Omega \qquad (21)$$

where k is Boltzmann constant, and Ω is the thermodynamic probability, that is, the number of allowed conformations of macromolecular chain which may be adopted as a result of segmental motion.

From this standpoint, for individual macromolecule, Boltzmann relation allows us to link macroscopic thermodynamic property - entropy - to microscopic structural behavior of polymer chain related to the segmental rearrangements, that is, to solve the principal problem of "Structural Physicomechanics". Let us discuss this problem in more details.

Under equilibrium conditions, isolated flexible macromolecule adopts the macro-conformation of macromolecular coil with the average size which may be estimated as mean-square end-to-end distance $\sqrt{h_0^2}$. However, this macromolecular coil can take a lot of conformations with the dimensions more and less than $\sqrt{h_0^2}$.

To describe the behavior of isolated macrochain, the problem is to find the distribution of mean-square end-to-end distance through the thermodynamic probability and entropy.

For this particular purpose, let us represent the polymer chain composed of *n* repeated units with the length *l* as the chain which consists of *N* segments with the length *Z*. In this case, the behavior of the chain with the specified valence angle and angle of restricted inner rotation may be discussed in the framework of the model of free-jointed chain with the mean-square end-to-end distance $\sqrt{h^2} = \sqrt{N}Z$.

For this system, each conformation with the specified $\sqrt{h^2}$ corresponds to the probability Ω via Gaussian distribution as follows

$$\Omega = \frac{b^3}{\pi^{3/2}} e^{-b^2 h^2}, \tag{22}$$

where *b* is constant. For free-jointed chain, $b^2 = \frac{3}{2}\frac{1}{NZ^2}$.

For this case, Fig. 8 shows the typical Gaussian distribution. As seen, with the increasing end-to-end distance the probability of the corresponding conformations goes through the maximum. In other words, for the conformations of dense macromolecular coil ($h \to 0$) as well as for the conformations of the completely extended polymer chain ($h \to L$ where L is the contour length) the probability is extremely low. The maximum at the above distribution corresponds to the most probable dimension of macromolecular coil

$$h_0 = \frac{1}{b} = \left(\frac{2N}{3}\right)^{1/2} Z. \tag{23}$$

Combining Eqs. (21) and (22), for entropy of isolated polymer chain, we obtain

$$S = c - kb^2 h^2, \tag{24}$$

where *c* is constant.

Deformation of macromolecular coil with external applied force *f* is associated with the changes of end-to-end distance. Under drawing, this value increases, and compression of macromolecular coil is accompanied by its decreasing. Taking into account Eq. (17),

$$f = -T\left(\frac{\partial S}{\partial h}\right)_T = 2kTb^2 h. \tag{25}$$

Substitution of the most probable value of *h* (Eq. (23)) gives the following expression

$$f = \frac{2kT}{h_0}\frac{h}{h_0}. \tag{26}$$

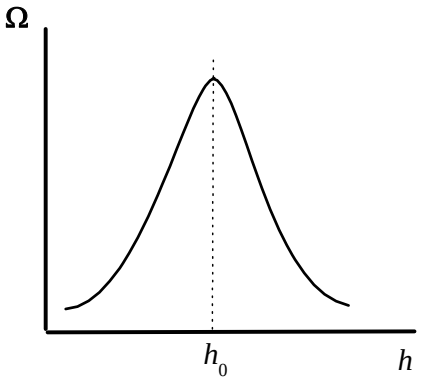

Figure 8. Typical Gaussian probability distribution of end-to-end distance.

For isolated macrochain, this expression predicts the linear correlation between the applied force f and strain h/h_0 with the coefficient $\frac{2kT}{h_0}$ similar to Hooke's law (Eq. (1)). From this formal standpoint, this coefficient may be considered as elastic modulus which with respect to the Eq. (23) is written as

$$E = \frac{\sqrt{2}\sqrt{3}k}{\sqrt{N}Z}T \qquad (27)$$

The above thermodynamic and statistical analysis allows the following speculations concerning the molecular mechanism of high-elasticity of macromolecular chain.

1. Deformation (drawing or compression) of isolated macromolecular coil is responsible for the disturbance of its equilibrium thermodynamic state and decreasing entropy. Under loading, this entropy loss is compensated by the applied external force;
2. Under unloading, when external force is released, deformed macromolecular coil tends to recover the initial thermodynamic equilibrium state with maximal entropy, and, as a result, recovery of size of macromolecular coil is observed. This thermodynamic behavior controls the reversibility of deformation;
3. The driving force of reversibility of deformation is the increasing entropy, and this entropic origin of elasticity is controlled by the chain chemical structure of macromolecule;
4. For macrochain, elastic modulus is reciprocal of the chain length N and proportional to temperature T. Hence, elastic modulus is expected to decrease with increasing the length of the chain (or its molar mass) and increase with increasing temperature.

In the framework of "Structural Physicomechanics", elastic behavior of ideal isolated macromolecule is controlled by its specific chain structural organization.

Can we apply the above speculations to description of high-elasticity of real rubbery substances? Obviously, in condensed rubbery body, macromolecules are not isolated. They interpenetrates, and, as a result, intermolecular physical interactions are well-pronounced. In other words, behavior of macromolecules in condensed body is expected to differ markedly from that for ideal macrochain with no energy interactions. Let us generalize the molecular mechanism of high-elasticity.

To solve this problem, at the first approximation, let us consider the structure of rubber as interpenetrated macromolecular coils (Ch. 3.1.) Obviously, in this case, segmental motion and thermal mobility of the chains are noticeably restricted as compared with the isolated ideal macromolecule. However, the surrounding of each segment of each macromolecule is expected to be, in general, the same. In connection with this, according to Flory, all possible conformations of a given macromolecular chain are adequate and occur with the same probability because they correspond to the same energy of interaction with the neighboring macrochains. As a result, in real rubbery substance, the properties of a given macromolecular coil (Gaussian distribution, correlation between the size of the coil and the length of the chain, *etc*.) are qualitatively the same as those for isolated macromolecular coil. These speculations

allow us to apply the above theoretical fundamentals concerning molecular mechanism of high-elasticity of isolated ideal macromolecule for the description of high-elastic properties of real rubbers.

To support the above idea, let us consider the following experimental evidence.

1. For high-elastic substances, theoretical speculations concerning the entropic origin of high-elasticity predicts the decreasing elastic modulus with increasing the length of the chain (see Eq. (27)) because $E \sim 1/N$. In other words, for rubbery polymers, elastic modulus is expected to be extremely small because of high molar mass. Note that the typical elastic modulus of real elastomers is lower for several orders of magnitude as compared with the low-molar-mass solids such as steel and quartz and comparable to that for gases.
2. Under heating, the uniaxially loaded sample of elastomer tends to shrink. This experimental behavior evidences the growth of elastic modulus of the elastomer with increasing temperature as predicted by the theoretical estimation (see Eq. (27)).
3. For real elastomer, the contributions from the entropic component f_S and energy component f_U to applied force f (see Eq. (18)) may be estimated form the experimental dependence force-strain obtained under the equilibrium conditions. For this case, Fig. 9 shows typical f - ε diagram. In the whole strain range, the changes of entropy control mainly elastomer deformation. In general, for elastomeric materials, change of inner energy is responsible for 5 ÷ 15 % of applied force.
4. Similar to gases and contrary to Hookean solids, under deformation, the sample of elastomer is heated, that is, deformation is characterized by the exo-effect. Recovery of the deformed elastomer results in the cooling of the sample because of endo-effect.

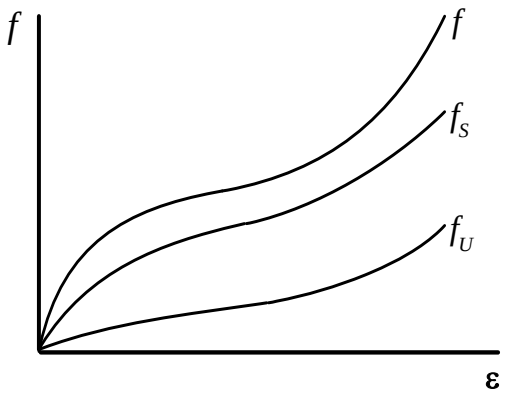

Figure 9. Typical force (f) - strain (ε) for elastomer and dependences of the entropic component f_S and energy component f_U on strain.

The above experimental evidence suggests the validity of the theoretical mechanism of high-elasticity of rubbers.

Similar to elasticity of gases, rubbery high-elasticity is mainly controlled by the changes of entropy associated with the conformational rearrangements because of well-pronounced segmental mobility.

3.2.2. Viscoelastic Behavior of Rubbers

To reveal the general features of the physical and mechanical behavior of rubbers, let us consider viscoelastic behavior of rubbers under *creep* and *stress relaxation* mechanical testing.

As mentioned in Ch. 2, under the ***creep*** testing, the sample is instantaneously subjected to stress σ at $t = 0$, and the stress is kept constant during experiment.

For linear rubber, typical time dependence of the resulting strain ε is shown in Fig. 10.At initial portion of the curve (up to point A) when the sample is subjected to the stress for time t_1, the linear increase in strain with time is observed. In general, this behavior may be associated with the Hookean deformation which is controlled by disturbance of physical, primarily, van der Waals interactions between neighbouring macromolecular coils or their fragments. Unloading of a sample after Hookean deformation results in immediate recovery of strain (curve 2).

With increasing deformation to point B because of increasing the loading time to t_2, time dependence of strain deviates from linearity. Unloading of a sample which was deformed within this region is also accompanied by complete strain recovery but, in this case, recovery do not proceed instantaneously and requires the finite period of time (curve 3).

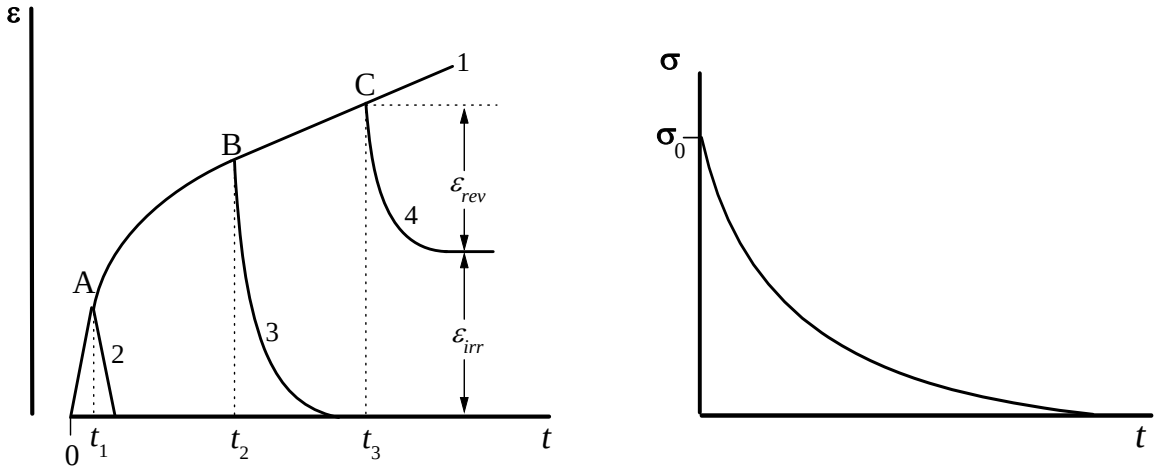

Figure 10. Typical time dependence of strain of linear rubber under creep conditions (1) and strain recovery curves after deformation for time t_1 (2), t_2 (3), and t_3 (4).

Figure 11. Stress relaxation in linear rubber.

With further increase in loading time, linear increase in strain with time takes place. Within this portion of deformation curve, for example, after deformation up to point C for time t_3, unloading does not lead to complete strain recovery (curve 4). In this case, strain involves reversible component ε_{rev} and irreversible component ε_{irr}, and may be represented as $\varepsilon = \varepsilon_{rev} + \varepsilon_{irr}$. Note that the following increasing loading time within this region results in the growth of contribution of irreversible component to total strain.

Under ***stress relaxation*** mechanical testing, the constant strain ε is immediately applied to a sample, and time dependence of resulting stress σ is studied.

For linear rubber, the resulting stress tends to zero in the finite period of time (Fig. 11).

Experimental results concerning creep (Fig. 10) and stress relaxation (Fig. 11) for linear rubbery amorphous polymer seem to be in good qualitative agreement with those obtained for combined model (Fig. 3) and Maxwell model (Fig. 1).

Real rubber demonstrates typical viscoelastic behavior which is characterized by

- the division of strain into reversible and irreversible components (i),
- time-dependent ratio between them (ii),
- and retarded origin of stress and strain relaxation (iii).

On the basis of above phenomenological description of linear viscoelasticity (Ch. 2), let us discuss the molecular mechanism of viscoelastic behavior of rubbery polymer in the framework of the model which considers the structure of linear rubbery polymer as interpenetrating macromolecular coils (Ch. 3.1).

For this structural model of amorphous polymer, one can recognize two basic types of kinetic units: segments and macromolecular coils. Viscoelastic behavior of rubbers is controlled by their mobility, that is, microscopic rearrangements or viscous flow. These microscopic rearrangements do not proceed instantaneously and require their own specified period of time which may be considered as relaxation time of segment and relaxation time of macromolecular coils. For simplicity, let us assume the single relaxation time of segments, τ_s, and single relaxation time of macromolecular coils, τ_{mc}. Obviously, relaxation time of segments is much less that that of macromolecular coils, and $\tau_s << \tau_{mc}$.

Under creep testing (Fig. 10), loading in the range not above point A proceeds within period of time which seems to be less that relaxation time of both segments and macromolecular coils ($t < \tau_s$ and τ_{mc}). As a result, both these kinetic units have no time to contribute to deformation, and mechanical response of rubber is controlled by only Hookean reversible deformation.

For the range of deformation to point B, loading time becomes higher than relaxation time of segments ($\tau_s < t < \tau_{mc}$). They have sufficient time for the mutual rearrangements and contribute to deformation. This range of loading is characterized by well-pronounced high elasticity. Under unloading, the strain recovers completely because of transition of excited macromolecular coils to initial equilibrium state via segmental mobility.

Transition to the range above point B is accompanied by the increasing loading time above relaxation time of macromolecular coils ($t > \tau_s$ and τ_{mc}). Their mutual rearrangements become noticeable, and we deal with well-pronounced flow because of slippage of macromolecular coils. Displacements of macromolecular coils relative to each other contributes to irreversible component of deformation which is stored in the sample after unloading. With increasing loading time the growth of irreversible component means that, in the range above point B, creep in rubbers is mainly controlled by viscous flow of macromolecular coils.

Specific feature of the viscoelastic behavior of rubbers may be attributed to the fact that the elastic reversible component of viscoelasticity is mainly associated with the high elastic deformation whereas the contribution of Hookean deformation is negligible. High elastic deformation and its recovery are controlled by segmental mobility within macromolecular coils. In rubbers, movements of segments are not free and proceed as a viscous flow of segments in viscous surrounding of neighbouring segments. This retardation of microscopic segmental mobility by the viscous surrounding results in time-dependent retarded high elastic response of rubbers to applied stress and its removal. This retarded character of the recovery of high elastic deformation is well seen in Fig. 10 (curve 3 and reversible portion of curve 4). As mentioned above, this behavior is referred to as *delayed elasticity*.

Under stress relaxation testing (Fig. 11), deformed polymer sample relaxes with the minimization of stress via the microscopic displacements of the same kinetic units - segments and macromolecular coils. At the initial portion of the stress relaxation curve, relaxation is mainly controlled by the segmental mobility. With increasing time mobility of macromolecular coils comes to a play providing the complete unloading of the deformed sample.

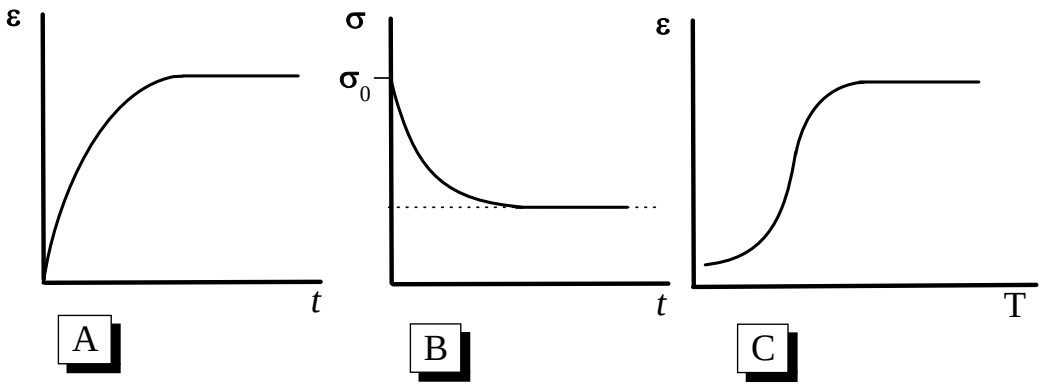

Figure 12. Time dependence of strain under creep conditions (A), stress relaxation (B), and thermomechanical curve (C) for cross-linked rubber.

Viscoelastic consideration of linear rubber deformation provides the fundamentals for design of modern rubbery-based polymeric materials which are usually identified as elastomers. The desired operating property of elastomers is their high elasticity. Appearance and storing of irreversible viscous component under operating conditions means the loss of stability of operating parameters of material. To prevent the development of viscous irreversible component of deformation, *vulcanization* of rubbers with appropriate chemical agents is carried out. Resulting cross-linking of macromolecular coils leads to the formation of *chemical network*. This structural modification of rubber prevents the displacements of macromolecular coils, and these kinetic units do not take part in deformation and relaxation. The fractions of chains between cross-links retain their ability to high elastic deformation via segmental mobility. As a result, under creep conditions, cross-linked rubbers exhibit only high elastic deformation (Fig. 12A). Their stress relaxation (Fig. 12B) proceeds only to equilibrium value σ_∞ in contrary to linear rubber (Fig. 11) for which stress relaxes down to zero. Thermomechanical behavior (Fig. 12C) suggests that, for cross-linked rubbers, viscous flow state is not observed, and they exist in high elastic rubbery state in the temperature range from T_g to temperature of thermal decomposition, T_{dec}.

Up to now, we discussed mechanical behavior of rubbers assuming the single relaxation time of segments and the single relaxation time of macromolecular coils. Actually, each segment as well as macromolecular coil are characterized by different surroundings, and, as a result, each segment and macromolecular coil are characterized by their own relaxation time. Hence, it is more correct to consider a *spectrum of relaxation times* of segments and spectrum of relaxation times of macromolecular coils. To simulate this situation, one can design *n* combined models (Fig. 3) in parallel. In this case, each combined model should include elastic units with different elastic modulus and viscous units with different viscosity.

3.2.3. Stress-Strain Behavior of Elastomers

In the previous Section, cross-linking was shown to prevent irreversible flow deformation of rubber. Cross-linked rubber, elastomer, demonstrate high elastic reversible deformation in the wide range (to thousand percents) of strain. In this section, stress-strain behavior of elastomers is analyzed when the sample is deformed with the constant strain rate $d\varepsilon / dt$.

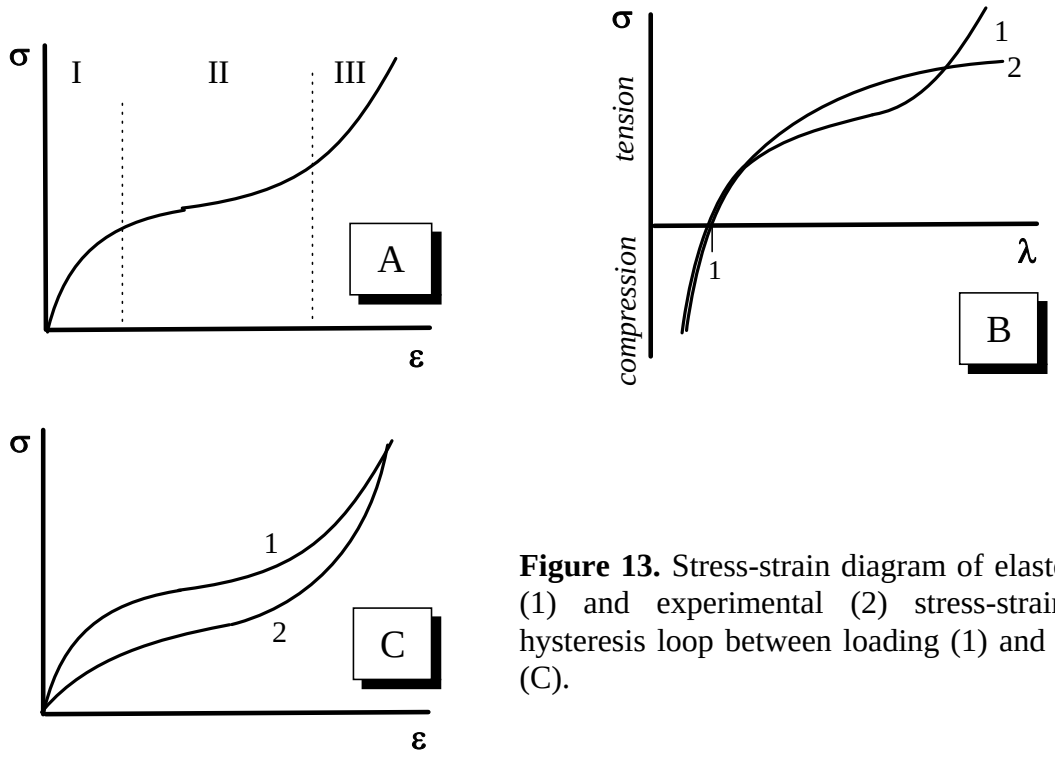

Figure 13. Stress-strain diagram of elastomer (A), theoretical (1) and experimental (2) stress-strain curves (B), and hysteresis loop between loading (1) and unloading (2) curves (C).

For elastomer sample, a typical resulting stress-strain relationship (*stress-strain diagram*) corresponding to uniaxial extension is shown in Fig. 13A. This stress-strain diagram may be divided into three well-pronounced regions. To explain this mechanical behavior, let us invoke the following structural model of elastomer.

Earlier, in Ch. 3.1 the structure of amorphous polymer was described in terms of physical network (Fig. 7). Cross-linking of amorphous linear rubber is responsible for formation of three-dimensional chemical network.

The structure of elastomer may be represented as superposition of a chemical and physical networks.

For chemical network, the junction points are chemical cross-links. For physical network, the junction points are fluctuation physical nods and entanglements. Note that this supramolecular network structure is characterized by defects such as loops when the same polymer chain is chemically cross-links and free chain ends which do not contribute to network formation. At first, let us consider the role of fluctuation physical network in stress-strain behavior of elastomer.

The initial portion of stress-strain diagram (Fig. 13A, region I) corresponds to the deformation of the above physical network without disruption of the physical nods. In this range of deformation, viscoelastic response of the material may be described in terms of *linear viscoelasticity*.

Under transition from region I to region II (Fig. 13A), noticeable structural rearrangements controlled by the disruption of physical nods take place. As a result, mobility of segments in rubber sample is enhanced. Enhancement of the segmental mobility facilitate deformation, and, within region II, increment of the stress per unit of strain $\Delta\sigma / \Delta\varepsilon$ is lower than that within region I. Structural rearrangements are accompanied by the change in the activation energy of segmental mobility, and resulting mechanical behavior can not be referred to as linear viscoelastic response. In this case, we deal with *non-linear viscoelasticity* which can not be described by the mechanical models discussed in Ch. 2.

Further deformation and transition to region III (Fig. 13A) results in the *orientation* of segments along the axis of drawing. This structural rearrangement is accompanied by increasing strength characteristics of polymer. As a result, within region III, the growth in $\Delta\sigma / \Delta\varepsilon$ is observed.

To solve the principal problem of "Structural Physicomechanics" for elastomers, let us find correlation between their specific microscopic structure associated with the appearance of physical and chemical network and resulting macroscopic physicomechanical parameters. Earlier, this correlation was found for linear rubbers (for example, Eqs. (24), (26), and (27)) when their high-elasticity was discussed in the framework of approach concerning the thermodynamics and statistics of ideal isolated polymer chain (Ch. 3.2.1).

To apply this approach to polymer network, let us assume that

- both in unstrained and deformed elastomer, the junction points which, in general, can be either chemical (cross-links) and physical (entanglements) in nature are fixed at their mean positions;
- the fragments of polymer chains between junction points composed of n repeated units with the length l are represented as the chain which consists of N segments with the length Z to describe the above chain fragments as free-jointed chain;
- when the elastomer is deformed the microscopic displacement of each chain is proportional to the corresponding increment in macroscopic dimension of the sample.

To consider large high-elastic deformation of elastomers, it is more convenient to operate with extension ratio λ than with strain ε.

Extension ratio λ is the ratio between the length of deformed sample and initial length of the sample.

For three-dimensional deformation, the axes of the extension ratios are chosen to coincide with the rectangular coordinate system. These speculations and above assumptions allow us to correlate the microscopic deformation of the sample and microscopic displacements of the chain fragments between cross-links or, for more convenience, microscopic displacements of the junction points.

Let us fix one junction point at a certain position. If, in the unstrained state, the coordinates of the other junction point is (x_0, y_0, z_0), after three-dimensional deformation, this junction point is displaced to the position with coordinates (x_{def}, y_{def}, z_{def}), and

$$\lambda_x = \frac{x_{def}}{x_o}; \lambda_y = \frac{y_{def}}{y_o}; \lambda_z = \frac{z_{def}}{z_o}. \quad (28)$$

Taking into account that $h^2 = (x^2 + y^2 + z^2)$, for entropy of the individual chain fragment between cross-links, Eq. (24) may be re-written as

$$S_0 = c - kb^2(x_0^2 + y_0^2 + z_0^2) \quad \text{(initial state)}$$

$$S_{def} = c - kb^2(\lambda_x^2 x_0^2 + \lambda_y^2 y_0^2 + \lambda_z^2 z_0^2) \quad \text{(deformed state)}$$

As a result of deformation, the corresponding change of entropy of individual chain fragment between cross-links is

$$\Delta S_i = S_{def} - S_0 = -kb^2\left[(\lambda_x^2 - 1)x_0^2 + (\lambda_y^2 - 1)y_0^2 + (\lambda_z^2 - 1)z_0^2\right]. \quad (29)$$

If the number of these chain fragments per volume unit of polymer sample is N, the number of the chains which have their ends initially in the vicinity ($dx \times dy \times dz$) of the point (x, y, z) is defined as dN and can be estimated from the Gaussian distribution function as

$$dN = N\left(\frac{b}{\sqrt{\pi}}\right)^3 \exp\left[-b^2(x^2 + y^2 + z^2)\right]dxdydz. \quad (30)$$

As a result of deformation, the total change of entropy is

$$\Delta S = \int \Delta S_i dN,$$

and, after integration,

$$\Delta S = \frac{1}{2} Nk\left(\lambda_x^2 + \lambda_y^2 + \lambda_z^2 - 3\right). \quad (31)$$

Hence, this equation correlates the change of entropy caused by deformation to the specified extension ratios and the number of the chain fragments between cross-links per unit volume. Taking into account that, in ideal case, deformation of rubber is accompanied by no change of inner energy and proceeds at constant volume (Ch. 3.2.1) and, as a result of deformation, $\Delta S < 0$, for isothermal deformation, the work of deformation per unit volume $A = -T\Delta S$ (Eqs. (13) and (14)). With respect to Eq. (31),

$$A = \frac{1}{2} NkT\left(\lambda_x^2 + \lambda_y^2 + \lambda_z^2 - 3\right), \quad (32)$$

where $NkT = G$ relates the work of deformation and applied strain and, from the formal standpoint, may be considered as the modulus of elastomer. Note that this mechanical parameter is proportional to temperature and the number of the chain fragments between cross-links per

unit volume N. Hence, for elastomers, the temperature dependence of modulus similar to that obtained for isolated macrochain (Eq. (27)). Parameter N may be expressed through the density of polymer ρ as follows

$$N = \frac{\rho N_A}{M_c} = \frac{\rho R}{M_c k},$$

and Eq. (32) may be rewritten as

$$A = \frac{\rho RT}{2M_c}\left(\lambda_x^2 + \lambda_y^2 + \lambda_z^2 - 3\right), \tag{33}$$

where N_A is Avogadro number and M_c is the number average molar mass of the chains between cross-links.

As a result,

$$G = \frac{\rho RT}{M_c}. \tag{34}$$

Hence, with increasing cross-link density, that is, decreasing the chain length between junction points M_c and resulting increase in N, modulus G is predicted to increase.

The general relationship between the work of deformation and extension ratios (Eq. (33)) allows one to predict stress-strain behavior of elastomer under the specified regime of loading. With respect to the fact that elastomers tend to deform at constant volume the product of the extension ratios is unity, that is, $\lambda_x\lambda_y\lambda_z = 1$.

For uniaxial tension or compression along the x axis, let us denote λ_x as λ. In this case, $\lambda_y = \lambda_z = 1/\lambda^{1/2}$, and Eq. (33) can be rewritten as

$$A = \frac{1}{2}G\left(\lambda^2 + \frac{2}{\lambda} - 3\right). \tag{34}$$

When the elastomer sample with initial cross-sectional area S_0 and length l_0 is uniaxially deformed by force f for dl, the work of deformation per unit volume is

$$dA = \frac{fdl}{S_0 l_0} = \sigma d(\lambda - 1) \approx \sigma d\lambda$$

and

$$\sigma = \frac{dA}{d\lambda} = G\left(\lambda - \frac{1}{\lambda^2}\right). \tag{35}$$

Note that, in this case, stress σ is the force f normalized to initial cross-sectional area of the sample. During deformation, cross-sectional area decreases, and, for true stress σ_{tr} normalized to the current cross-sectional area, the corresponding equation is

$$\sigma_{tr} = G\left(\lambda^2 - \frac{1}{\lambda}\right). \tag{36}$$

To estimate the validity of the above theoretical speculations, let us compare stress-strain behavior predicted by the Eq. (35) (Fig. 13B, curve 2) and experimental stress-strain curve (Fig. 13B, curve 1).

For ***uniaxial compression***, the theoretical curve agrees well with experimental stress-strain diagram for vulcanized rubber.

In the case of ***uniaxial extension***, the agreement between theoretical and experimental curves is observed at rather low elongations when $\lambda < 1.5$.

At $1.5 < \lambda < 5$, the theoretical stress is higher than experimental value. When λ becomes more than 5, theoretical and experimental curves drastically deviate. Hence, the above theory concerning mechanical behavior of polymer networks predicts experimental results at $0.4 < \lambda < 1.5$.

At high strains, the lack of agreement between theoretical and experimental curves may be attributed to the following factors. At first, the loops and free ends of the chains do not contribute to elastic deformation. As a result, experimental mechanical behavior and behavior predicted by theory based on the consideration of ideal network deviate. Secondly, at high strains, Gaussian model does not reflect correctly the behavior of polymer coil. With increasing extension, end-to-end distances of polymer chains can not be described by Gaussian distribution, and more sophisticated distribution functions should be invoked. Third, at these strains, well-pronounced orientation of polymer molecules along the axis of drawing is responsible for the noticeable change in the mechanism of mechanical response of polymer body to applied loading (see Ch. 5). In the framework of the above model concerning rubber deformation, when the end-to-end distance of a coil becomes comparable to one-half of the contour length, the elastic force is larger than that predicted by Eq. (26). Fourth, structural changes associated, primarily, with crystallization in the material induced by the orientation (see Ch. 4.2.2) complicate mainly mechanical behavior of elastomer.

To describe ***stress-strain behavior of elastomers at moderate elongations***, several empirical approaches were proposed. For example, according to Mooney,

$$\sigma = 2C_1\left(\lambda - \frac{1}{\lambda^2}\right) + 2C_2\left(1 - \frac{1}{\lambda^3}\right) \tag{37}$$

or

$$\frac{\sigma}{2\left(\lambda - \frac{1}{\lambda^2}\right)} = C_1 + C_2\frac{1}{\lambda}, \tag{38}$$

where C_1 and C_2 are constants.

Comparison of Eqs. (37) and (35) gives $C_1 = G$ when constant C_2 characterizes the deviation of experimental and theoretical behavior. Equation (38) indicates the linear dependence between $\frac{\sigma}{2\left(\lambda - \frac{1}{\lambda^2}\right)}$ and $\frac{1}{\lambda}$. Extrapolation of this experimental dependence allows one to estimate C_1 and, hence, network parameters such as N and M_c (Eqs. (32) and (34)). The slope of this line gives C_2 and allows one to estimate the deviation of the mechanical behavior of a given polymer sample from that predicted by theory.

Hence, despite of the above assumptions and limitations, thermodynamic analysis and statistical theory allowed us to predict macroscopic stress-strain behavior of elastomer of the basis of consideration of its molecular chain structure and supramolecular three-dimensional network structure (i) and find correlation between macroscopic mechanical parameter (for example, elastic modulus) and parameters of microscopic structure (for example, the density of chain fragments between junction points N and their molar mass M_c) (ii).

Another important aspect of stress-strain behavior of elastomers which is not predicted by the above theory is associated with the appearance of *mechanical hysteresis* during cyclic loading-unloading regime of deformation. When deformed elastomer sample is unloaded with the same strain rate $d\varepsilon / dt$, relaxation of the polymer is accompanied by the complete high elastic recovery (Fig. 13C), and unloaded sample retains its initial shape and dimension. However, loading and unloading curves do not coincide, and mechanical hysteresis manifests itself as an area between loading and unloading curves. In general, the appearance of hysteresis loop is controlled by the relaxation nature of deformation - strain proceeds more slow than stress, that is, strain lags behind applied stress. In other words, hysteresis phenomenon is a macroscopic manifestation of microscopic relaxation processes which takes place during deformation. In details, hysteresis and its relationship with relaxation is discussed in forthcoming section.

3.3. Hysteresis Phenomena and Relaxation

To discuss the origin and molecular mechanism of hysteresis phenomena in amorphous polymers, let us consider cyclic deformation in the region of *linear viscoelasticity* (region I, Fig. 13A).

Cyclic deformation implies loading and unloading of the test sample with a given strain rate $d\varepsilon / dt$.

For elastomer, Figure 14 shows typical cyclic stress-strain diagram – loading (curve1) and unloading (curve 2). As mentioned above, the appearance of hysteresis loop between loading and unloading curves is controlled by the well-pronounced relaxation processes in polymer sample. In general, for elastomers, deformation proceeds via transition of segments from one position to another position as was discussed in Ch. 2 (Fig. 4). This segmental movements are restricted by the viscous resistance of surrounding, and, in other words, deformation is controlled by the viscous flow of segments. These elementary jumps of segments from one state to another state require the finite period of time, that is, relaxation time τ. The constant strain rate implies the constant loading time t, and, from the standpoint of Deborah number (Ch. 2), the mechanical response of elastomer is controlled by the ratio t/τ.

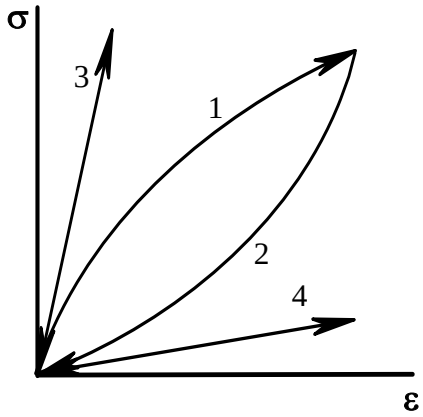

Figure 14. Typical stress-strain behavior of elastomer under cyclic loading-unloading deformation.

When $t << \tau$, that is, $d\varepsilon / dt$ is extremely high, segments have no enough time for mutual rearrangements, and typical Hookean elastic response takes place (Fig. 14, curve 3). In this case, loading and unloading curves coincide, and hysteresis is absent. In contrary, when $t >> \tau$, at each stage of loading, segments have enough time for mutual displacements. As a result, at each stage of deformation, polymer sample approaches equilibrium state, and equilibrium high elastic deformation takes place. This equilibrium deformation is also characterized by the coincidence of loading and unloading curves and the absence of hysteresis (Fig. 14, curve 4).

When $t \sim \tau$, segments have enough time to contribute to deformation, but their rearrangements and resulting macroscopic strain lags behind the applied stress. This factor provides non-equilibrium nature of deformation which manifests itself as hysteresis phenomenon (Fig. 14, curves 1 and 2).

Hysteresis is associated with the relaxation origin of deformation and is controlled by the degree of equilibrium observed during loading.

The above experimental evidence allows us to reveal the following aspects of high elastic deformation. As for the Hookean elastic deformation, high elastic deformation is completely reversible. The principal difference between them is associated with the fact that Hookean deformation is completely equilibrium process, and, at each stage of cyclic deformation, resulting strain is directly related to applied stress and *vice versa*. High elastic reversible deformation is non-equilibrium process, and, at each stage of cyclic loading, the strain corresponds to a pair of stress values. This mechanical behavior, that is, combination of

reversibility and hysteresis is called *anelasticity* in contrary pure elasticity which is characteristic of Hookean bodies.

In general, viscoelastic bodies combines elastic and anelastic strains. This situation is clearly demonstrated by the behavior of combined model (Fig. 3). Elastic spring of modulus E_1 models the Hookean elastic component of reversible portion of strain. Voigt-Kelvin unit which consists of the spring of modulus E_2 and viscous dashpot of viscosity η_2 controls anelastic component of reversible portion of strain. Note that, in the framework of this terminology, the proceeding and development of irreversible strain which is simulated by the dashpot of viscosity η_3 is called *inelasticity*.

To estimate hysteresis phenomenon quantitatively, let us consider the following procedure. The area under the loading curve (Fig. 14, curve 1) given by the $\int_0^{\varepsilon^*} \sigma^* d\varepsilon$ describes mechanical work of deformation normalized to the sample volume. It is easy to demonstrate as follows

$$\sigma d\varepsilon = \frac{F}{S}\frac{dl}{l_0} = \frac{Fdl}{V} = \frac{A}{V}$$

where F is applied force, S is cross-section area of a sample, dl is increment of linear dimension of a sample because of deformation, l_0 is initial length of a sample, V is a sample volume, and A is a work.

Similar to that, the area under unloading curve (Fig. 14, curve 2) given by $\int_{\varepsilon^*}^{0} \sigma^* d\varepsilon$ corresponds to the part of mechanical work of deformation which is reversibly recovered during unloading. The difference between these two areas

$$S = \int_0^{\varepsilon^*} \sigma^* d\varepsilon - \int_{\varepsilon^*}^{0} \sigma^* d\varepsilon$$

is the area of hysteresis loop, that is, the difference of the mechanical work of deformation and mechanical work which is reverted during cyclic loading. In other words, hysteresis area corresponds to a portion of mechanical work which is lost during loading-unloading test.

From the physical viewpoint, the loss of a certain fraction of mechanical work under cyclic loading is controlled by the viscous flow of segments which is responsible for deformation. This viscous flow is accompanied by the appearance of inner friction which controls the dissipation of mechanical work as a heat. Hence, the area of hysteresis loop is a quantitative measure of a portion of the mechanical work which is dissipated due to relaxation origin of high elastic deformation.

The above consideration of cyclic loading allows us to conclude that high elastic reversible deformation manifests its viscoelastic nature as the co-existence of viscous component which is lost during loading-unloading cycle and pure elastic component which completely recovers during unloading.

From the applied standpoint, prediction of the behavior of polymeric materials which are subjected to cyclic deformation is of prime importance. Actually, a variety of practical application involves periodical long-term loading. The prime example is the work of car tyres which, during car driving, are subjected to continuous cyclic loading.

To gain a deeper insight to the relaxation origin of polymer behavior as well as to predict physicomechanical behavior of polymeric materials, let us invoke the *dynamic mechanical testing*.

Dynamic mechanical analysis is based on the application to the sample sinusoidal stress or strain.

When sinusoidal strain

$$\varepsilon = \varepsilon_0 \sin \omega t$$

is applied to the ***ideal elastic body***, according to Hooke's law, the resulting stress is

$$\sigma = E\varepsilon = E\varepsilon_0 \sin \omega t = \sigma_0 \sin \omega t .$$

For Hookean elastic body, there is no phase lag between applied strain and resulting stress. In other words, ***ideal elastic body*** just immediately responses to applied deformation.

When sinusoidal stress

$$\sigma = \sigma_0 \sin \omega t$$

is applied to ***ideal viscous liquid***, resulting strain can be estimated through Newton's law

$$\sigma = \eta \frac{d\varepsilon}{dt} \Rightarrow \frac{d\varepsilon}{dt} = \frac{\sigma_0 \sin \omega t}{\eta} .$$

After intergration

$$\varepsilon = \varepsilon_0 \sin\left(\omega t - \frac{\pi}{2} \right)$$

where $\varepsilon_0 = \sigma_0 / (\eta\omega)$.

For ***Newtonian viscous liquid***, resulting strain lags behind applied stress for the phase angle equal to $\pi / 2$.

Mechanical behavior of linear viscoelastic bodies is controlled by co-existence of elastic and viscous modes of deformation.

For ***viscoelastic bodies***, the phase lag between applied and resulting parameters is expected to lay between zero and $\pi / 2$.

When sinusoidal strain

$$\varepsilon = \varepsilon_0 \sin \omega t$$

is applied to ***linear viscoelastic polymer***, resulting stress

$$\sigma = \sigma_0 \sin\left(\omega t - \delta \right)$$

lags behind it for phase angle δ (Fig. 15).

In *x-y* plot, sinusoidal change in strain can be pictorially represented as rotation of strain vector around zero point with a specified angular frequency ω (Fig. 16). In this case, the phase lag between applied strain and resulting stress is the angle δ between strain vector and stress vector. Stress vector can be divided to two components: σ' which is in phase with strain and σ'' which is $\pi / 2$ out of phase with strain. From this standpoint, resulting stress and elastic modulus can be represented as a sum of real and imaginary parts

$$\sigma^* = \sigma' + \sigma'' i \Rightarrow \frac{\sigma^*}{\varepsilon} = \frac{\sigma'}{\varepsilon} + \frac{\sigma''}{\varepsilon} i \Rightarrow E^* = E' + E'' i ,$$

where E^* is complex modulus, E' is storage modulus, and E'' is loss modulus.

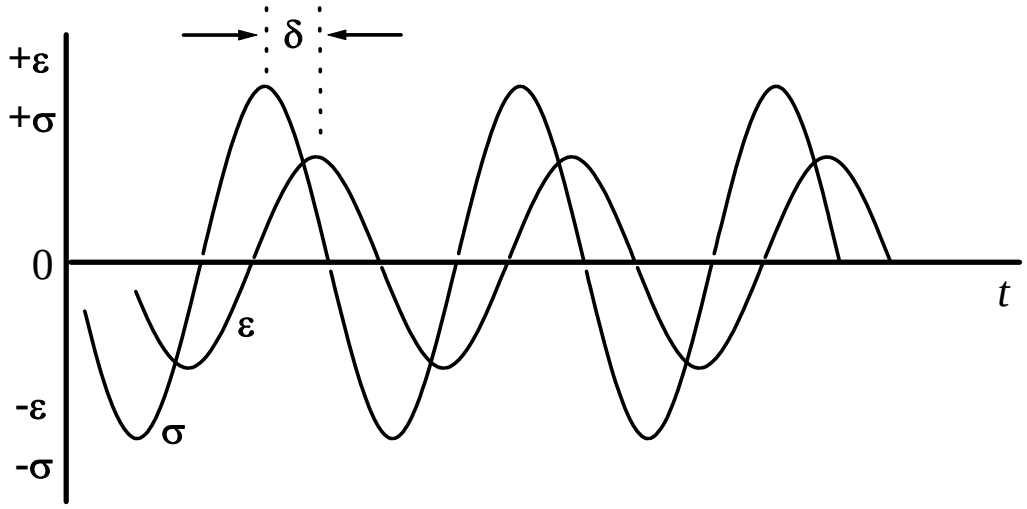

Figure 15. The variations of stress **σ** and strain **ε** with time for viscoelastic body under cyclic loading.

Storage modulus E' characterizes the fraction of mechanical work of deformation which is stored in deformed sample as elastic energy and is reverted during unloading. Loss modulus E'' characterizes the fraction of mechanical work which is dissipated in each cycle as a heat. The other important parameter of cyclic loading is $tg\delta = \sigma''/\sigma' = E''/E'$ which is called *loss tangent*.

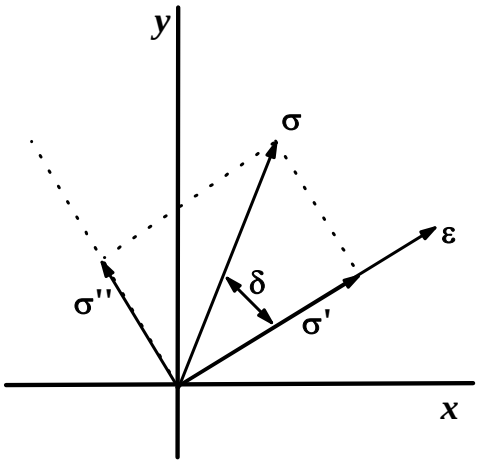

At constant test temperature, frequency dependences of both E' and $tg\delta$ are shown in Fig. 17. In the vicinity of specified frequency ω^*, the marked increase in storage modulus is observed while loss tangent goes through the maximum. In other words, within this frequency range, well-pronounced increase in rigidity of the sample is accompanied by maximal dissipation of mechanical work as a heat.

Figure 16. Representation of sinusoidal changes of applied strain **ε** and resulting stress **σ** in *x-y* plot.

As discussed earlier, linear viscoelastic behavior of rubbers is mainly associated with segmental mobility. Mobility of segments is controlled by their relaxation time which is temperature-dependent. At constant test temperature, relaxation time of segments seems to be constant during testing. Taking into account the fact that frequency of loading is reciprocal to loading time, we can conclude that, at frequencies much less than ω^* (Fig. 17), the corresponding loading times are much higher that relaxation time of segments. As a result, well-pronounced high elasticity is observed, and storage modulus is rather low. At $\omega >> \omega^*$, the corresponding loading times are much less that relaxation time of segments. Mechanical response of the sample to applied loading is controlled by Hookean elastic deformation, and storage modulus is high. At the transient frequency range when $\omega \sim \omega^*$, relaxation time of segments becomes comparable to the loading time. Under these conditions, a small increment in frequency results in noticeable increase in storage modulus, and well-pronounced "damping" effect is observed. The latter is associated with the high growth in the loss of mechanical work as a heat.

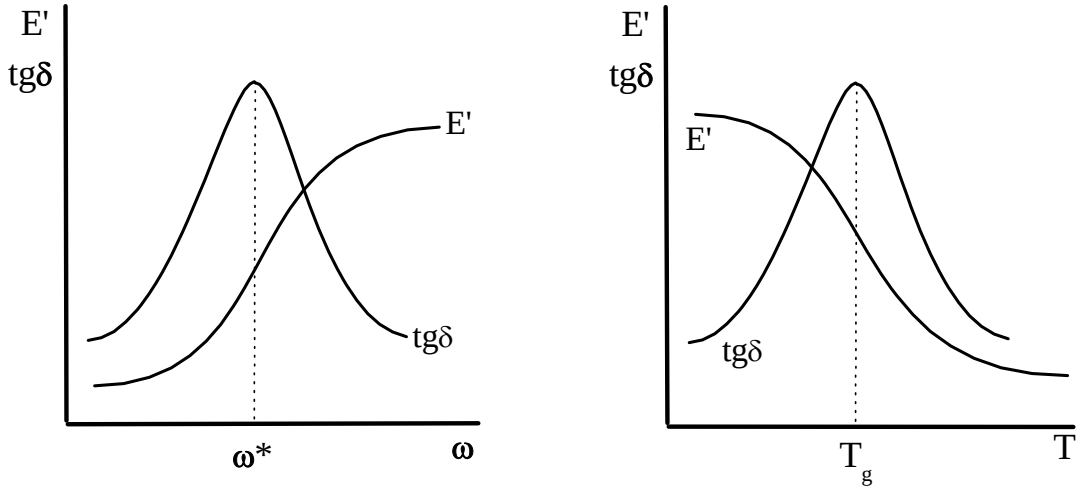

Figure 17. Frequency dependences of storage modulus *E*' and loss tangent tgδ for amorphous polymer.

Figure 18. Temperature dependences of storage modulus *E*' and loss tangent tgδ for amorphous polymer.

Hence, the value of hysteresis, that is, $tg\delta$ is characterized by the high sensitivity to proceeding of relaxation processes. Maximum in frequency dependence of $tg\delta$ suggests the occurrence of relaxation transition in polymer which is associated with the ratio between relaxation time and loading time. These microscopic processes control the dramatic changes of macroscopic parameters such as elastic modulus.

The similar behavior of amorphous polymer is observed when the sample is loaded with the constant frequency while the test temperature is changed (Fig. 18). Under these testing conditions, loading time is constant, and relaxation time of segments decreases with increasing temperature. Noticeable change in mechanical response of the body to applied loading takes place within a specified temperature range when loading time becomes comparable with relaxation times of segments. This temperature range is referred to as glass transition. Earlier, when we discussed thermomechanical behavior of amorphous polymers, glass transition was attributed to the occurrence of segmental mobility in polymer. Dynamic mechanical testing allows us to reveal the nature of glass transition in more details.

Glass transition is controlled by the ratio between loading time and relaxation time of segments, that is, this transition is of relaxation origin. The relaxation origin of glass transition can be easily demonstrated as follows. Figure 19 show temperature dependences of storage modulus and loss tangent which were obtained at different frequencies. Increasing frequency of loading results in the shift of T_g toward higher temperatures.

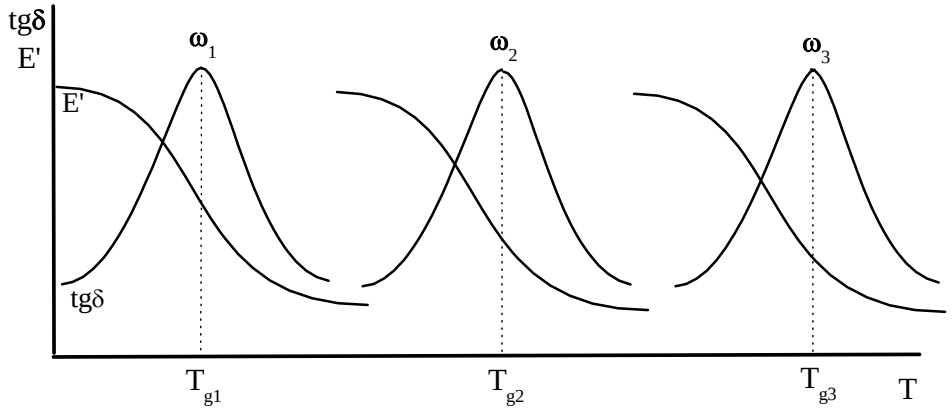

Figure 19. Temperature dependences of storage modulus *E*' and loss tangent tgδ for amorphous polymers at frequencies $\omega_1 < \omega_2 < \omega_3$.

Changing in E' and peaks of *tg*δ are sensitive to occurrence of the particular types of molecular motions in polymer. Apart from the glass transition, amorphous polymer exhibits secondary relaxation transitions. In general, amorphous polymer is characterized by the following transitions (Fig. 20) which are denoted, as a rule, α-, β-, and γ-transitions. Alpha-transition, as we saw earlier, is controlled by the appearance of segmental mobility in polymer sample. The origin of β-transition is associated with the temperature-induced mobility of fragments of backbone which are less than segment. Appearance of γ-transition is attributed to temperature-induced mobility of side groups.

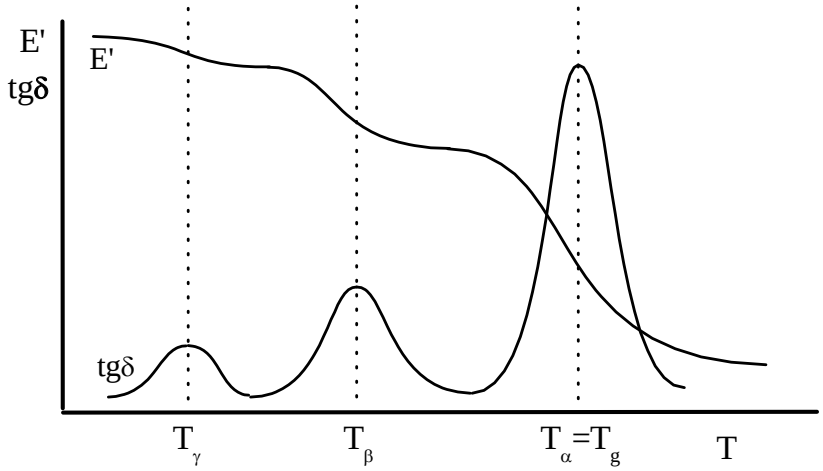

Figure 20. Typical temperature dependences of storage modulus *E*' and loss tangent tgδ for amorphous polymer.

Let us generalize the above discussion.

Mechanical response of polymer is controlled by the ratio between loading time and relaxation time.

The same mechanical behavior of the material can be realized via changing loading time, that is, frequency or strain rate at constant relaxation time, that is, at a given test temperature, and *vice versa*.

It means the general equivalence between time and temperature which is formalized as *time-temperature superposition*.

3.4. Time-Temperature Superposition

For amorphous polymer, Figure 21 shows the set of frequency dependences of storage modulus which are obtained at different test temperatures.

At a specified frequency decreasing test temperature results in increasing storage modulus.

The above equivalence between time and temperature allows remarkable procedure, that is, superposition of all these curves by keeping one of them fixed and shifting each other parallel frequency axis.

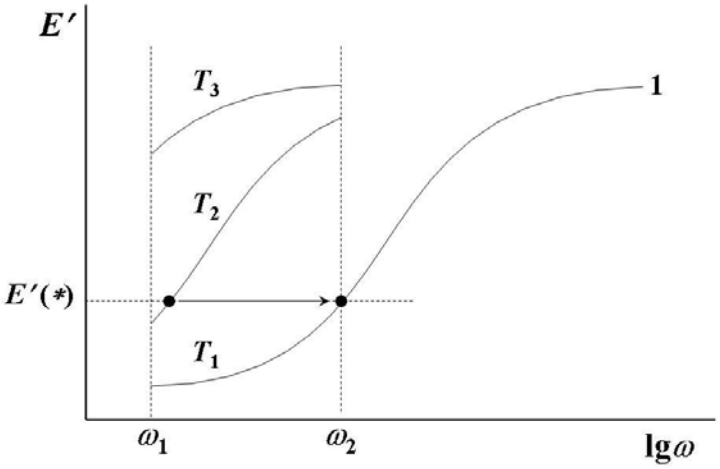

Figure 21. Typical frequency dependences of storage modulus of amorphous polymer obtained at temperatures $T_1 > T_2 > T_3$, and master curve (1). Details are given in the text.

For this purpose,

one should select some reference temperature T_{ref} (for example, T_1) and reference frequency ω_{ref} (for example, ω_2). This pair of experimental parameters controls the specified mechanical response of material, in this case, storage modulus $E'(*)$.

If ω is the frequency at which the same value of storage modulus is observed on the other curve at different temperature T_2, this curve is required to be shifted for ($\log \omega_{ref} - \log \omega$) relative to reference curve to superpose with it.

In this case, the "*shift factor*" can be written as follows

$$\log a_T = \log \omega_{ref} - \log \omega = \log\left(\frac{\omega_{ref}}{\omega}\right). \qquad (39)$$

Performance of this procedure for each curve allows complete superposition of all these curves and, as a result, construction of *master curve* (Fig. 21, curve 1).

Note that, in general, "shift factor" depends on temperature, and for accurate data handling, this fact should be taken into account.

This approach concerning time-temperature superposition was elaborated by Williams, Landel, and Ferry. The following expression for “shift factor” was proposed

$$\log a_T = \frac{-C_1\left(T - T_{ref}\right)}{C_2 + \left(T - T_{ref}\right)}, \tag{40}$$

where C_1 and C_2 are constants.

This equation which is called WLF equation is well applied for a variety of polymers tested in the vicinity of glass transition temperature.

From the practical viewpoint,

Construction of the resulting master curve allows prediction of mechanical behavior of polymers in extremely wide range of frequencies which can not be attained experimentally.

3.5. Glass Transition

Earlier, under thermomechanical testing and dynamic mechanical testing, we saw that, within a specific temperature interval, mechanical response of amorphous polymer changes from stiff glassy to soft rubbery. This temperature transition was referred to as glass transition, that is, transition from glassy state to rubbery state.

In general, when amorphous polymer goes through glass transition, there are also marked changes in various physical properties.

Figure 22 shows typical temperature dependences of a variety of mechanical and physical properties of amorphous polymer.

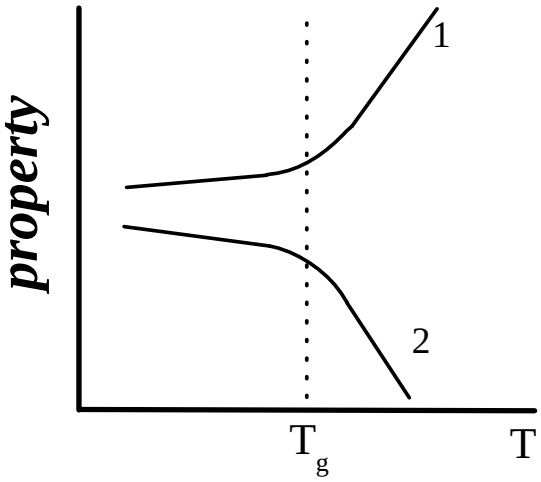

The behavior described by curve 1 corresponds to the temperature dependences of state functions (volume, entropy, *etc*.). For dynamic parameters of the material such as elastic modulus, viscosity, *etc*., the temperature dependences associated with curve 2 are observed.

Note that the temperature coefficients of the above polymer characteristics show well-pronounced jump in the vicinity of glass transition. This behavior allows one to identify glass transition with second-order phase transition.

Figure 22. Temperature dependences of various physical properties of amorphous polymer. Comments are given n the text.

To discuss the structural aspects of glass transition, one should find experimental approaches which allow one to study glass transition.

To gain a deeper insight into the nature of glass transition, let us consider the temperature-induced changes in volume of amorphous polymer in the vicinity of glass transition using *dilatometry*.

Dilatometry is based on the measuring the temperature dependence of specific volume (volume of mass unit) of material.

Typical dependence of specific volume on temperature is shown in Fig. 23 (curve 1). In the vicinity of T_g a well-pronounced inflection of the curve associated with the sharp growth in thermal expansion coefficient is observed. To analyze this behavior of amorphous polymer, the concept of *free volume* is useful.

In general, *free volume* in condensed body is a space which is not occupied by molecules. Hence, the total volume of a sample involves the volume occupied by molecules V_0 and free volume V_f

$$V = V_0 + V_f.$$

Note that the temperature dependence of occupied volume goes through glass transition with no changes (Fig. 23, curve 2). In other words, for amorphous polymer, increasing thermal expansion coefficient is controlled by the sharp growth in free volume at temperatures above T_g.

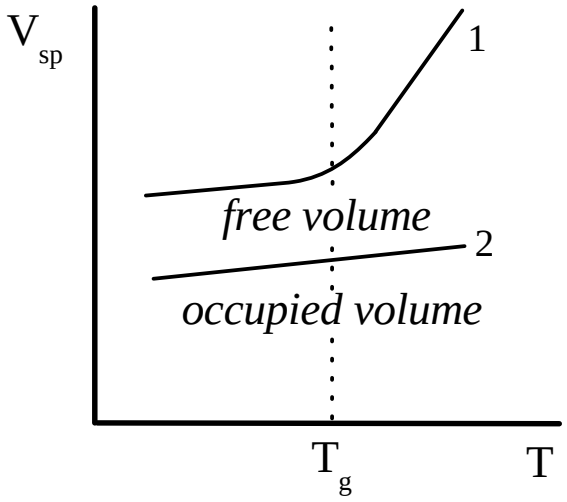

It is more convenient to insert fractional free volume f

$$f = V_f / V. \qquad (41)$$

Figure 23. Typical temperature dependences of specific volume (1) and occupied volume (2) for amorphous polymers.

At temperatures below T_g, fractional free volume $f_g = \frac{V_{fg}}{V}$ seems to be constant.
At temperatures above T_g, with increasing temperature increasing free volume is observed (Fig. 23).

From this standpoint, above T_g free volume can be expressed as follows

$$V_f = V_{fg} + \left(T - T_g\right)\left(\frac{\partial V}{\partial T}\right).$$

Division of this expression by V yields

$$f = f_g + \left(T - T_g\right)\alpha_f, \qquad (42)$$

where α_f is the thermal expansion coefficient of free volume, that is, the difference between the thermal expansion coefficients of the glassy polymer and rubber.

For the most amorphous polymers, f_q was found to be of the order 0.025 and α_f is approximately 4.8×10^{-4} K^{-1}.

Note that T_g determined from the temperature dependence of specific volume depends on rate of changing temperature.

The lower the rate of changing temperature, the lower the experimental value of T_g

Shift of T_q with changing heating rate is unambiguous evidence of the relaxation origin of glass transition.

At the temperatures above T_g, polymer sample is likely to be in equilibrium state. Cooling the sample with the constant rate disturbs the equilibrium, and the sample tends to relax and attain equilibrium state under these conditions. In this case, we deal with *structural relaxation* associated with the decreasing free volume. This process is controlled by structural rearrangements controlled by segmental mobility. With decreasing temperature, relaxation time of segments increases. As a result, at a specified temperature, segments have no time to relax during cooling at a given rate. This microscopic process manifests itself macroscopically as the glass transition. Obviously, at lower cooling rate, termination of segmental relaxation is observed at lower temperatures, and experimental T_g decreases.

As for the changes in the physicomechanical behavior of amorphous polymer at T_g, the concept of free volume allows consideration at greater length. Earlier, we discussed the transition from glassy state to rubbery state in terms of appearance of segmental mobility in polymer sample. Segmental mobility appears, at first, at temperatures when thermal energy becomes sufficient to provide mutual rotation and translation of segments. Secondly, appearance of mobility of segments requires sufficient space between them, i.e. sufficient free volume.

This dual origin of glass transition

Glass transition is controlled by both temperature activation of segmental mobility and realization of sufficient fraction of free volume.

These speculations indicate the distinctive feature of glass transition. As any relaxation transition, glass transition is controlled by the "freezing – unfreezing" of the particular type of molecular motion, in this case, segmental mobility. On the other hand, transition from rubbery to glassy state is accompanied by the noticeable structural changes which are associated with the "freezing" of a certain fraction of free volume. For secondary γ- and β-types of relaxation transitions, we deal only with the appearance of particular modes of molecular mobility whereas the structural changes do not occur.

Influence of the Chemical Structure on Glass Transition Temperature

The dual nature of glass transition controls the specific features of the influence of chemical structure of macromolecules on T_g of polymers.

For polymers, ***the correlation "chemical structure – glass transition temperature"*** should be discussed in terms of the influence of chemical structure of the macrochain flexibility (i) and on the fractional free volume in polymer sample (ii).

Flexibility of macromolecule is associated with the rotation of chemical groups around chemical bonds. This rotation is controlled by both intramolecular and intermolecular interactions.

Low values of T_g for polymers such as polyethylene, polybutadiene, and poly(ethylene oxide) (Table 1) are associated with high flexibility of macrochains because of easy rotation around single carbon-carbon and carbon-oxygen bonds. For polyethylene, wide dispersion of experimental values of T_g is a result of well-pronounced crystallization which complicate precise determination of glass transition temperature. Incorporation of chemical groups which impede rotation (for example, benzene rings) results in increasing rigidity of macrochains and growth in T_g for poly(*p*-xylylene) and poly(ethylene terephthalate).

Side groups have a marked influence on T_g because of restriction of the rotation around chemical bonds. For polystyrene, bulk side benzene ring results in increasing rigidity of macrochain and growth in T_g as compared with polypropylene. For poly(vinyl chloride), poly(vinyl alcohol), and polyacrylonitrile, polar side groups have more pronounced influence on flexibility of macrochains and on T_g because of marked growth in intermolecular interaction. This is a reason that polar side group results in more noticeable increasing T_g than non-polar side groups with the equivalent size (compare poly(vinyl chloride) and polypropylene).

Table 1.

Glass transition temperature T_g for various polymers

Polymer	**T_g, K**
Polyethylene	150-240
Polybutadiene	200
Poly(ethylene oxide)	206
Poly(p-xylylene)	353
Poly(ethylene terephthalate)	350
Polypropylene	250
Polystyrene	373
Poly(vinyl chloride)	354
Poly(vinyl alcohol)	358
Poly(acrylonitrile)	370
Nylon-3	383
Nylon-6	343
Nylon-11	315
Poly(methyl methacrylate)	378
Poly(ethyl methacrylate)	338
Poly(butyl methacrylate)	298
Poly(methyl methacrylate)	
syndiotactic	433
isotactic	317
heterotactic	378

Parallel influence of both intramolecular and intermolecular effects on T_g may be clear demonstrated for polyamides (nylons). Chemical structure of nylons is characterized by two types of chemical bonds: carbon-carbon bonds around which rotation is rather easy and carbon-nitrogen bonds in amide groups around which rotation is not allowed because of quasi-conjugation nature of these bonds. Hence, the flexibility of nylon macrochains is expected to be controlled by the ratio between *C-C* and *C-N* chemical bonds. On the other hand, nylons are characterized by high intermolecular interaction because of hydrogen bonding between amide *CONH* groups of the neighboring macromolecules. For these two reasons, increasing content of *CONH* groups controls dramatic growth in T_g under transition from nylon-11 to nylon-3.

It is notable that, in some cases (poly(methyl methacrylate) as an example), T_g is very sensitive to stereo-isomerism of polymer. For syndio-tactic PMMA, higher value of Tg as compared with that for iso-tactic PMMA is associated with the fact that iso-tactic polymer has higher amount of allowed conformations. As a result, the flexibility of iso-tactic PMMA is higher, and T_g is lower. For hetero-tactic PMMA which is a mixture of syndio- and iso-tactic isomers, T_g is intermediate.

Note that, for poly(methyl methacrylate), poly(ethyl methacrylate), and poly(butyl methacrylate), T_g decreases with increasing the size of side group whereas, as discussed above, the opposite behavior is expected. For poly(alkyl methacrylate)s, increasing the size of side groups results in increasing free volume in polymers. In this case, increasing free volume is deciding factor as compared with restriction of flexibility caused by bulkier side groups.

Competition between these opposite effects of side chemical groups on T_g (restriction of flexibility of macrochain and increasing free volume) is well-pronounced for branched polymers. At small density of branches, they control decreasing T_g via increasing free volume in polymer. With increasing density of branches, T_g increases because of marked restriction of flexibility of macromolecules.

Cross-linking of linear polymers leads to increasing T_g because of restriction of segmental mobility and decreasing free volume. For example, cross-linking of polyisoprene (natural rubber) is accompanied by increases in T_g from 200 K to 353 K when concentration cross-linking agent (sulfur) changes from 0 to 30 %. In this case, rather interesting behavior is observed. When cross-linking is carried out at a given temperature, polymer undergoes the transition from rubbery state to glassy state, Hence, glass transition may be caused not only by changing temperature but also by chemical cross-linking.

For more complicated polymer systems such as copolymers, T_g depends mainly on their structure. Block- and graft-copolymers are characterized by multiple glass transitions at temperatures which are close to T_g of constituent homopolymers. Random copolymers have the single T_g which is intermediate between T_g's of corresponding homopolymers.

3.6. Glassy Polymers

Glassy polymers or *polymer glasses* are considered as amorphous polymers for which operating temperature is below their T_g.

As discussed in Ch. 3.5, cooling of rubbery polymer is accompanied by the decreasing intensity of translation and vibration mobility of segments, increasing viscosity of a system, and decreasing free volume. When fractional free volume approaches the value of about 0.025, segmental mobility comes out of play, and transiton to glassy state takes place. This relaxation transition is observed at temperature which is referred to as glass transition temperature. On the other hand, dynamic mechanical analysis (Ch. 3.3) predicts the fact that, as a result of cooling, exceeding of relaxation time of segments over loading time is responsible for the transition from high elastic response which is characteristic for rubber to Hookean elastic response which is characteristic for glassy polymer.

Transition from rubbery state to glassy state is accompanied by “freezing” of segmental mobility and a certain fraction of free volume.

Under cooling with the constant rate dT / dt, when polymer sample approaches glass transition region increasing relaxation time of segments is responsible for the fact that segments have no enough time to rearrange adequately and provide transition of polymer sample to equilibrium state. As a result, at T_g, non-equilibrium structure is fixed.

Glassy polymer is considered as non-equilibrium frozen polymer liquid or metastable system.

Obviously, the higher cooling rate, the non-equilibrium is glassy polymer is more pronounced. In ideal case, at infinitely low cooling rate, glassy polymer which is characterized by equilibrium state may be prepared. In industry, polymeric materials based on glassy polymers (plastics, for example) are processed from melts, and this technological procedure involves the cooling of as-obtained article down to temperatures below T_g with the finite cooling rate. To diminish non-equilibrium nature of such materials, the above cooling rate should be rather small. In same cases, *annealing*, that is, thermal treatment of finished article at $T \sim T_g$ is used followed by the slow cooling down to ambient temperature.

Note that degree of equilibrium is well correlated to the fractional free volume which is frozen in glassy polymer under the transition through T_g. The higher fractional free volume, the more non-equilibrium state of polymer. When cooling rate is fixed, the above fractional free volume is mainly controlled by the flexibility of the backbone for a given polymer. For flexible-chain polymers, under glass transition, segmental rearrangements are enhanced. As a result, the more dense package of macrochains is observed, and polymer sample is more close to equilibrium state. For stiff macromolecules, the resulting structure is loosely packed, and polymer sample is characterized by well-pronounced non-equilibrium.

Non-equilibrium nature of glassy polymers manifests itself as a time-dependent change in polymer physicomechanical properties, for example, specific volume V_{sp}. At $T < T_g$, with time specific volume decreases and tends to constant value. This time-dependent decreasing V_{sp} reflects the proceeding of inner molecular rearrangements which are responsible for the *structural relaxation*, that is, the trend of the non-equilibrium system to approach equilibrium state. Obviously, the higher temperature, the smaller time is required for complete relaxation. For polystyrene with T_g = 80°C, at 60°C, this time is about 10 hours, and, at room temperature, this time increases up to several years.

3.6.1. Stress-Strain Behavior of Glassy Polymers

Studies in stress-strain behavior of the material are of particular importance because they provide an important information concerning mechanical parameters such as elastic modulus, strength, yield characteristics, and ultimate strain as well as mechanism of deformation.

Figure 24 shows a typical stress-strain diagram for the uniaxial drawing of ductile glassy polymer. The initial portion of the curve is characterized by linear dependence of stress on strain and obeys Hooke's law. Note that Young modulus is estimated from the slope. With increasing strain resulting stress goes through the peak which is called *yield* point with corresponding *yield stress* σ_y and *yield strain* ε_y. Typically, for glassy polymers, yield strain is about 5 – 10 %, and yield stress is in the range 10 – 100 MPa. Decreasing the stress under transition through yield point is attributed to *strain softening* of the material caused by applied loading. Macroscopically, yielding is accompanied by *necking*, that is, formation of the *neck* – local lateral contraction of the sample. With the further increase in strain, deformation proceeds via propagation of the neck along the sample at approximately constant stress. When the whole sample is necked, increasing stress with increasing strain is observed. This behavior is associated with the *strain hardening* of polymer.

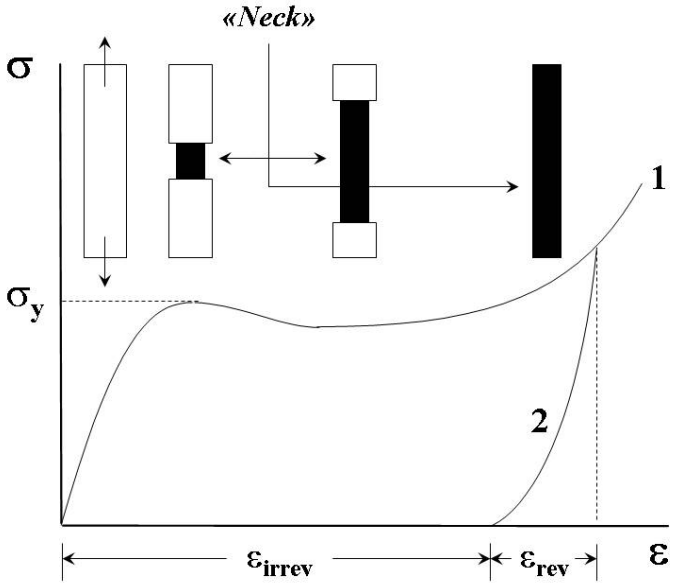

Figure 24. Typical stress-strain diagram for ductile glassy polymer. Uniaxial drawing. Loading (1), unloading (2).

Qualitatively, this behavior does not seem quite different as compared with that observed for conventional plastic materials, for example, metals. However, stress-strain behavior of polymers shows a well-pronounced time or strain rate dependence, that is, well-pronounced viscoelastic nature. These specific features will be discussed below in more details.

For uniaxial compression, stress-strain diagram of glassy polymer is similar to that obtained for uniaxial drawing. However, for compression, necking does not take place, and deformation proceeds via *shear yielding* which is associated with the localization of deformation in microscopic *shear bands* distributed throughout the polymer sample.

The formation of shear bands and their propagation through the polymer is responsible for the strain softening of material. The following loading proceeds via the widening of shear bands. Hence, in general, glassy polymers show the capacity for development of ductile deformation up to tens – hundreds percents when the critical applied stress σ_y is attained.

After unloading with the same rate (Fig. 24, curve 2), polymer samples are characterized by residual or irreversible strain ε_{irrev}, which is stored in the sample for the limitless period of time. As mentioned earlier, under loading and unloading, macroscopic mechanical behavior of glassy polymers seems to be similar to plastic deformation. As compared with conventional plasticity, specific feature of plastic deformation of polymer glasses is associated with the fact that residual strain recovers completely under heating of deformed polymer sample up to $T \geq T_g$. As a result, polymer sample retains its initial shape and dimension. Taking into account the fact that, above T_g, segmental mobility comes to a play, macroscopic recovery may be assigned to microscopic relaxation of extended polymer chains (macromolecular coils) via rearrangements of segments. From this standpoint, deformation of glassy polymers is also controlled by segmental mobility. These considerations provoked the following theories to describe yielding in polymer glasses.

3.6.2. Theoretical Approaches to Yielding

Consideration of glassy polymers as frozen liquids allows one to discuss yielding in the framework of the theory developed by Eyring[1] to describe viscous flow in liquids and adopted by Aleksandrov[2] to describe mechanical behavior of glassy polymers. In amorphous polymers, deformation proceeds via viscous flow of segments, that is, movements of segments from initial position to adjacent position. These transitions proceed with the overcoming of potential barrier and required a certain activation energy. The origin of this potential barrier is associated with intermolecular interaction between neighboring segments or, in general, with the reaction of the viscous surrounding. The frequency of the transition of segments from one position to another position ν_s which is reciprocal to relaxation time of segments τ_s is described by Eq. (12).

Note that, for liquids and rubbers, thermal energy is sufficient to provide forward and backward transition from one potential dwell to adjacent potential dwell through the potential barrier. The external stress applied to sample along a certain axis controls mainly the preferential direction of the above segmental transitions and, as a result, the direction of macroscopic deformation.

For glassy polymers, at $T < T_g$, thermal energy is not sufficient to provide overcoming of potential barrier, and segmental mobility is frozen. In this case, applied stress σ tends to reduce activation energy of above transitions of segments from initial to adjacent positions providing increasing frequency of transitions and decreasing relaxation time as follows

$$\tau = \frac{1}{\upsilon} = Ae^{\frac{U-\gamma\sigma}{kT}}, \qquad (43)$$

where γ is a coefficient which is sensitive to the polymer structure.

[1] Henry Eyring (1901-1981) – Mexican-born American theoretical chemist.
[2] A.P. Aleksandrov (1903-1994) – Soviet and Russian Physicist. Academician (from 1953) and president of the Academy of Sciences of the USSR (1975-1986).

When σ attains σ_y, stress activation of segmental mobility results in the appearance of viscous flow of segments, and development of deformation of glassy polymer. After unloading, when $\sigma = 0$, extended macromolecular coils are fixed in deformed glassy polymer providing the storing of residual strain. In this case, noticeable entropic recovery of excited macromolecular coils is not observed because, at this temperature, segmental motion is forbidden without external loading. Recovery of residual strain takes place only at temperatures above T_g as a result of relaxation of macromolecular coils via thermal activated segmental mobility.

From this standpoint, molecular mechanism of deformation of glassy polymers is similar to that for rubbers and involves deformation of macromolecular coils via viscous flow of segments. The distinctive feature of the deformation of glassy polymers is associated with the fact that segmental mobility is forced by applied stress. This is a reason that in Russian literature deformation of glassy polymers is called *forced elasticity*.

Note that the coefficient γ in Eq. (43) has a dimension of volume and is called *activation volume*. This is a volume of the polymer kinetic unit which should be moved to provide flow deformation. In general, for glassy polymers, this kinetic unit is estimated to be of the volume of several polymer segments, typically, from 2 to 10. However, activation volume is effective value, and there is no correct correlation between its dimension and dimension of the particular moiety of polymer chain.

3.6.3. Ductile-Brittle Transition

The above theoretical consideration of yielding (Eq. (43)) allows one to conclude that, in general, activation of segmental mobility takes place under parallel action of temperature and stress or, in other words, at appropriate balance between thermal and mechanical contributions (thermal term kT and mechanical term $\gamma\sigma$ in Eq. (43)). This superposition between temperature and stress action on the mechanical behavior of polymer is demonstrated in Fig. 25.

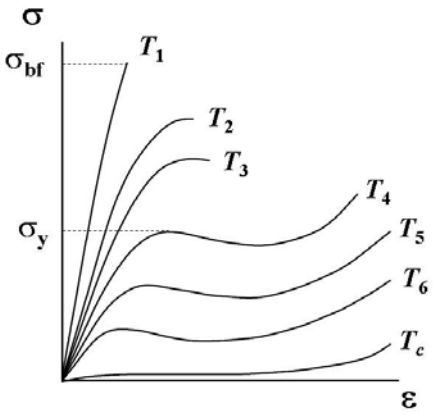

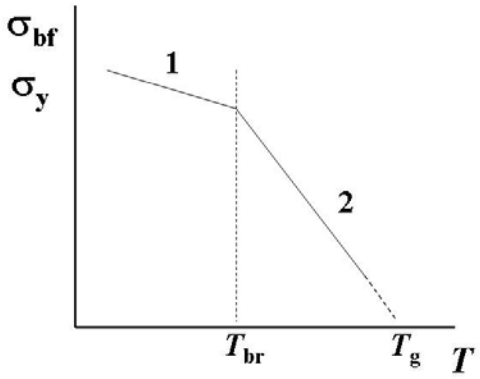

Figure 25. Stress-strain diagrams for glassy polymer at temperatures $T_1 < T_2 < T_3 < T_4 < T_5 < T_6 < T_g$.

Figure 26. Temperature dependences of strength σ_{bf} and yield stress σ_y of glassy polymer.

At a constant strain rate, increasing temperature of deformation (transition from T_4 to T_6) is accompanied by the decreasing σ_y.

At higher temperatures, that is, at higher level of thermal activation, the less mechanical activation is required to realize yielding via segmental mobility in glassy polymer.

When temperature approaches T_g, thermal term becomes sufficient to provide segmental mobility without external loading. In this case, yielding is not observed, and high elastic deformation comes to a play.

With decreasing deformation temperature (transition to $T_3 - T_1$), deformation mechanism changes from ductile to brittle, and typical brittle fracture is observed at temperature T_1. In this case, the most important mechanical characteristic of the polymer is strength, that is, the stress σ_{bf} at which brittle fracture occurs.

Ductile-brittle transition takes place at *brittleness temperature* T_{br}. The reason is that, at T_{br}, to provide forced segmental mobility required external stress becomes higher than the stress of polymer fracture. These experimental data are generalized in Fig. 26. Extrapolation of temperature dependence of σ_y to zero stress gives the value of polymer T_g.

Hence,
glassy polymers are characterized by well-pronounced ductility and ability to large deformation in the temperature range $T_g - T_{br}$.

From the applied standpoint,
for plastics based on the amorphous polymers, T_q is the upper operating temperature, and T_{br} is the lower operating temperature.

For some polymers, the corresponding temperatures are listed in Table 2.

Table 2

Glass transition temperatures and brittleness temperatures for various polymers

Polymer	T_g, °C	T_{br}, °C
Polystyrene	100	90
Poly(methyl methacrylate)	120	40
Polyvinylchloride	80	-90
Vulcanized polyisoprene	-60	-80

The influence of the chemical structure of polymer on $T_g - T_{br}$ is mainly controlled by the effect of structure on packaging of macromolecules and resulting free volume discussed above. For flexible-chain polymers, dense package of macromolecules restricts segmental mobility required for yielding and reduces $T_g - T_{br}$. For loosely packed polymers, the ability for well-pronounced ductility remains down to low temperatures, and T_{br} is rather low. In general, cross-linking results in increasing T_{br} and decreasing $T_g - T_{br}$.

At a fixed testing temperature, with increasing strain rate σ_y increases, and, at a certain strain rate, ductile-brittle transition is observed. This experimental evidence suggests the superposition between the influence of both testing temperature and loading time (strain rate) on yielding in amorphous polymers. This typical viscoelastic behavior reflects the relaxation nature of ductility and ductile-brittle transition.

Chapter 4. SEMICRYSTALLINE POLYMERS

Crystalline phase state of solids is characterized by three-dimensional crystalline lattice which is specified as a regular set of repeating atomic groups. These repeating units are called *unit* (*elementary*) *cells*. Unit cell is described quantitatively by three vectors $\vec{a}, \vec{b}, \vec{c}$ and angles between them α, β, γ.

In dependence on the ratio between the above vectors and corresponding angles the following seven basic crystal systems are recognized:

1. cubic,
2. tetragonal,
3. hexagonal,
4. rhombic (orthorhombic),
5. rhombohedral (trigonal),
6. monoclinic,
7. triclinic.

Note that macromolecules are crystallized with the formation of latter six crystal systems. For polymers, cubic crystal system is not known.

The specific feature of polymer crystals is associated with the fact that the single macromolecule takes part in the formation of a numerous unit cells. This situation is demonstrated by well-studied crystalline structure of linear polyethylene (Fig. 27). Polyethylene macrochains in the lowest-energy stable planar zig-zag conformations (all bonds are in *trans* positions) are crystallized with the formation of orthorhombic unit cell with the dimension 0.742 × 0.495 × 0.254 nm^3.

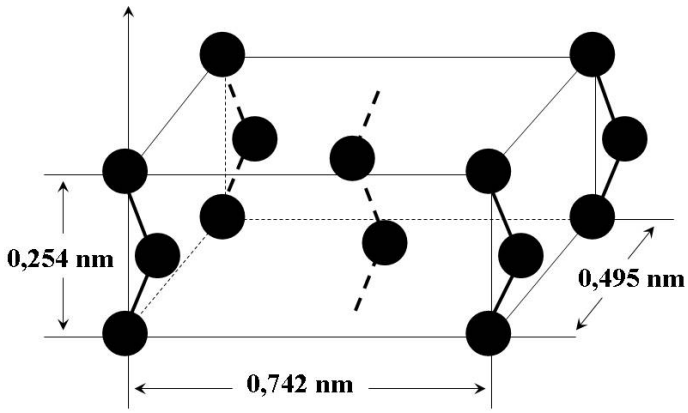

Figure 27. Elementary cell of polyethylene. Dark circles represents – CH_2 – groups of polymer. The arrow shows the axis of macromolecules.

The axis of macrochains coincide with the $\vec{c}$ vector while hydrogen atoms lie in the planes parallel to *ab* plane. The polyethylene unit cell is formed by the fragments of five macromolecules: four of them are in the corners and the fifth one is in the middle. In the unit cell and, in general, in crystal, the molecules are held together by the van der Waals interactions between the chain atomic groups.

For polymers with side groups bulkier than hydrogen, planar zig-zag conformation is characterized by noticeable steric repulsion. To minimize the energy, the macromolecules take the helical conformation providing the most appropriate arrangements of side groups relative to each other. Crystallization of these macromolecules proceeds as the packaging of the above helices. To describe quantitatively the above conformational isomers (planar zig-zag and helices), the following nomenclature is used.

In general, both planar and helical conformations are described as *A*u / t*, where *A* indicates the class of helix, that is, the amount of sceletal atoms in the asymetric unit of the chain; *u* is the number of the above units; and *t* is the number of turns of the helix which corresponds to the crystallographic repeat.

For various polymers, the parameters of unit cell and helix as well as the type of crystal system are given in Table 3.

Table 3

The parameters of crystalline structure of various polymers

Polymer and Repeated Unit	**Unit Cell Parameters, *a*×*b*×*c*, Å *α, β, γ,* °**	**Helix Parameters**	**Crystal System**
Polyethylene - CH_2 -	7.42 × 4.94 × 2.54 90, 90, 90 8.10 × 2.52 × 4.79 90, 107.9, 90	1*2/1 1*2/1	Orthorhombic Monoclinic
Polytetrafluoroethylene - CF_2 -	5.59 × 5.59 × 16.88 90, 90, 119.3 5.66 × 5.66 × 19.5 90, 90, 120	1*13/6 1*15/7	Triclinic Trigonal
Polyoxymethylene - CH_2 - O -	4.47 × 4.47 × 17.4 90, 90, 120 4.76 × 4.66 × 3.56 90, 90, 90	2*9/5 2*2/1	Trigonal Orthorhombic
Poly(vinyl alcohol) - $CH_2 – CHOH$ -	7.81 × 2.51 × 5.51 90, 91.7, 90	2*1/1	Monoclinic
Poly(vinyl fluoride) - $CH_2 – CHF$-	8.57 × 4.95 × 2.52 90, 90, 90	2*1/1	Orthorhombic

As for the low-molar-mass crystals,

polymorphism, that is, the ability to exist in more than one crystal systems is observed for crystalline polymers.

For example, deformation of orthorhombic polyethylene is accompanied by formation of monoclinic crystalline structure. Monoclinic crystal system is also formed by the polyethylene macromolecules with planar zig-zag conformations similar to that for orthophombic structure. The only difference between these two crystalline forms is associated with differences in the parameters of unit cell (Table 3). Polyoxymethylene exists in trigonal and orthophombic crystal systems. At the temperatures below 19°C, polytetrafluoroethylene exists in trigonal modification. When the temperature increases above 19°C, polytetrafluoroethylene crystallizes in trigonal crystal system.

In general, for a given polymer, different crystal systems occur as a result of deformation or changes in the crystallization conditions.

The above general crystallographic considerations allow one to describe the structure of polymer crystals which are commonly called crystallites in terms of basic parameters of unit cells, that is, by three vectors and the angles between them. Note that, for the crystalline polymers with a given unit cell, a variety of supramolecular structures is observed. Formation of different supramolecular is mainly controlled by the conditions of crystallization.

4.1. Supramolecular Structure of Semicrystalline Polymers

For some polymers, single crystals may be prepared by the precipitation from the dilute solutions. The prime example is the polyethylene single crystals. The single plate-like crystal is called *lamella*. Note that the thickness of polyethylene lamellae is of the order of 10 *nm* when the length of polyethylene chains is of thousand nanometers. The packing of these long macromolecules in lamellae was suggested to be achieved via folding of macrochains. Schematic representation of the lamellae with folded macromolecules is given in Fig. 28.

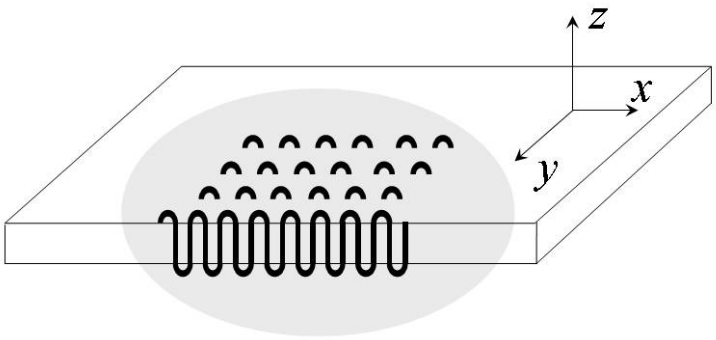

Figure 28. Schematic representation of lamella structure.

The thickness of the lamellae and length of the fold are controlled by the nature of solvent used and temperature of crystallization. For solution-grown polyethylene lamellae, increasing temperature from 50 to 90°C increases the lamellae thickness from 9 to 15 *nm*. Increasing solution concentration and the rate of crystallization are responsible for the formation of more complicated supramolecular structures. In this case, lamella are layered over each other, and stepped crystals appear.

When the rate of evaporation of the solvent is rather high, fibrillar crystals with the high ratio between length and thickness are formed. Fibrillar crystals are considered as degenerated lamellar structure when the growth of the crystal in one predominant direction takes place. Under crystallization from supercooled solutions, dendrite crystals appear as a result of the aggregation of small lamella.

The above speculations concerning the formation of polymer supramolecular structure are also applicable for the polymers crystallized from the melts. The general feature of polymer crystallization from both concentrated solutions and melts is associated with the fact that individual chains take part in the formation of several crystallites and provide inter-crystallites links. These tie chains constitute amorphous regions.

Hence,

except single crystals, supramolecular polymer structures are characterized by the co-existence of the crystalline and amorphous phases.

In connection with this,

crystalline polymers are called *semicrystalline*.

During crystallization from the concentrated solutions and supercooled melts, spherulites with circular shape are most often appear. The size of spherulies reaches thousands of microns, and they are easily viewed by the optical microscopy. Spherulites are built up from lamellar crystals which grow from the single center and constitute the radii of the spherulite. These lamellae are interconnected by the tie-chains which constitute the spherulitic amorphous regions. In the radial spherulites, radii are constructed from planar lamella. In some cases, during the growth, lamella twist with the formation of helix. The spherulites with the helical lamellar radii are called ringed spherulites.

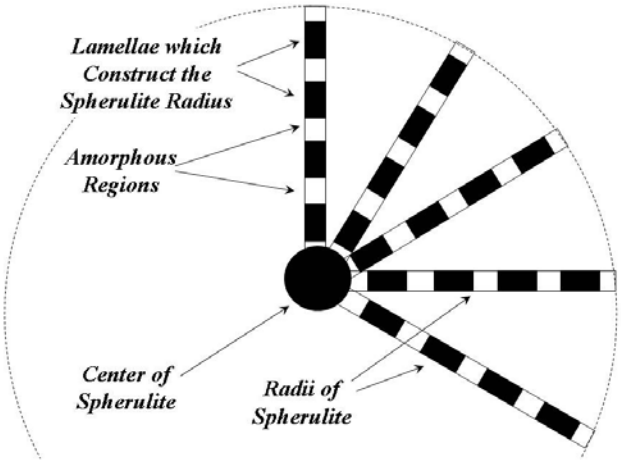

Figure 29. Schematic representation of spherulite structure.

The above considerations allow us to conclude that the general structural feature of the semicrystalline polymers is associated with the co-existence of the interconnected amorphous phase and crystalline phase with the folded macrochains. For quantitative estimation of the above co-existence of amorphous and crystalline phases, a specific parameter - *degree of crystallinity* is invoked

Degree of crystallinity, χ_c, is defined as mass (or volume) fraction of the crystalline phase as follows

$$\chi_c = \frac{M_c}{M} = \frac{\rho_c V_c}{\rho V}, \tag{44}$$

where M and M_c are total mass of the sample and mass of crystalline phase, respectively; ρ and ρ_c are total density of the sample and density of crystalline phase, respectively; and V and V_c are total volume of the sample and volume of crystalline phase, respectively.

Note that

$$\rho V = \rho_c V_c + \rho_a V_a,$$

where V_a and ρ_a are volume and density of amorphous phase, respectively,

and

$$\frac{V_c}{V} = \frac{\rho - \rho_a}{\rho_c - \rho_a}. \tag{45}$$

Substitution of the Eq. (45) in Eq. (44) yields

$$\chi_c = \frac{\rho_c}{\rho}\left(\frac{\rho - \rho_a}{\rho_c - \rho_a}\right). \tag{46}$$

This expression relates degree of crystallinity with the density of the sample studied and densities of crystalline and amorphous phases and provides determination of χ_c by flotation in a density-gradient columns. This experimental technique allows estimation of the sample density ρ. The density of crystalline phase ρ_c is a calculated value. The density of amorphous phase ρ_a may be determined experimentally for the total amorphous sample prepared via quenching of polymer melt (see Ch. 4.2.3) or by extrapolation of the densities of a series of semicrystalline samples to zero crystallinity.

To determine degree of crystallinity, wide-angle X-ray scattering (WAXS) seems to be rather powerful. Typical plots of intensity of X-ray scattering versus diffraction angle are characterized by the sharp peaks due to scattering from the crystalline regions and broad underlying bands due to scattering from the non-crystalline regions. In principle, degree of crystallinity is the ratio between areas under the crystalline peaks and amorphous band.

Another experimental approach to estimate degree of crystallinity is based on the determination of the changes in the enthalpy of melting by differential scanning calorimetry (DSC). Degree of crystallinity is calculated as a ratio between experimental value of the enthalpy of melting and enthalpy of melting for the completely crystalline polymer. Spectroscopic methods such as nuclear magnetic resonance (NMR) and infra-red spectroscopy can be also used.

4.2. Crystallization in Polymers

4.2.1. Structural Criteria of Crystallization

Crystallization is associated with the incorporation of the fragments of polymer chains in the ordered three-dimensional crystalline lattice. To provide the dense packaging of macrochains in crystalline lattice, stereoregularity of macromolecules is required.

Only polymers with the regular configuration show capacity to crystallization. In terms of tacticity of polymer chain, isotactic and syndiotactic polymers crystallize whereas, for heterotactic polymers, the ability to crystallization is suppressed.

However, there are some exceptions to this rule.

The prime examples of these exceptions are poly(vinyl fluoride) and poly(vinyl alcohol). In these cases, the sizes of the side groups are smaller than the corresponding dimension of unit cell, and even heterotactic configuration isomers easily from crystalline lattice similar to that for polyethylene (see Table 3).

Note that the size of side groups is also considered as determining factor which controls mainly the ability of polymer to crystallization. For methacrylic polymers, under transition from poly(methyl methacrylate) to poly(ethyl methacrylate) to poly(propyl methacrylate), increasing size of side groups suppresses crystallization completely even for stereoregular samples.

The additional structural factor which favors crystallization is the presence in macromolecule polar groups. For example, for polyamides, the strong hydrogen bonding between the amide groups controls the close packing of the macromolecules in crystalline lattice, and, as a result, crystallization is enhanced. The same situation is observed for poly(vinyl alcohol) in which side hydroxyls also form hydrogen bonds.

Obviously, macromolecules or their fragments can be incorporated in crystalline lattice when they are in most appropriated conformation which allows the most dense package. As mentioned earlier, in most cases, crystallization proceeds via folding of macrochains. The folding require high flexibility and existence of well-pronounced conformational isomerism.

Hence, from the structural standpoint,

polymer ability to crystallization is controlled by configuration and conformation isomerism, size of side groups, and the polarity of atomic groups in the macromolecule. These structural aspects are responsible for the general division of polymers into crystallizable and non-crystallizable.

4.2.2. Thermodynamics of Crystallization

As any physical and chemical process, crystallization proceeds spontaneously when decreasing Gibbs energy ΔG takes place

$$\Delta G = \Delta H - T\Delta S < 0 \qquad (47)$$

as a result of appropriate balance between enthalpy change ΔH and entropy change ΔS of crystallization.

As for the entropy of crystallization, one should take into account the fact that crystallization is a typical "disorder - order" transition which is accompanied by the negative change in entropy. Hence, crystallization is expected to proceed when negative change in entropy is compensated by appreciable negative change in enthalpy.

At melting temperature, T_m, equilibrium "crystallization - melting" is observed. At this temperature, $\Delta G = 0$, and $\Delta H = T_m \Delta S$. When temperature decreases below T_m, ΔG becomes negative, and crystallization proceeds spontaneously. Hence, crystallization temperature, T_{cr}, should be selected below T_m to provide noticeable crystallization or, in other words, the difference between the above temperatures $\Delta T = T_m - T_{cr}$ which is called *supercooling parameter* should be positive.

In general, crystallization involves two stages: nucleation and growth of crystals. In details these stages will be discussed in the next section from kinetic viewpoint. Nucleation proceeds via side-by-side packing of several molecules of fragments of several macrochains with the formation of crystalline embryo in polymer melt. Aggregation of molecules is associated with the following changes of Gibbs energy. At first, appearance of crystalline particle (nucleus of crystallizatrion) which is characterized by a specified surface energy controls increasing Gibbs energy, and $\Delta G = G_{crystal} - G_{melt}$ becomes positive. Secondly, as discussed earlier, at appropriate temperatures, when reduction of enthalpy compensates entropy penalty ($\Delta H > T\Delta S$), incorporation of molecules in crystalline particle is accompanied by decreasing Gibbs energy, and $\Delta G = G_{crystal} - G_{melt}$ becomes negative.

Obviously, the competition of the above factors which influence on ΔG in opposite ways is controlled by the surface-to-volume ratio of the crystalline particle. The dependence of ΔG on size of particle goes through maximum at critical size, d_{cr}. When $d < d_{cr}$, appearance and growth of crystalline embryo is accompanied by the growth of positive ΔG because, at this high surface-to-volume ratio, increasing Gibbs energy as a result of formation of crystal surface prevails over the decreasing Gibbs energy caused by incorporation of molecules in crystal volume. When d becomes higher than d_{cr}, the lowering of surface-to-volume ratio and resulting opposite balance between the above factors control the change of sign of ΔG. The negative values of ΔG provides the formation of stable nuclei of crystallization and following spontaneous growth of crystals. The peak at the curve ΔG - d may be considered as energy barrier. From this standpoint, at a given crystallization temperature, this barrier is overcome by the sufficient thermal fluctuations.

The peculiar feature of polymers is associated with their ability to crystallize during drawing and orientation at temperatures at which crystallization of isotropic sample thermodynamically is not allowed. The prime example is crystallization of rubbers during their drawing.

Let at a given temperature,

$$\Delta G = \Delta H - T\Delta S > 0 .$$

For rubbery sample, high elastic deformation is accompanied by orientation and ordering of segments and macromolecules, and, as a result, decreasing entropy of amorphous polymer S_{am} takes place. This factor is responsible for increasing entropy term $T\Delta S \equiv T(S_{cr} - S_{am})$. When this growth in entropy term becomes sufficient to cause the change of the sign of ΔG, in oriented polymer sample, crystallization proceeds spontaneously. Obviously, unloading of the sample results in recovery of high elastic deformation and melting of crystals.

For real crystalline phase, change in Gibbs energy can be represented as follows

$$\Delta G_{cr} = G_{cr}^{\infty} + \sigma s + \gamma , \qquad (48)$$

where G_{cr}^{∞} is Gibbs energy of ideal crystalline phase, σ is surface energy, s is the surface of crystal, and γ is responsible for the defects of structure.

In general, under crystallization from melt, sizes of crystals is mainly controlled by the number of nuclei of crystallization. The growth of each crystal is terminated when the neighboring crystals approach each other, and close contact between them is realized. As a result, the less number of growing crystals, the higher their final size.

For polymers, the peculiar feature of their crystallization is associated with the fact that macromolecules are crystallized via folding within crystallite. The thickness of crystallite is controlled by the length of the fold.

From the thermodynamic point of view, folding mechanism of crystallization can be explained as follows. In the crystalline lattice, the vibration of some fragments of macrochains are correlated. With increasing the length of the above fragments this correlation becomes more pronounced. This is accompanied by the decreasing energy of intermolecular interaction, that is, increasing the term γ in Eq. (48). As a result, Gibbs energy of crystal increases. Hence, when the critical length is achieved, the folding of the macrochain takes place.

With increasing crystallization temperature the thickness of crystallites is expected to increase. When supercooling parameter is very small (not more than 1 degree), crystallization proceeds with formation of extended-chain crystals. In extended-chain crystals, macromolecules are packed like pencils in a box. These crystals may be prepared when polymer molar mass is not very high (for example, for polyethylene with molar mass 10.000) and crystallization conditions are close to equilibrium. To realize the latter requirement, crystallization is carried out at high pressures about 1 GPa.

4.2.3. Kinetics of Crystallization

Crystallization involves two distinct steps: nucleation and growth of crystals. Nucleation is classified as *homogeneous* and *heterogeneous*.

Kinetic analysis of polymer crystallization is based on the following assumptions.

- Under cooling below melting point, the random and spontaneous homogeneous nucleation, that is, formation of the nuclei of crystallization takes place in the melt. Thermodynamic features of the homogeneous nucleation were considered in the previous section. From the kinetic standpoint, the above nuclei may be formed instantaneously, and after that their amount does not change (the case of instantaneous homogeneous nucleation), or the appearance of nuclei takes place with the constant rate during crystallization (the case of sporadic nucleation). In the latter case, the amount of nuclei changes with time as $n = V_{sp.n.} \times t$, where $V_{sp.n.}$ is the rate of sporadic nucleation.
- The growth of nuclei may be, in general, uni-, two-, and three-dimensional. This factor controls the formation of rod-like, plate- or disc-like, and spherical types of supramolecular crystalline structure, respectively.

However, in the majority of cases, heterogeneous nucleation takes place on the foreign inclusions such as dust particles as well as on the walls of the vessel. In both cases, nuclei of crystallization add macromolecules, and, as a result, growth of crystals starts.

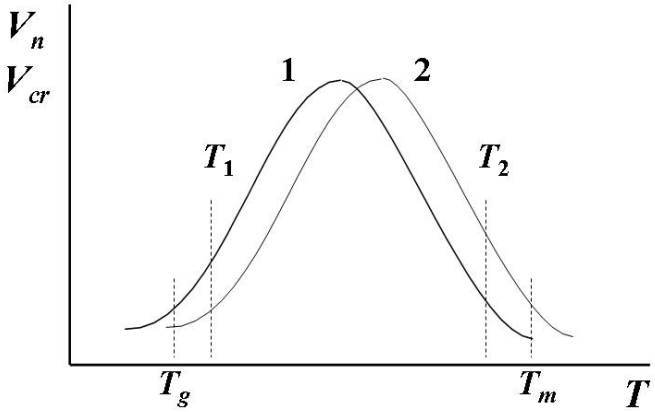

The rate of nucleation V_n as well as crystal growth rate V_{cr} are dependent on crystallization temperature (Fig. 30). Both V_n and V_{cr} go through maximum in the temperature interval between glass transition temperature and melting temperature. Note that the plot of V_n versus temperature lags behind the plot of V_{cr} versus temperature.

Figure 30. Temperature dependences of the rate of nucleation V_n (1) and crystal growth rate V_{cr} (2).

Molar mass of polymer was found to effect on the rate of crystal growth. At a given temperature of crystallization, the rate of crystallization decreases when molar mass of polymer increases.

An appearance of the maximum in the plot V_{cr} versus temperature is associated with the competition of the following factors. From thermodynamic viewpoint, crystallization starts spontaneously when crystallization temperature becomes lower that T_m. With further decreasing T_{cr}, thermodynamic driving force for crystallization increases. This factor is responsible for the increasing V_{cr}. On the other hand, decreasing T_{cr} results in the growth of viscosity of a system, and, as a result, transport of macromolecules to the growing crystals slows down. This is a reason for the decreasing V_{cr} when T_{cr} decreases, despite of the fact, that, in this case, thermodynamic driving force continues to grow. At T_g, crystal growth rate tends to zero.

Crystallization takes place at temperatures above T_g when segmental mobility is well-pronounced.

To elucidate the situation, let us invoke the following experimental procedure.

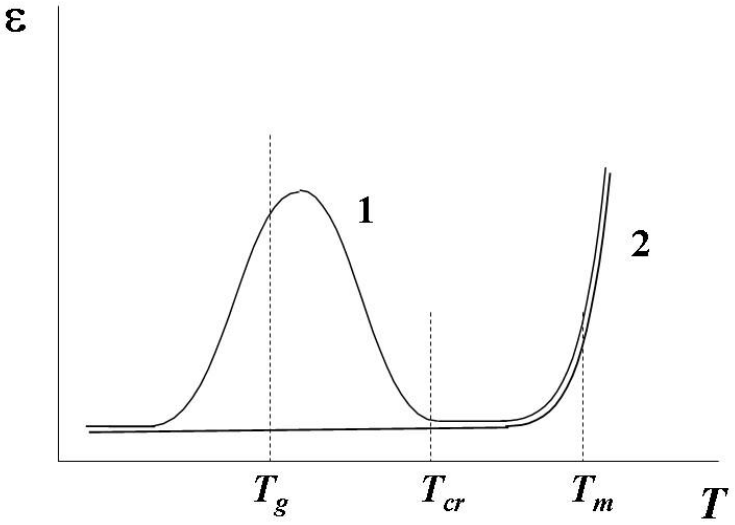

When melt of the crystallizable polymer is rapidly cooled down to the temperatures below T_g, crystallization is kinetically suppressed because kinetic units responsible for crystallization have no time to form the crystalline lattice. This procedure is called *quenching*. Hence, at the temperatures below T_g, the quenched polymer sample is crystallizable polymer in amorphous phase state. For quenched polymer sample, thermomechanical curve is shown in Fig. 31 (curve 1).

Figure 31. Thermomechanical curve of quenched (1) and crystalline polymer (2).

At temperatures below T_g, deformation of quenched polymer sample in glassy state is rather low and comparable with that for amorphous non-crystallizable polymer. At T_g, appearance of segmental mobility is responsible for the marked growth in deformation because of transition from glassy state to rubbery state. For quenched polymer sample, further increasing temperature is accompanied by the decrease in deformation which remains rather low up to T_m. The trend observed is attributed to crystallization of quenched polymer sample within T_g - T_m temperature range. From this standpoint, crystallization is associated with the appearance of segmental mobility, and segments are considered as the principal kinetic units responsible for crystallization. At T_m, melting of the crystalline phase controls noticeable increasing deformation of the polymer sample. Obviously, for crystalline polymer sample, the change in deformation takes place only at T_m (Fig. 31, curve 2).

The above ratio between V_n and V_{cr} (Fig. 30) allows one to control the structural parameters of semicrystalline polymers. Crystal grows till it meets the adjacent crystal. After that, crystal growth is terminated. In a given direction, the linear dimension of the growing crystal l with crystallization time may be expressed as follows $l = V_{cr} \times t$.

Crystal dimension is mainly controlled by the amount of nuclei in melt.

The lower amount of nuclei, the more space is available for the growth of crystals. At crystallization temperature close to T_m, the crystal growth rate exceeds markedly the rate of nucleation. As a result, the number of crystallites is rather low and their size is rather high. The opposite case is observed when crystallization temperature tends to T_g. The fact that V_n exceeds V_{cr} controls high amount of crystallites and their small size.

To estimate the kinetics of crystallization quantitatively, Avrami equation may be invoked. This equation was derived to describe the kinetics of isothermal crystallization of low-molar-mass substances and based on the following assumptions. When melt is cooled down to crystallization temperature below T_m, nucleation is assumed to be homogeneous and both nucleation rate and crystallization rate are constant. In other words, both number of nuclei and the size of crystals are proportional to the crystallization time. In this case, crystallization kinetics may be estimated as the rate of the increasing fraction of crystalline phase as follows

$$\frac{M_c}{M_0} = 1 - e^{-kt^n}, \tag{49}$$

where M_0 and M_c are the initial mass of melt and the mass of crystalline phase which was formed during time t, respectively; k is crystallization constant; and n is Avrami exponent which is controlled by the type of crystallization structure.

For semicrystalline polymers, the fraction of crystalline phase M_c / M_0 is considered as the degree of crystallinity, χ_c. According to Avrami equation, with increasing crystallization time t, degree of crystallinity tends to unity. In practice, degree of crystallinity which is equal to unity is never achieved for semicrystalline polymers. In connection with this, to describe the kinetics of increasing degree of crystallinity, Avrami equation is modified as follows

$$\chi_c = \chi_c^{\infty}\left(1 - e^{-kt^n}\right) \tag{50}$$

where χ_c^{∞} is a limiting degree of crystallinity which can be achieved at a given crystallization temperature.

Experimentally, to study the kinetics of crystallization, it is much easier to follow the decreasing volume of the sample during crystallization using dilatometry.

The sample of crystallizable polymer is placed in dilatometer, melt at temperature above T_m, and cool down to a given crystallization temperature.

The volume decreasing is monitored from the decreasing height of the liquid. In this case, time dependence of the corresponding experimental parameters is written as follows

$$\frac{V_t - V_\infty}{V_0 - V_\infty} = \frac{h_t - h_\infty}{h_0 - h_\infty} = e^{-kt^n}, \quad (51)$$

where V_0, V_∞, and V_t are initial, final, and current volume at time t, respectively; h_0, h_∞, and h_t are initial, final, and current height of the liquid in dilatometer at time t, respectively.

From the slope of the linear portion of the plot $\log\left\{\ln\left[\frac{h_t - h_\infty}{h_0 - h_\infty}\right]\right\}$ versus log t, Avrami exponent n is estimated. When crystallization is three-dimensional, n is equal to 4. For polymers, this case corresponds to crystallization with the formation of the spherullites. For two-dimensional crystallization, n is equal to 3, and lamella grow. Uni-dimensional crystallization is associated with n = 2, when polymer melt is mainly crystallized as fibrils. Actually, in the most cases, experimental values of Avrami exponent are fractional because of superposition of homogeneous and heterogeneous nucleation, changes of the types of crystalline strauctures during crystallization, and influence of molar-mass distribution on the crystallization. From this standpoint, this approach to estimate Avrami exponent and corresponding type of crystalline structure is considered as qualitative.

The specific feature of the kinetics of polymer crystallization is associated with the marked influence of crystallization temperature on the crystallization rate. This trend is most pronounced at the small values of supercooling parameter, that is, at crystallization temperature close to T_m. Increasing crystallization temperature for several degrees is accompanied by the decreasing crystallization rate for several orders of magnitude.

4.2.4. Relaxation Processes Accompanying Crystallization and Melting

Crystallization of polymers is associated with incorporation of macromolecules in crystalline lattice via their folding. The transition of macromolecules and segments from melt or solution to crystal does not proceed instantaneously and requires a specified period of time which may be identify as relaxation time.

Crystallization has a well-pronounced relaxation nature and is time-dependent process.

During isothermal crystallization, increasing crystallization time controls the increasing degree of crystallinity. When crystallization of polymer sample is carried out via the cooling with constant rate, increasing cooling rate is responsible for the decreasing degree of crystallinity. If cooling rate is extremely high, kinetically, crystallization is not allowed, and quenched polymer sample is prepared. To discuss relaxation nature of both polymer crystallization and melting, let us consider the changes in the specific volume of polymer samples during heating and cooling with the constant rate.

For low-molar-mass substances, the typical plot of the specific volume versus temperature is shown in Fig. 32A. Note that both melting and crystallization take place at a specified temperature $T_m = T_{cr}$, and corresponding curves coincide.

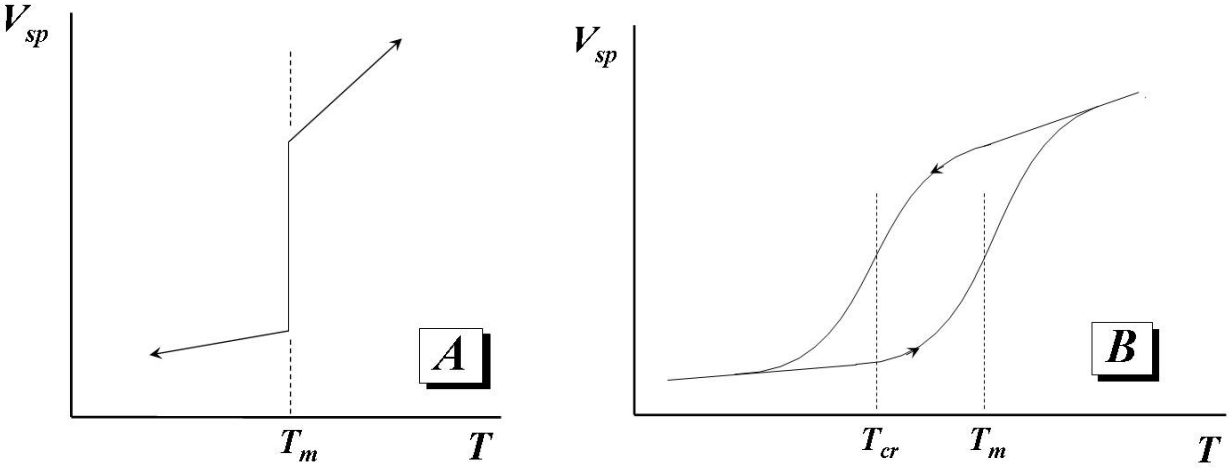

Figure 32. Temperature dependences of specific volume for low-molar-mass substances (A) and polymers (B) under heating and cooling.

For crystallizable polymer sample, melting and crystallization curves are shown in Fig. 32B. This experimental evidence allows the following conclusions.

- For crystalline polymer sample, there is no single T_m, and melting is observed in a certain temperature interval. From this standpoint, when we speak about polymer melting temperature we mean the midpoint of the above melting interval. The same trend is observed for crystallization.
- Melting and crystallization curves do not coincide, and hysteresis between them takes place. Note that the appearance of hysteresis is the direct confirmation of the relaxation nature of the phenomenon. The relaxation origin of the melting is also followed from the fact that, with increasing the rate of heating, melting temperature shifted toward higher temperatures.

The absence of the single melting point for polymers is explained by the higher irregularity polymer crystals as compared with low-molar-mass crystalline substances. The defects in polymer crystalline lattice arise from the obvious irregularities in the macromolecule chemical structure. Stereoregular polymers with a specified configuration always contain non-regular chain fragments which contribute to the imperfection of crystalline lattice. As any crystalline material, polymer crystals possess the general imperfections such as point defects and dislocations. The long-chain nature of macromolecules adds to the appearance of these defects which include chain ends, local folding, molecular kinks, *etc*. Moreover, the folds of the macrochains at the polymer crystal surface may be considered as defects.

Apart from the above "macromolecular" reasons, defectiveness of polymer crystals is controlled by the following factors. For the crystallites which appeared at the late stage of crystallization, growth is hindered because of the presence of preliminary formed crystallites. These steric hindrances result in the distortion in the crystalline lattice and contribute to the increasing the number of structural defects.

Hence, the appearance of the above defects is responsible for the fact that polymer crystals are much less perfect as compared with low-molar-mass crystals.

A various types of disorder in polymer crystalline structure are formalized in terms of *paracrystallinity*. In the framework of this concept, for polymer *paracrystal*, the parameters of unit cell, primarily, the angles α, β, and γ between basic vectors $\vec{a}, \vec{b},$ and $\vec{c}$ vary from one cell to another cell.

Note that the different crystallites are characterized by the different defectiveness and types of defects. The more defective crystallite, the lower its own melting temperature.

The other reason for the polymer melting in the wide temperature range is associated with the different size of crystallites, that is, with wide distribution of crystallites throughout their sizes. The smaller crystallite, the higher ratio between the surface area and volume. As a result, the smaller crystallites melt at the lower temperatures than those for crystallites with larger sizes.

Hence, within the melting interval, first melt the more defective and small crystallites. With increasing temperature, crystallites with less defectiveness and larger size start to melt and so on. Obviously, to narrow melting interval and shift it toward higher temperature, one should decrease defectiveness and increase the dimension of crystallites. Taking into account the relaxation origin of crystallization, it can be achieved by the increasing crystallization temperature, that is, decreasing supercooling parameter and increasing crystallization time. In this case, less defects appear in polymer crystallites, and crystallites are more uniform in size. For the finished semicrystalline polymer, one can obtain the same results using *annealing* of the sample. To anneal, polymer sample is kept at temperatures close to T_m. Under these conditions, secondary crystallization is responsible for the perfection of crystalline phase, and, as a result, melting temperature increases. On the other hand, during annealing, one crystalline from may transform to another more equilibrium form because of polymorphism which is characteristic for a variety of polymers.

4.3. Control for the Melting Temperature and Crystalline Structure

The above considerations concerning thermodynamic, kinetic, and relaxation aspects of polymer crystallization provide the possibilities to control melting temperature and crystalline structure of polymeric materials, primarily, fibers and plastics, based on semicrystalline polymers.

Melting temperature is the upper operating temperature of semicrystalline polymer, and the value of T_m is responsible for the operating temperature range of the material.

The desirable properties of polymeric material are controlled by the microscopic structure, and modification of supramolecular crystalline structure provides development of required operating parameters.

4.3.1. Factors Affecting Melting Temperature

In general, the factors such as molar mass and chemical structure which control glass transition temperature(see Ch. 3.5) affect on melting temperature in a similar way.

As for T_g, T_m increases with molar mass of polymer approaching approximately constant value for high-molar-mass polymers. The influence of molar mass on T_m may be understood from the following viewpoint.

For linear polymers, chain ends introduce the defects in crystalline structure lowering T_m. To estimate the influence of molar mass on T_m, let us consider chain ends as impurities incorporated in polymer crystal.

From the general physicochemical viewpoint, the influence of impurities on T_m is expressed as follows

$$\frac{1}{T_m} - \frac{1}{T_m^\infty} = \frac{R}{\Delta H_f} n, \qquad (52)$$

where T_m^∞ is equilibrium melting temperature; ΔH_f is enthalpy of fusion per mole of repeat unit; and n is mole fraction of impurity.

Taking into account the fact that each macrochain of linear polymer have two chain ends, mole fraction of impurity is $\frac{2}{\overline{P}_n}$ where $\overline{P}_n$ is degree of polymerization, and Eq. (52) may be written as

$$\frac{1}{T_m} - \frac{1}{T_m^\infty} = \frac{R}{\Delta H_f} \frac{2}{\overline{P}_n}. \qquad (53)$$

Hence, T_m is expected to tend to T_m^∞ when $\overline{P}_n \to \infty$.

The influence of chemical structure on T_m may be demonstrated as follows (Table 4).

At first, in general, the influence of chemical structure on T_m is controlled by the balance between flexibility and rigidity of polymer chain. The higher flexibility, the lower T_m, and *vice versa*. For flexible polymers (polyethylene as a prime example) T_m is rather low. For poly(ethylene oxide), the following increase in flexibility via incorporation in backbone - *O* - group results in decreasing T_m. In contrary, for poly(*p*-xylylene), increasing stiffness because of the presence of benzene ring is responsible for enormous growth of T_m.

The second factor which affects markedly on T_m is the type and size of side groups. Incorporation of side groups restricts chain flexibility and increases T_m. The bulkier side group, the higher T_m. As a result, transition from polyethylene to polypropylene to polystyrene is accompanied by noticeable increase in T_m. However, the long aliphatic side groups may decrease T_m because of loosening crystalline structure.

Third, incorporation of polar groups in backbone increases intermolecular interaction and increase T_m. For aliphatic polyamides (nylons) when crystalline structure is stabilized by hydrogen bonding between amide *CONH* groups, transition from nylon-6 to nylon-4 to nylon-3 results in increasing T_m because of increasing the content of amide groups in backbone.

Forth, as for the low-molar-mass organic compounds, T_m of polymers is sensitive to configuration isomerism of molecules. As a rule, trans-isomers are characterized by the higher T_m as compared with that for cis-isomers. For diene polymers, such as polyisoprene and polybutadiene, transition from cis- to trans-isomers is accompanied by the marked growth of T_m.

Table 4.

Average melting temperature T_m for various polymers

Polymer	**T_m, K**
Polyethylene	373-393
Poly(ethylene oxide)	355
Poly(*p*-xylylene)	475
Polypropylene	415-425
Polystyrene	500
Nylon-3	610
Nylon-4	535
Nylon-6	510
1,4-polyisoprene	
cis-	300
trans-	345
1,4-polybutadiene	
cis-	273
trans-	420

Chain branching always depresses T_m, and, when density of branches is high enough, crystallization is completely suppressed. For semicrystalline polymers with low density of branches, decreasing T_m is controlled by the same reasons as discussed above for linear polymers. As chain ends, branches may be considered as impurities which are responsible for imperfections in crystal structure. In this case, Eq (.53) may be written as

$$\frac{1}{T_m} - \frac{1}{T_m^{\infty}} = \frac{R}{\Delta H_f}\frac{m}{\overline{P}_n}, \qquad (54)$$

where m is the amount of the chain ends per chain.

Copolymerization also has a pronounced influence on copolymer T_m. In graft and block copolymers, separate crystallization of one or another block may take place. Random copolymerization results in distortion of regularity of polymer chain and may suppress crystallization completely. For example, polyethylene and polypropylene homopolymers are characterized by high crystallinity while random poly(ethylene-*co*-propylene) with the feed monomer composition 50/50 is completely amorphous. Small amount of comonomer units does not suppress crystallization. However, they reduce T_m of resulting polymer because of appearance of non-crystallizable units in polymer backbone. If these non-crystallizable units are considered as impurities they decrease T_m according to Eq. (52) where n is their mole fraction.

Hence, for crystallizable homopolymers, the influence of chemical structure on T_m is similar to that on T_g of amorphous polymers (see Ch. 3.5). Both T_m and T_g are controlled mainly by the balance flexibility - rigidity of the backbone. As a result, the same factors seem to be responsible for parallel changes in both T_g and T_m. Semicrystalline polymers combine both amorphous phase which is characterized by T_g and crystalline phase with T_m, and exhibit both glass transition and melting. For them, correlation between T_g and T_m was found. When these temperatures are expressed in Kelvins, $\frac{T_g}{T_m} \approx \frac{2}{3}$. This empirical observation suggests that, for homopolymers, T_g and T_m can not be changed separately. In some case, copolymerization of appropriate monomers provides a possibility to control T_g and T_m independently. Incorporation of a small amount of foreign comonomer units with the similar chemical structure does not affect markedly of the flexibility of the chain, and noticeable changes in T_g are not observed. However, T_m decreases because of increasing irregularity.

4.3.2. Factors Affecting Crystalline Structure

As discussed in Chs. 4.2.2 and 4.2.3, the dimension of crystallites increase markedly when T_{cr} tends to T_m and overcooling parameter tends to zero. This trend is well-pronounced for polymers characterized by lamellar supramolecular structure (polyethylene is a prime example). For polyethylene, crystallization near T_m results in growth of lamellae thickness up to more that 100 nm.

Crystallization under applied external pressure is accompanied by following increase in lamellae thickness. At pressures up to 5 kbar and low supercooling, lamellae with the thickness up to ~ 10 μm were obtained. This enormous growth of lamellae thickness is responsible for the fact that these lamellae are formed by macrochains with fully extended conformations. This *chain-extended* morphology controls the noticeable increase in polymer density up to 0.996 g/cm^3 and degree of crystallinity up to 95 - 98 %. Note that, for conventional polyethylene, the corresponding values are 0.95 g/cm^3 and 65 - 70 %.

The observed increase in both density and degree of crystallinity controls the growth of elastic modulus and strength of as-prepared materials. However, the growth of these desirable operating parameters is accompanied by increasing brittleness of material, and this factor restricts the field of industrial application.

Note that the appearance of chain-extended morphology under parallel action of pressure and temperature is observed for polyethylene crystallized from melt. Polyethylene crystallization from solutions under pressure up to 5 kbar is not accompanied by the noticeable increase in lamellae thickness, and they are characterized by the typical thickness of about 10 - 15 nm.

Chain-extended lamellae morphology is also observed for polychlorinetrifluoroethylene crystallized from the melt under pressure about 1 kbar as well as for polytetrafluoroethylene crystallized from melt at atmospheric pressure.

For some polymers (polypropylene, poly(methylene oxide)), parallel increase in both temperature and pressure does not affect on the lamella thickness.

Similar extension of macrochains during crystallization and resulting increasing lamella thickness take place when uniaxial mechanical loading, that is, drawing accompanies crystallization. In this case, macrochains are oriented along the axis of drawing, and enhancement of crystallization of these macrochains aligned in parallel controls increasing both crystallinity and density. Application of external stress to the material during crystallization is widely used in industry when polymers are processed via spinning, molding, extrusion, *etc*.

Obviously, increasing stiffness of macromolecules favors crystallization with formation of chain-extended crystallites. For stiff polymers, crystallization proceeds without chain folding with formation of rod-like crystalline fibrils which are characterized by parallel alignment of macrochains along fibril axis.

Note that, for chain-extended crystalline structure, polymer molar mass may have pronounced influence on the crystalline morphology when the dimension of crystallite becomes comparable with the length of macromolecule.

Increasing molar mass controls increase in crystallite dimension.

For polymer crystallization, another peculiar possibility is associated with the crystallization during polymerization. For example, emulsion polymerization of polytetrafluoroethylene is accompanied by the formation of fibrillar crystallites in which macrochains are aligned in parallel along fibril axis without folding. To minimize surface energy, these fibrils tend to coil with formation of dense globule with diameter of about 0.2 μm. As-prepared polytetrafluoroethylene is characterized by degree of crystallinity close to 100 %.

Under appropriate polymerization conditions, for some polymers (polyethylene is a prime example), growth of macrochains is accompanied by the immediate crystallization via folding when the rate of polymerization is comparable with the rate of crystallization. In this case, the parallel polymerization and crystallization are responsible for the appearance of crystallites with low amount of defects and rather perfect structure.

4.4. Physicomechanical Behavior of Semicrystalline Polymers

Obviously, physicomechnanical behavior of semicrystalline polymers is mainly controlled by the coexistence of crystalline and amorphous phases.

Hard crystalline phase contributes to the rigidity of polymer while soft amorphous phase contributes to ductility of material.

To discuss the contributions of both amorphous and crystalline phases in the development of physicomechanical behavior of polymer, let us invoke thermomechanical testing (Fig. 33).

Crystalline phase is characterized by melting temperature T_m and amorphous phase is characterized by glass transition temperature T_g and flow temperature T_f.

Note that T_g is always lower than T_m. As for the ratio between T_f and T_m, two following cases should be taken into account. For semicrystalline polymer with $T_f < T_m$ (Fig. 33A), high rigidity and low deformation is observed up to melting temperature.

Note that, in this case, there are no marked changes in deformation when polymer goes through T_g and T_f. The reasoning for this behavior is associated with the fact that crystallites act as cross-links for macrochains and, as a result, both segmental and molecular mobility in amorphous phase is suppressed. In other words, physicomechanical behavior of this polymer is mainly controlled by crystalline phase without regard to the state of amorphous regions.

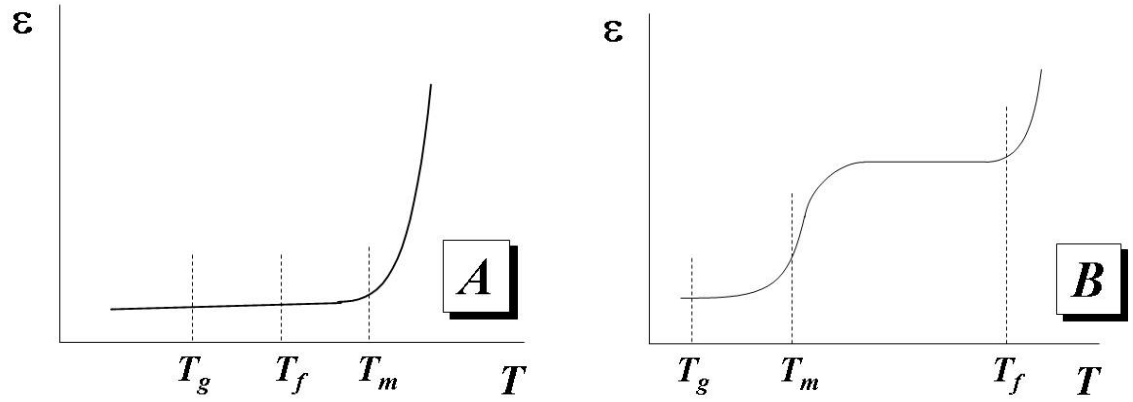

Figure 33. Thermomechanical curves for semicrystalline polymers. $T_f < T_m$ (A), $T_f > T_m$ (B).

For semicrystalline polymer with $T_f > T_m$ (Fig. 33B), the situation is more complicated.

At T_m, there is melting of crystallites, and, as a result, transition of semicrystalline polymer to total amorphous polymer which is in temperature range between T_g and T_f. Obviously, in this case, realization of rubbery state is observed. When temperature increases up to T_f, there is the transition of amorphous polymer to viscous flow state. Hence, thermomechanical behavior of semicrystalline polymer is controlled by the corresponding behavior of amorphous and crystalline phases.

Note that the above speculations are applicable for the deformation within linear viscoelastic region when no structural rearrangements take place. To follow structural pattern of the development physicomechanical behavior of semicrystalline polymer, let us consider its stress-strain behavior.

4.4.1.Stress-Strain Behavior

For semicrystalline polymers, Figure 34 shows a typical stress-strain diagram under the drawing with the constant rate.

Macroscopically, mechanical behavior of semicrystalline polymer seems to be similar to that for the amorphous ductile polymer (Fig. II.26). When the applied stress achieves yield point, yielding is accompanied by the necking of polymer sample, and strain softening is observed. Propagation of neck through the sample proceeds at approximately constant stress, and strain hardening takes place when the whole sample is necked.

The precise structural studies of neck using, for example, electron microscopy and small-angle X-ray scattering showed well-pronounced anisotropic fibrillar structure. The main structural unit of fibrillar structure is asymmetric fibril with high ratio between length and diameter (Fig. 35).

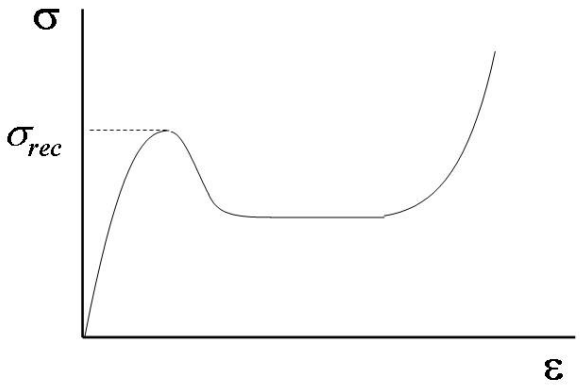

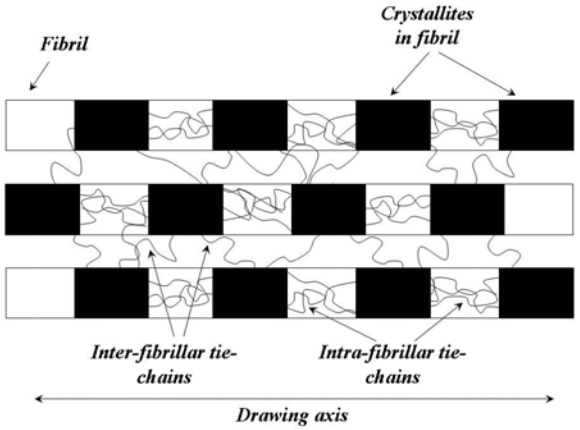

Figure 34. Typical stress-strain diagram for semicrystalline polymer.

Figure 35. Schematic representation of the structure of “neck”.

The fine crystalline fibril structure is characterized by the crystallites with folded macrochains. These crystalline regions are interconnected with the tie-chains which constitute the intrafibrillar amorphous regions. Note that the individual macromolecule may be incorporated in several crystalline regions within individual fibril as well as in the crystalline regions of neighboring fibrils. In the latter case, the corresponding tie-chains constitute interfibrillar amorphous phase.

The structural rearrangements which accompany transformation of initial polymer structure to fibrillar structure are most studied for initial spherulitic and lamellar structure. These studies made it possible to advance the following deformation mechanism.

For initial spherulitic structure, uniaxial drawing is responsible for elongation of spherulites along the axis of drawing followed by the breakage of initial spherulites, and, as a result, fibrillar morphology appears. From the standpoint of structural rearrangements on a finer structural level within spherulite amorphous and crystalline phase, the above process proceeds at initial stage of drawing via homogeneous deformation of spherulite which is provided by shearing of crystals relative to each other. This shear deformation is allowed by soft amorphous phase. With the following increasing strain deformation of crystalline regions comes to a play. Deformation of crystallites is accomapnied by their distortion and breakage followed by the formation of new fibrillar structure.

For initial lamellar structure characterized by regular folded macrochains, uniaxial drawing controls distortion and breakage of initial lamellae, unfolding of the macrochains, and formation of fibrillar structure. In some cases, crystalline regions of this fibrillar structure are formed by folded macrochains, for example, for polyethylene. For polypropylene, chain-extended conformations of polymer macromolecules in fibril crystalline regions seem to be more preferable. In general, superposition of both mechanisms is expected. Note that, in both cases, reorientation of crystallites is observed.

To generalize, let us consider the structure of crystalline polymer as coexistence of randomly oriented crystallites with folded macrochains and amorphous phase constituted by tie-chains. At strain below yield point, deformation of amorphous phase is responsible for preferable orientation of crystallites along the axis of drawing. At yield point, breakage of crystallites takes place, and resulting small crystalline species form fibril.

To understand the origin of microstructural rearrangements which take place at the yield point, let us invoke the following speculations. Any polymer sample is characterized by the presence of both surface and volume structural microdefects. Surface defects, for example, scratches may appear during polymer processing. Inner volume defects may also appear during processing (dust particles, air bubbles, *etc*.) or may have their origin because of density fluctuations or microvoiding as a result of the concentration of free volume. These defects act as the stress concentrators. In the vicinity of the defect the local stress may exceed the applied external stress for several times, and local overloading takes place. Macroscopically, this local overloading results in the formation of neck. Microscopically, local overloading is associated with breakage of crystallites and parallel alignment of their fragments along the axis of drawing with formation of new fibrillar structure.

Transition from the initial polymer structure to the new fibrillar structure under applied stress may be considered as *recrystallization*. In connection with this, for semicrystalline polymers, yield stress is called *recrystallization stress* σ_{rec} (Fig. 34).

In some cases, necking may proceed without recrystallization and appearance of fibrillar structure. Electron microscopy shows that necking sometimes is controlled by deformation of spherullites to elipsoidal shape without their breakage and transition to fibrils. Another possibility is associated with the occurrence of typical plastic deformation (as in metals) controlled for polymers by the sliding of supramolecular structural units relative to each other on slip planes. At temperature of liquid nitrogen, for crystalline *iso*-propylene with perfect spherullitic structure, necking proceeds without distortion of spherullites via their sliding on amorphous regions. This mechanism allows proceeding of rather high deformation up to 100 - 150 %.

The general feature of stress-strain behavior of semicrystalline polymers is associated with the fact that, when the sample is necked, strain hardening (Fig. 34) takes place. Strain hardening, that is, sharp growth of stress with strain implies increasing mechanical response of polymer along the axis of drawing. Obviously, these changes in mechanical behavior are controlled by the above structural transformations which accompany necking. In any case, as a result of deformation, molecular and supramolecular units tend to orient along the axis of loading, that is, *orientation* of polymer material is observed. In details, orientation phenomena in polymers will be discussed in the forthcoming chapter.

4.4.2. Factors Affecting Stress-Strain Behavior

As for the amorphous glassy polymers, the stress required for the recrystallization in semicrystalline polymers increases when the rate of deformation is increased at the fixed deformation temperature. At the fixed rate of deformation, recrystallization stress increases with decreasing deformation temperature.

Note that, ultimately, the increasing rate of deformation as well as decreasing deformation temperature result in brittle-ductile transition for semicrystalline polymer. This well-pronounced time-temperature dependent mechanical behavior implies relaxation origin of necking.

The above structural pattern of recrystallization indicates that this process proceeds via stress activated molecular and segmental mobility. These molecular and segmental rearrangements which are responsible for recrystallization do not occur instantaneously and require the specified period of time, that is, relaxation time. From this standpoint, to discuss the deformation behavior of semicrystalline polymer, one should take into account the ratio between the rate of deformation (loading time) and relaxation time of the above molecular rearrangements.

Relaxation time is controlled by both thermal and stress activation of molecular kinetic units responsible for the recrystallization. At a certain rate of deformation or deformation temperature, macromolecules and segments have no time for the corresponding rearrangements, and brittle fracture occurs till recrystallization point. Hence, to provide recrystallization and necking in semicrystalline polymer one should find the appropriate balance between the rate of deformation and deformation temperature. Successful solution of this problem allows orientation of polymer sample due to formation of fibrillar supramolecular structure.

From the applied standpoint, the search for correlation between deformation temperature and characteristic temperatures of semicrystalline polymer, that is, T_g and T_m is of prime importance.

At deformation temperatures below T_g, vitrification of amorphous phase restricts markedly molecular and segmental mobility, and semicrystalline polymer demonstrates brittle behavior. At temperatures above T_m, semicrystalline polymer behaves itself as viscous liquid or rubber (Fig. 43).

When deformation temperature is in the range between T_g and T_m, well-pronounced molecular mobiltiy within rubbery amorphous phase controls well-pronounced necking, recrystallization, and orientation.

Molar mass has a noticeable influence on stress-strain behavior of semicrystalline polymers. Polymer with low molar mass break at low strains without necking.

The effect of structural organization on stress-strain behavior of semicrystalline polymers is complicate and changes markedly for polymers with specified initial structure. In general, polymer with chain-extended morphology of crystallites tend to be deformed without necking and are characterized by high brittleness. The similar tendency id observed for semicrystalline polymers with stiff chains and polymers with low degree of crystallinity.

Chapter 5. ORIENTATION AND ORIENTED POLYMERS

Orientation of polymeric materials is one of the most important approach for their modification to improve physicomechanical characteristics. Note that production of modern high-modulus and high strength polymeric materials is based, primarily, on polymer orientation.

As considered earlier, during uniaxial drawing, segments, macromolecules, and supramolecular structural units (crystallites) tend to be partially parallel aligned (oriented) along the axis of deformation. For example, during high-elastic deformation, the straightening of the macromolecular coils results in the orientation of segments and macromolecules along the axis of drawing. Obviously, under unloading of deformed rubber, these oriented molecular units tend to the initial positions to increase entropy of the system. As a result, recovery of high elastic deformation is observed, and orientation obtained during deformation is lost. For rubbers, that is, amorphous polymers at temperatures above T_g, the driving force of both deformation and its recovery is well-pronounced segmental mobility. From the structural viewpoint, the similar macromolecular rearrangements provide orientation of glassy amorphous polymers during their yield (forced elastic) deformation. For oriented glassy polymer, unloading is expected not to be accompanied by the recovery of deformation because, at temperatures below T_g, segmental mobility is not observed. However, orientation of polymer glasses is not, generally, possible because of their brittleness. Orientation via uniaxial drawing is well-pronounced for semicrystalline polymers, especially, at deformation temperatures between T_g of amorphous phase and T_m of crystalline phase.

Orientation is observed for polymers in various physical and phase states and may be considered as a general feature of their mechanical behavior.

5.1. Factors which Control Orientation and General Features of Oriented Polymers

In general, during drawing, orientation of isotropic polymer is controlled by extension of macrochains and their fragments along the axis of loading. In other words, orientation is associated with noticeable intramolecular rearrangements via appearance and following increase in extended chain conformations. These conformational transitions result in the parallel alignment of macrochains or their fragments. Obviously, this process is responsible for marked growth of intermolecular interaction, and, as a result, effective stiffness of macrochain and segment size increase, and above conformational transitions responsible for orientation are much restricted. Hence, proceeding of orientation requires more and more loading to provide molecular rearrangements at the final stage of the process. In this case, the external stress may cause the breakage of polymer chains and decrease the final operating parameters of oriented material. Obviously, the above conformational transitions has the relaxation origin and may be controlled by changes of the rate of orientation drawing and temperature of orientation. These speculations emphasizes the important role of technological regime of orientation to obtain oriented polymeric material with desired operating parameters.

Note that the relaxation phenomena play a significant role in the orientation and stability of final oriented polymer. On one hand, the above consideration concerning the relaxation origin of orientation allows one to conclude that the lower relaxation time, the easier conformational transitions, and extension and orientation of macrochains are enhanced. On the other hand, oriented polymer structure is characterized by well-pronounced excited and non-equilibrium

nature. Under unloading, this non-equilibrium state tends to relax to equilibrium state via deorientation. When relaxation time is small enough, deorientation proceeds during or just after unloading as was discussed for orientation-deorientation of rubbery polymer. Hence, to provide a stability of oriented polymer large relaxation time is required. In its turn, large relaxation time much complicate orientation.

From molecular standpoint, relaxation time is controlled by the balance between flexibility and rigidity of polymer chain. Flexible polymers are expected to orient and relax easily while, for stiff polymers, orientation is complicated but stability of final oriented material is rather high. Obviously, optimal combination of orientation and deorientation is observed for polymers with optimal flexibility-rigidity ratio.

From physical viewpoint, to decrease relaxation time one may decrease viscosity of a system via increasing temperature or dissolution of polymer in appropriate solvent. Well-pronounced flow of both polymer melts and solutions provide the orientation of macrochains. For polymers oriented in melt and solution, the following cooling or evaporation of solvent decrease dramatically relaxation time and provide high stability of oriented structure. Industrial aspects of these approaches will be discussed in the next section.

Another factor which has a significant influence on orientation and properties of final oriented materials is associated with the fact that, in general, isotropic polymer systems (polymer solids, rubbers, melts, and concentrated solutions) are characterized by well-pronounced chain entanglements. From this standpoint, orientation of isotropic material should involve disentanglement of macromolecules to provide their parallel alignment along the axis of deformation. During orientation of isotrpic viscous polymer systems, disentanglement of macromolecules is very complicated process which, in general, can not be completed. In the majority of cases, during loading of entangled systems, stress is accumulated in fragments of polymer chains in the vicinity of entanglement. When this stress is high enough, the breakage of macromolecule takes place. When breakage is not observed, in the vicinity of entanglement polymer chains remain stressed in final oriented material. Both above factors are responsible for lowering of mechanical properties of oriented polymers. Hence, the challenging problem concerning the preparation of advanced oriented polymeric materials may be considered as a problem to avoid entanglements in initial polymer system. The possible solution of this problem will be discussed in the next section.

As for the final properties of oriented polymeric materials, the following general considerations should be taken into account. Orientation is accompanied by parallel alignment of segments, macrochains, and fibrillar supramolecular units along the axis of drawing. As a result, oriented polymer is typical anisotropic material, and its properties are quite different in normal directions. The reasoning of it is associated with appearance of two different types of interactions between atomic groups. Along the axis of previous orientation oriented polymer is characterized by strong covalent bonds which control the enormous growth of mechanical response to applied loading. In normal direction, oriented macromolecular units are held together by weak physical interactions. As a result, in this direction, mechanical behavior is controlled by the response of these weak physical bonds to applied loading, and decreasing mechanical properties is observed. In other words, uniaxial orientation is accompanied by increasing mechanical characteristics of oriented polymer in the direction of orientation and their decreasing in perpendicular direction. From this standpoint, uniaxial orientation can be effectively used only for polymer fibers which always work along the fiber axis. For polymer

films or plastic sheets, biaxial or multiaxial orientation in plane should be carried out to provide adequate mechanical response of oriented polymer in different directions.

Obviously, increasing strength properties of oriented polymer because of orientation of molecular and supramolecular units along a given axis is accompanied by decreasing ductility and deformability. From the standpoint of industrial application, advanced polymer materials should combine high strength with low brittleness, that is, with rather high deformability. Deformability is controlled by the mobility of some kinetic units which can relax during loading and provide non-brittle mechanical response. In contrary, relaxation of the above kinetic units is expected to be responsible for deorientation and loss of desirable mechanical characteristics of orients polymer. In other words, to obtain the optimal combination of strength and ductility peculiar combination of relaxing structural units is required.

For low-molar-mass oriented materials, this situation can not be realized because mobility and relaxation of molecules immediately results in deorientation and decreasing strength properties. When the molecules are fixed in appropriate positions, high-strength oriented body becomes rigid and brittle. Chain chemical structure of polymers provides a unique possibility to design oriented material with desired properties. In this case, molecular and supramolecular structural units with high relaxation time (for example, oriented macrochains and crystallites in fibrils) control the stability of oriented structure and high strength. Structural units with low relaxation time (segments and tie-chains in fibrils) contribute to ductility and elasticity of material.

Hence, to prepare oriented polymeric material with desired operating parameters we should take into account the above kinetic, relaxation, and structural features of orientation and physicomechanical behavior of oriented systems. The possible ways of technological realization of these fundamentals as well as the advantages of oriented polymers will be discussed in forthcoming sections for ductile semicrystalline and glassy polymers and brittle polymer glasses.

5.2. Orientation of Ductile Polymers

As discussed earlier, for isotropic semicrystalline and ductile glassy polymers, orientation is easily carried out via necking of the polymer sample under the drawing with constant strain rate which is usually called *cold drawing* (Fig. 36, curve 1).

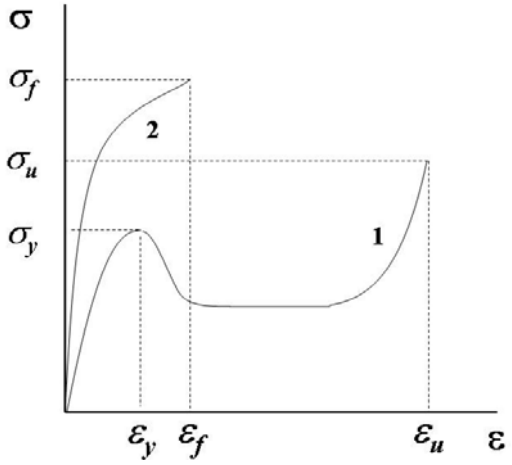

For the unloaded necked, that is, oriented sample, the stress-strain diagram is shown in Fig. 36 (curve 2). Obviously, for oriented polymer sample, yielding is not observed, and fracture takes place within stress-strain region close to linear. To understand the possibilities of orientation drawing to improve mechanical properties of polymeric materials, let us compare the mechanical parameters of initial isotropic and oriented necked polymer samples.

Figure 36. Stress-strain diagrams for isotropic ductile polymer (1) and oriented necked sample (2).

Initial ductile polymer is characterized by the following set of mechanical parameters: elastic modulus E, yield stress σ_y and yield strain ε_y, ultimate stress σ_u (strength) and ultimate strain ε_u. Oriented polymer sample is characterized by the elastic modulus E', strength σ_f and corresponding ε_f. For oriented sample, the strength and elastic modulus are much higher as compared with that for initial isotropic polymer, that is, $\sigma_f > \sigma_u$ and $E' > E$. However, orientation is accompanied by the marked decreasing ultimate strain, and $\varepsilon_f < \varepsilon_u$. Hence, orientation drawing is associated with the gain in strength and loss in ultimate strain.

On the other hand, from the operating viewpoint, isotropic samples are used at the stress and strain not above σ_y and ε_y. When the applied stress or strain exceed the above values, the yielding and necking are responsible for the loss in stability of polymeric material. In connection with this, the operating parameters of isotropic semicrystalline polymer are σ_y and ε_y, and, for oriented material, they are σ_f and ε_f. Comparison of these parameters shows the complete gain in mechanical properties for the oriented polymer: $\sigma_f > \sigma_y$ and $\varepsilon_f > \varepsilon_y$.

The above procedure to orient ductile (primarily, semicrystalline) polymers via uniaxial drawing is suitable well for the polymer fibers. Orientation of isotropic semicrystalline fiber is responsible for the drastic increasing both elastic modulus and strength along the fiber axis.

The above gain in operating parameters is associated with the transformation of initial isotropic structure to oriented structure, and, after orientation, macroscopic mechanical response of oriented polymer is controlled by specific behavior of fibrillar structure under mechanical loading.

Fibrillar structure (Fig. 35) consists of individual fibrils which are characterized by the set of crystalline regions interconnected with tie-chains. These tie-chains compose intrafibrillar amorphous regions. Fibrils are held together by physical interactions and interfibrillar tie-chains. Under loading, stiff crystalline regions are responsible for increase in stiffness of oriented polymer and resulting growth of strength properties. In both intra- and interfibrillar amorphous regions, tie-chains contribute to ductility and elasticity of oriented material obtained by cold drawing. However, these tie-chains are “weak” sites of fibrillar structure and, when stress is sufficiently high, they are broken down, and macroscopic rupture of material takes place.

Hence, despite of positive contribution to ductility of oriented material, amorphous regions of fibrillar structure may be considered as “structural defects” which restrict the possibilities for improvement of final mechanical parameters via cold drawing. To avoid these disadvanatges and make oriented crystalline structure more perfect, the following technological approach is widely used for production of polymer fibers.

Processing of polymer fibers involves crystallization and orientation The main problem is to realize these two processes in a continuous way just in the course of fiber processing. In industry, fibers are produced via *spinning*. When fibers are fabricated from polymer melts this technological technique is called *melt spinning*. Fiber production from polymer solutions is carried out via *solution spinning*.

During melt spinning, polymer melt is forced through the spinneret, a plate with tens to thousands holes. The individual fibers produced via the pumping of polymer melt through the holes of spinneret are used as monofilaments or twisted together with formation of yarn. When fibers leave the spinneret, solidification (crystallization) takes place because of the sharp cooling of the material. Using a suitable wind-up devices, as-prepared fibers are stretched to provide the

required orientation. It is important to orient polymer fibers simultaneously with their crystallization. During orientation, the alignment of macromolecules along the axis of orientation favors crystallization and increases degree of crystallinity of the final polymeric material. Both increasing crystallinity and orientation are responsible for the improvement of the operating properties of resulting polymer fibers. Widely used nylon (polyamide) fibers are produced via melt spinning.

Note that only polymers with high thermal stability can be processed via melt spinning. Polymer which tend to decompose at the temperatures required for melt spinning are processed via solution spinning. These are two versions of this processing technique - dry spinning and wet spinning.

For the dry spinning, polymer solutions in the volatile solvent are used. When fibers leave the spinneret, evaporation of the solvent is accompanied by solidification and crystallization of polymer. Orientation of the drying polymer fiber enhances the crystallization similar to that for melt spinning. Note that this processing technique is more complicated as compared with melt spinning, Evaporation of the solvent from the fiber surface results in formation of solidified surface layer and make the evaporation from the core more difficult. This diffusion-controlled solvent evaporation results in the appearance of the irregularities on the surface and in the core of the resulting fiber. Moreover, dry spinning requires the additional technological stages to utilize or recycle the solvent used. Acrylic fibers, primarily, polyacrylonitrile, are produced via dry spinning.

In wet spinning, solution is forced through the spinneret into coagulation bath with precipitator. Precipitation controls the solidification of as-formed polymer fibers. Obviously, precipitation starts at the fiber surface, and structural inhomogeneties appear both along the fiber and in normal direction. Note that the pick-up rates in wet spinning should be much lower as compared with the above spinning techniques to provide the complete coagulation and stabilization of precipitated polymer fibers. Cellulose fibers are the prime example of the polymers produced via wet spinning.

The above spinning processes are more advantageous as compared with cold drawing of isotropic fiber. However, both melts and solutions which are subjected to orientation via spinning are characterized by well-pronounced chain entanglements. As discussed in previous section, chain entanglements complicate orientation and, as a result, restrict the growth of final operating parameters. To avoid these disadvantages, recently, *gel-technology* is used to prepare advanced oriented polymer materials.

Gel-technology involves preparation of polymer precursor from dilute polymer solution in which macromolecular coils are completely isolated. In other words, this polymer system is characterized by no entanglements of macromolecules. Orientation of the above precursor is accompanied by separate uncoiling of the individual macromolecular coils and parallel alignment of extended macrochains.

5.3. Orientation of Polymer Glasses

In general, for amorphous glassy polymers, orientation via drawing of the films and sheets can not be carried out because of their brittleness. Under the drawing of polymer glasses, brittle fracture takes place at the stress and strain much lower than those required for yielding and resulting orientation. To orient, glassy polymer is drawn at elevated temperatures close to or above glass transition temperature. At these temperatures, alignment of both segments and macromolecules along the axis of drawing proceeds rather easily, and orientation of polymeric material is observed. To prepare oriented glassy polymer, after orientation drawing at elevated temperatures, the sample is cooled down in the stressed state followed by the unloading at the ambient temperature.

The comparison of the mechanical behavior of initial isotropic and oriented polymer samples indicates the complete gain in the mechanical parameters as a result of orientation. For oriented polymer sample, elastic modulus, strength, and ultimate strain are much higher as compared with the initial polymer. Moreover, orientation increases markedly the work of fracture estimated as the area under corresponding stress-strain curves.

The work of fracture is a measure of the very important operating parameter such as impact strength (or toughness) which controls the resistance of polymeric material to the impact loading. For oriented polymer glasses, impact strength exceeds markedly the corresponding parameter for the initial polymer, and, in other words, orientation provides decreasing brittleness of polymer glasses.

As mentioned above, uniaxial orientation results in increasing mechanical parameters along the axis of drawing and decreasing those in the normal direction. To obtain oriented polymer films and plastics with comparable mechanical properties in any direction, they are oriented biaxially or multiaxially.

Chapter 6. FRACTURE OF POLYMERS

During deformation, when the applied stress approaches a critical value, the fracture of material takes place. This critical stress is identify as strength of a given material, and corresponding strain is called as ultimate strain.

Modern materials are classified as “brittle” and “ductile” materials.

Low-molar-mass brittle materials such as inorganic glasses breaks down at rather low ultimate strain which is typically not more than percent. Ductile materials, for example, metals demonstrate plastic deformation to high strain before failure, and, for them, ultimate strain is rather high.

Polymers also show both types of fracture behavior depending on their structural organization and test conditions. In general, glassy polymers, highly oriented polymers, semicrystalline polymers with high degree of crystallinity, chain-extended crystalline polymers are considered as brittle materials which fail at relatively low strain. Isotropic semicrystalline polymers are characterized by well-pronounced ductility in the temperature range between T_g and T_m and undergo cold drawing before fracture. Decreasing test temperature below T_g is accompanied by increasing their brittleness, and brittle fracture becomes preferable. For elastomers, fracture is observed after high elastic deformation to hundreds percents of strain. As mentioned in Sections 3.6.3 and 4.4.2, for polymers, the particular fracture mode is mainly controlled by the balance between testing temperature and strain rate. For both amorphous and semicrystalline polymers, ductile-brittle transition is observed at specified temperature and strain rate.

Hence, the fracture behavior of polymers seems to be rather complicated as compared with that for low-molar-mass materials. In this section, we consider both general features of fracture and particular fracture behavior for various polymeric materials.

6.1. Theoretical Tensile Strength

In general, strength of any material is controlled by the energy of interaction between atoms, atomic groups, and molecules which compose the physical body.

Theoretical strength is the energy of dissociation of a given covalent or physical bond multiplied by the amount of these bonds in cross-section area.

Figure 37 shows profile of potential energy U versus the distance between two particles. These particles are in equilibrium when the attractive and repulsive components of their interaction are compensated, and potential energy is minimal. Let us denote the corresponding distance between the particles as x_0. Any external excitation disturbs equilibrium, and U increases. The general correlation between potential energy and inter-particle distance x may be expressed by semi-empirical Morze function

$$U = E_d e^{-2b(x-x_0)} - 2E_d e^{-b(x-x_0)} \qquad (55)$$

where E_d is the energy of dissociation, and b is a constant for a given bond.

In the case of tensile deformation when x increases, the resulting force goes through maximum at $x = x_{max}$. At $x_0 < x < x_{max}$, attraction forces between particles resist the external loading, and, when $x > x_{max}$, the energy of inter-particle interaction dramatically falls down. From this standpoint, F_{max} is the critical force, and when it is attained the particles are separated, and macroscopic fracture of a solid takes place.

Taking into account that

$$F = \frac{dU}{dx} = -2bE_d e^{-2b(x-x_0)} + 2bE_d e^{-b(x-x_0)} \tag{56}$$

and, at $x = x_{max}$, $dF/dx = 0$, the value of x_{max} can be found.

Substitution of x_{max} in (56) gives

$$F_{\max} = \frac{bE_d}{2}. \tag{57}$$

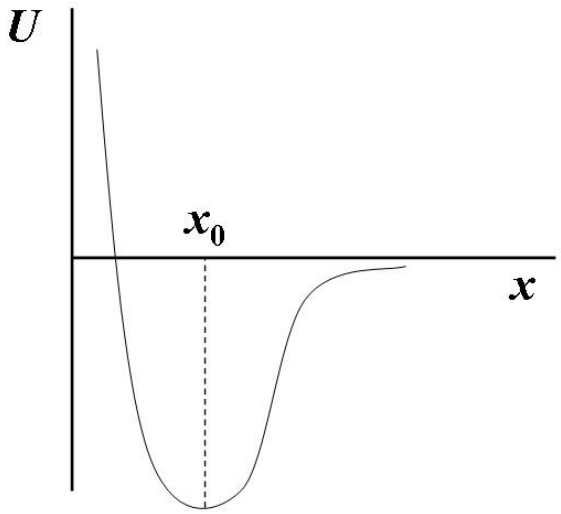

For a given bond, dissociation energy and constant b can be determined experimentally and are tabulated. Using these parameters, F_{max} may be estimated for a particular type of covalent and physical bonding. For polymers, when the type of packaging of macromolecules is known from X-ray scattering data, the amount of macrochains in cross-section area may be estimated, and multiplication of this value by F_{max} gives theoretical strength.

Figure 37. Profile of potential energy U versus the distance x between two particles.

The above speculations allow us to estimate also theoretical elastic modulus.

According to Hooke's law

$$E = x_o \left(\frac{dF}{dx}\right)_{x \to x_0}. \tag{58}$$

Let us assume that, Hooke's law is obeyed till $x = x_{max}$.
Substitution of F (Eq. (56)) to Eq. (58) gives

$$E_{theor} = 2b^2 E_d x_0. \tag{59}$$

Note that, for a variety of materials, theoretical strength differs markedly from experimental value of strength (Table 5). The prime reasoning of this fact is associated with the presence of a lot of defects in real physical body. The role of defects in fracture will be discussed in the next section. On the other hand, the theoretical consideration of fracture implies instantaneous cooperative breakage of all bonds in a given cross-section. Actually, fracture of real materials involves crack propagation through the body, and macroscopic fracture is observed when this crack propagates through cross-section.

Fracture is likely to be controlled by kinetic factors.

As discussed in Section 3.3, mechanical work delivered to material is, in general, divided into two components one of which is stored in material as elastic energy and the second of them is dissipated as a heat. In its turn, during fracture the elastic energy stored in the sample is released via formation of two new surfaces within body (i) and rearrangements of some structural units at the tip of the growing crack (ii). The latter factor is responsible for appearance of internal friction and dissipation of a certain fraction of energy as a heat.

Table 5.
Theoretical strength and strength of the commercial grades of various materials

Material	**Theoretical strength, GPa**	**The strength of commercial grades, GPa**
Steel	46	2 - 4
Sodium chloride (crystal)	2	5×10^{-3}
Graphite	122 - 138	101 - 117
Polyethylene	26 - 27	4.0 - 6.5
Polypropylene	11 - 12.5	2.0 - 3.5
Poly(vinyl chloride)	14 - 17	2.7 - 4.0
Nylon-6	23 - 27	4 - 7
Cellulose	16 - 26	2.7 - 7.0

These factors have a pronounced influence on the fracture behavior of polymers and are responsible for high sensitivity of polymer experimental strength to testing parameters such as duration and rate of loading, loading temperature and stress, geometry and dimension of testing sample, *etc*. There are two basic concepts to describe and predict fracture behavior of solids - Griffith's theory of brittle fracture and fatigue.

6.2. Griffith's Theory

To explain the great difference between theoretical and experimental strength values, Griffith suggested the existence in real body a lot of defects which decrease strength properties of material. This decrease in strength is associated with the fact that, at the edge of any defect such as surface scratch, volume flaw, and microcrack, localized stress exceeds applied external stress for several times.

Defects cause stress concentration in the vicinity of their tips.

Figure 38 shows the distribution of applied stress σ in the sample with volume flaw. The local stress σ^* is maximal at flaw tip and exceeds applied stress. With increasing distance from notch tip the local stress decreases and tends to σ.

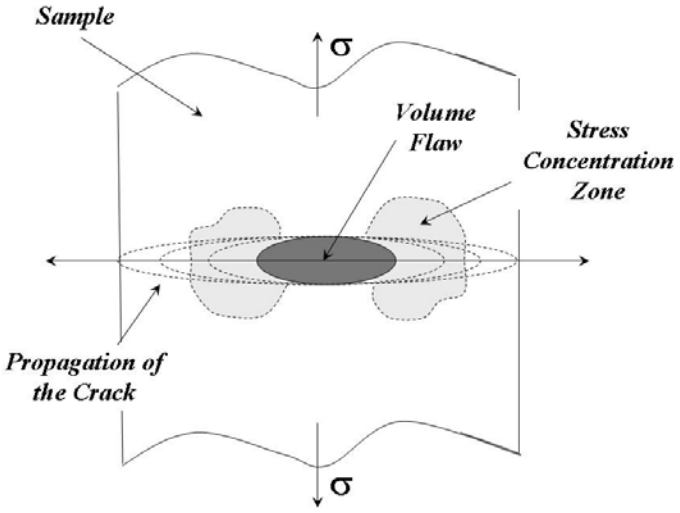

For pre-existing volume elliptical crack, the local stress σ^* at its tip is given by

$$\sigma^* = \sigma\left(1+2\frac{a}{b}\right), \qquad (60)$$

where σ is applied stress, a and b are major and minor axes of ellipse, respectively.

Figure 38. Schematic representation of the stress concentration in the vicinity of flaw tip and following propagation of the crack in the sample.

Equation (60) predicts the larger σ^* for larger ratio a/b. The ratio between a and b axes may be formalizad as radius of curvature of the sharper end of ellipse $r = b^2/a$, and Eq. (60) may be written as

$$\sigma^* = \sigma\left(1+2\sqrt{\frac{a}{r}}\right). \qquad (61)$$

The sharper crack tip, the larger stress concentration in its vicinity.

From this standpoint, the loading of the sample is accompanied by noticeable stress concentration at the tips of pre-existing defects. When this stress concentration is sufficient to break chemical of physical bonds, the crack starts to grow and propagate through the material.

Statistically, at first, the most “weak” defects, primarily, surface notches and scratches come to a play under loading. The propagation of cracks initiated at these defects is accompanied by decreasing cross-section area. As a result, effective stress grows, and other defects become activated. Hence, the appearance and growth of primary cracks initiate the appearance and growth of secondary cracks, and fracture takes place as a result of their coalescence.

Within the framework of Griffith’s theory, mechanical work delivered to a sample is released completely via formation of two new surfaces under crack propagation. From this standpoint, the critical stress, that is, strength is written as follows

$$\sigma_f = \sqrt{\frac{2\alpha E}{\pi l_0}}, \qquad (62)$$

where α is specific surface energy, E is elastic modulus, and l_0 is the length of pre-existing defect.

Griffith's theory developed to describe the brittle fracture of glasses predicts adequately the fracture behavior of brittle polymers such as polystyrene and poly(methyl methacrylate).

The principal result of Griffith's theory is the dependence of strength on the size of intrinsic defects in a brittle body which is actually observed for a variety of materials.

The brilliant support of the idea concerning the significant role of surface defects in fracture behavior was provided by experiments carried out by Ioffe[1]. Under tensile loading, the crystal of salt was continuously rinsed with hot water to disslove the surface layer and eliminate surface defects. Under these testing conditions, experimental strength of the salt specimen was close to theoretical value. The same increasing strength was observed for glass samples which were previously etched in hydrofluoric acid.

The main disadvantages of Griffith's theory are the following.

At first, dissipation of energy as a heat is not taken into account. Note that, for polymers, even at brittle fracture, yielding is likely to take place in the vicinity of the tip of growing crack. Yielding is controlled by stress-induced rearrangements of segments, and, as a result, internal friction and dissipation of energy are observed.

Secondly, Griffith's theory predicts the fracture of material when the stress approaches the critical value. In other words, at lower stress, fracture is not possible. Actually, the fracture takes place even at stress which is much less than the critical stress when this material is loaded for along period of time. This phenomenon is called *fatigue* and considered in the next section.

6.3. Fatigue

A variety of materials fail when they are subjected to the stress much less than critical stress predicted by Griffith's theory. This time-dependent fracture behavior is identified as *fatigue*.

This behavior is associated with the fact that the distribution of thermal energy in material is not homogeneous. The fluctuation of thermal energy means the probability of concentration of thermal energy in local microvolume. Such local concentration of thermal energy on some stressed chemical or physical bonds is accompanied by their disruption, and, as a result, appearance of microcracks takes place. Appeared microcracks are accumulated in material with time till macroscopic fracture is observed.

Disruption of both chemical and physical bonds in stressed sample is a result of parallel action of thermal and mechanical energy.

These speculations provide the basis for kinetic theory of fracture developed by Zhurkov[2].

[1] A.F. Ioffe (1880-1960) – Soviet physicist. "Father" of Soviet physics.
[2] S.N. Zhurkov (1905-1997) – Soviet physicist.

The higher stress, the higher probability of disruption of bonds at a given temperature and *vice versa*.

In the framework of Zhurkov' theory, this approach is formalized as follows

$$\tau_f = \tau_0 e^{\frac{U-\gamma\sigma}{RT}}, \qquad (63)$$

where τ_f is durability of material, that is, the period of time till fracture, U is activation energy of disruption of a given bond when $\sigma \to 0$, and γ is a coefficient which is controlled by structure of material.

For polymers, γ increases with orientation, and decreases as a result of plasticization.

The main disadvantages of Zhurkov' theory are the following.

The linear character of the dependences of durability on stress and temperature is observed in restricted range of stresses. With increasing stress, the safe stress is approached. Safe stress does not influence on fracture of polymer, and, as a result, durability increases enormously. Zhurkov' theory does not predict the safe stress as well as critical stress of fracture.

Under operating conditions, polymer materials are often undergone by periodic or cyclic deformation. In this case, the *dynamic fatigue* takes place, and fracture is observed after a certain number of cycles. The number of cycles to failure is very important operating parameter of material. The main reason of dynamic fatigue is associated with the fact that, in each cycle, the heat is released. When the heat remove is not sufficiently effective, the local overheating is observed. Obviously, this factor accelerates disruption of both chemical and physical bonds and leads to fracture.

Dynamic fatigue may be formalized as follows.

Let us assume that, during each cycle, fatigue cracks grow with a small increment, and this crack propagation is accumulated in loaded material. From this standpoint, durability τ_f can be represented as a set of time intervals Δt_1, Δt_2, ... , Δt_n within which applied stress is constant.

In each cycle, relative decrease in durability is $\frac{\Delta \tau_i}{\tau_f}$. Taking into account that $\Delta t_1 + \Delta t_2 + ... + \Delta t_n = \tau_f$,

$$\sum_{i=1}^{n} \frac{\Delta t_i}{\tau_f} = \frac{\tau_f}{\tau_f} = 1. \qquad (64)$$

When $\Delta t \to 0$, Eq. (64) may be written as

$$\int_0^{\tau_f} \frac{dt}{\tau_f} = 1, \qquad (65)$$

where τ_f is durability described by Eq. (II.63) under applied stress when loading time tends to zero.

6.4. Factors which Control Fracture of Polymers

Chain chemical structure of macromolecules is responsible for specific features of fracture behavior of polymeric materials.

At first, in the majority of cases, fracture of polymers has a well-pronounced relaxation origin.

Secondly, in general, there are two types of interactions which resist fracture of any material: covalent intramolecular interactions and physical intermolecular interactions. From this standpoint, the fracture occurs as a result of slippage of molecules with disruption of intermolecular interactions and via molecular rupture. ***As compared with low-molar-mass materials, for polymers, fracture behavior is controlled by unique combination of above types of interaction and modes of rupture.***

Third, chain chemical structure is responsible for formation of complicated and unique supramolecular structures with specific response to applied loading.

Forth, polymers are characterized by appearance of specific inhomogeneities associated with the above supramolecular structures. Note that these inhomogeneities or structural defects may serve as nuclei of crack initiation and following propagation and enhance fracture. On the other hand, these inhomogeneities provide rearrangements of molecular kinetic units, occurrence of relaxation, and termination of growing cracks.

The fracture of polymeric material is controlled by the specific combination of the above factors.

Let us consider the following types of materials.

For ***high-molar-mass high-oriented polymers*** with parallel alignment of extended macrochains, activation energy of breakage E_a (see Eq. (63)) was estimated to be close to the energy of covalent bonds between atomic groups in backbone and coincide with the activation energy of thermal destruction of corresponding polymer. These estimations allow us to conclude that, for high-oriented polymeric materials, breakage is controlled by rupture of covalent bonds via their thermal destruction. According to Zhurkov' approach (Section 6.3), localized thermal destruction of chemical bonds is controlled by fluctuations of thermal energy and its statistical concentration in a given microvolume of polymer body. External mechanical loading favors the above thermal activation of the rupture of covalent bonds. Hence, for oriented materials with parallel alignment of macrochains, strength properties are expected to be associated with intramolecular chemical interactions based on the covalent bonding of atomic groups in polymer backbone. However, cooperative intermolecular physical interactions between extended macrochains play a significant role in polymer resistance to breakage because they prevent the slippage of macrochains relative to each other and, as a result, appearance and growth of cracks in intermolecular regions.

For ***oriented polymers with fibrillar structure*** (Fig. 34), rigid crystallites contribute to increasing material stiffness and restrict slippage of macrochains in intrafibrillar amorphous regions. Interfibrillar tie-chains as well as interfibrillar physical interaction prevent slippage of fibrils relative to each other. Under deformation, loading of tie-chains in amorphous regions results in their rupture, appearance of the cracks and their propagation till the complete breakage of material.

For ***isotropic polymeric materials***, intermolecular physical interactions contribute mainly in strength properties. Under loading, preferential breakage of rather weak physical bonds is responsible for slippage of macrochains and resulting macroscopic rupture.

Actually, polymeric materials combine both types of fracture. To make a conclusion concerning preferential mechanism of fracture, experimental techniques which are capable to monitor the occurrence molecular rupture may be used. For example, electron spin resonance spectroscopy allows one to detect the production of free radicals which are produced via the fracture of covalent bonds during loading. Under rupture, the most pronounced amount of free radicals was observed for oriented crystalline fibers and cross-linked elastomers. This experimental evidence suggests the preferential molecular rupture of material during breakage. For these materials, crystallites and cross-links restrict the slippage of macromolecules, and rupture of polymer is mainly controlled by disruption of covalent bonds. For a majority of polymers, low amount of appeared free radicals evidences that their failure occurs primarily via molecular slippage with disruption of intermolecular physical interactions.

As mentioned in Section 6.2, at the tip of growing crack, the stress is maximal. Chain chemical structure of polymers provides relaxation of this localized stress via rearrangements of structural units in the vicinity of crack tip. Note that relaxation time decreases markedly with increasing stress (Eq. (43)), and relaxation processes become more enhanced. As a result, mechanical work delivered to polymer dissipates, localized stress relaxes, and crack growth is terminated. These relaxation processes accompany fracture of even brittle polymeric materials such as polymer glasses, poly(methyl methacrylate) as a prime example. The above consideration concerning the relaxation origin of fracture of polymers may be used to explain the lowered brittleness of glassy polymers as compared with conventional silicate and inorganic glasses.

For ***polymers characterized by well-pronounced yielding***, relaxation phenomena determine mainly fracture behavior. In this case, yield deformation at the tip of growing crack is accompanied by orientation of polymer, resulting reinforcement of material, and termination of crack. For these materials, fracture is observed at rather high strain when the polymer sample is necked.

> At temperatures below T_g, brittle fracture at low strain takes place when the rate of crack propagation is higher than the rate of orientation and yielding of polymer.

Obviously, the rate of orientation is controlled by relaxation time of kinetic units (segments) which are responsible for yielding. With increasing temperature relaxation time decreases, and transition from brittle fracture to fracture via yielding takes place. At fixed testing temperature, the same trend is observed when the rate of loading decreases. At temperatures above T_g when amorphous polymers are in rubbery state, appearance and growth of crack is accompanied by well-pronounced orientation of the material at the tip of growing crack as a

result of high elastic deformation. For rubbers and elastomers, fracture takes place at high strain when disruption of both inter- and intramolecular interactions become noticeable.

For amorphous isotropic polymer, the fracture is associated with above discussed competition between crack propagation and orientation which reinforces polymer. At temperatures below brittleness temperature T_{br}, orientation is suppressed and brittle fracture prevails. When temperature tends to glass transition temperature T_g, orientation comes to a play, and strength grows. At temperatures higher T_g, rubbery polymer orients easily. However, elevated temperature activates enormously breakage of both physical and chemical bonds, and high oriented rubber fails at rather low stress.

Molar mass affects strength as follows. For low-molar-mass polymer homologues, strength increases markedly with increasing molar mass. When critical degree of polymerization (appr. 500 - 600) is attained, the following increase in molar mass does not have noticeable influence on the strength parameters. This behavior is associated with the fact that, for low-molar-mass polymers, flexibility of short chains is rather poor, and during loading above reinforcing orientation phenomena via yielding and high elastic deformation are not pronounced. As compared with high-molar-mass polymers with cooperative nature of intermolecular physical bonding, polymers with short chains are characterized by low resistance of intermolecular interactions to applied loading.

As for the structural aspects of fracture

- Strength is higher for stiff polymers which contain atomic groups with high energy covalent bonds such as phenolic rings, intramolecular cycles, double and triple bonds, *etc*.
- Incorporation of atomic groups which are capable to specific physical interactions, for example, hydrogen bonding increases strength because of increase in the energy of intermolecular interactions.
- Formation of supramolecular structures via crystallization, orientation, and cross-linking results, in general, in the growth of strength.
- In contrary, structural factors which complicate packaging of macromolecules, for example, branching decrease strength.

For ***fibers***, the peculiar factor which affects noticeably on the strength is fiber diameter. For both polymeric fibers and fibers based on inorganic glasses (for example, boron and quartz fibers), decreasing diameter is responsible for marked growth of their strength. Strength of quartz fibers approach almost theoretical value when diameter is about several micrometers. For polydiacetylene single crystal fibers, decreasing diameter from 150 to 50 μm results in increasing strength from 0.5 to 1.5 GPa. Statistically, this behavior is associated with the fact that the probability of appearance of both surface and volume defects is proportional to surface area and cross-section area which decrease with decreasing fiber diameter. As a result, the thinner fibers contain less defects, and their strength characteristics increase.